

THE UNIVERSITY OF MICHIGAN
INDUSTRY PROGRAM OF THE COLLEGE OF ENGINEERING

AN ANALYTICAL AND EXPERIMENTAL STUDY OF THE
PRESTRESSED BOWSTRING ARCH

Movses J. Kaldjian

A dissertation submitted in partial fulfillment
of the requirements for the degree of
Doctor of Philosophy in the
University of Michigan
1959

September, 1959

IP-385

ACKNOWLEDGMENT

The investigation described in this study has been carried on under the direction of Professor Lawrence C. Maugh, chairman of the doctoral committee, to whom I am indebted for his valuable advice, for the time he has generously given for consultation, and for reviewing the manuscript and offering numerous helpful suggestions. I also wish to thank the other members of my committee for their assistance: Professor Robert C. F. Bartels, Assistant Professor Glen V. Berg, Associate Professor Samuel K. Clark, and Professor Leo M. Legatski. The Department of Civil Engineering supplied the funds for the "model study." The Statistical Research Laboratory made available the high-speed digital computer, without which the computation could not have been made. The typing, drafting, and reproduction were done by the staff of the Industry Program of the College of Engineering. I wish to express my thanks to each of these persons for their assistance.

TABLE OF CONTENTS

	<u>Page</u>
ACKNOWLEDGMENT.....	ii
LIST OF TABLES.....	iv
LIST OF FIGURES.....	v
NOMENCLATURE.....	vii
CHAPTER	
I. INTRODUCTION.....	1
II. THE STRAIN-ENERGY METHOD.....	6
III. THE MEMBRANE-ANALOGY METHOD.....	19
IV. EXPERIMENTAL STUDY.....	33
V. SUMMARY AND CONCLUSIONS.....	42
APPENDIX A. RELATION BETWEEN THE VERTICAL COMPONENTS OF THE DEFLECTION OF THE ARCH RIB AND THE TIE-GIRDER.....	47
APPENDIX B. SAMPLE CALCULATION.....	50
APPENDIX C. INFLUENCE LINE DIAGRAMS AND GRAPHS FOR PRELIMINARY DESIGN WORK.....	56
REFERENCES.....	81

LIST OF TABLES

<u>Table</u>		<u>Page</u>
I	VALUES OF EQUATION (2.4) (ARCH RIB CENTERLINE) AND ITS DERIVATIVES.....	10
II	BENDING MOMENTS AND AXIAL FORCES WITH PARTIAL DERIVATIVES - IN ARCH.....	11
III	BENDING MOMENTS AND AXIAL FORCES WITH PARTIAL DERIVATIVES - IN TIE-GIRDER.....	12
IV	AXIAL FORCES WITH PARTIAL DERIVATIVES - IN SUSPENSION RODS.....	13
V	ANALYTICAL AND EXPERIMENTAL VALUES OF HORIZONTAL FORCE X_1 COMPARED.....	36
VI	VALUES OF $\sin(i\pi k)$ FOR DIFFERENT "i" AND "k".....	54
VII	VALUES OF $10/i\pi (k^4 - 2k^3 + k)$ FOR DIFFERENT "i" AND "k".....	55

LIST OF FIGURES

<u>Figure</u>		<u>Page</u>
1	Analytical and Experimental Values of Bending Moment Compared for $m_I = 2.62$	37
2	Analytical and Experimental Values of Bending Moment Compared for $m_I = 5.30$	38
3	Bending Moment Along Arch and Girder for Different m_g and m_r Values.....	57
4	Influence Lines for Bending Moment at Panel Point X_4 for Different m_g and m_r Values.....	58
<u>For Vertical Load</u>		
5	Influence Lines for Horizontal Force X_1	59
6	Influence Lines for Suspension-Rod Force X_2	60
7	Influence Lines for Suspension-Rod Force X_3	61
8	Influence Lines for Suspension-Rod Force X_4	62
9	Influence Lines for Bending Moment at Panel Point X_2 for Arch.....	63
10	Influence Lines for Bending Moment at Panel Point X_3 for Arch.....	64
11	Influence Lines for Bending Moment at Panel Point X_4 for Arch.....	65
12	Influence Lines for Bending Moment at Panel Point X_2 for Tie-Girder.....	66
13	Influence Lines for Bending Moment at Panel Point X_3 for Tie-Girder.....	67
14	Influence Lines for Bending Moment at Panel Point X_4 for Tie-Girder.....	68
<u>For Horizontal Load</u>		
15	Bending Moment at Panel Point X_4 for Different Values of L/r_c and m_I for Tie-Girder.....	69

LIST OF FIGURES (CONT'D)

<u>Figure</u>		<u>Page</u>
16	Bending Moment at Crown for Different Values of L/r_c and m_I for Arch.....	70
17	Horizontal Force X_1 for Different L/r_c and m_I Values..	71
18	Suspension-Rod Force X_2 for Different L/r_c and m_I Values.....	72
19	Suspension-Rod Force X_3 for Different L/r_c and m_I Values.....	73
20	Suspension-Rod Force X_4 for Different L/r_c and m_I Values.....	74
<u>For Horizontal Gap Δ</u>		
21	Bending Moment at Panel Point X_4 for Different Values of L/r_c and m_I for Tie-Girder.....	75
22	Bending Moment at Crown for Different Values of L/r_c and m_I for Arch.....	76
23	Horizontal Force X_1 for Different L/r_c and m_I Values..	77
24	Suspension-Rod Force X_2 for Different L/r_c and m_I Values.....	78
25	Suspension-Rod Force X_3 for Different L/r_c and m_I Values.....	79
26	Suspension-Rod Force X_4 for Different L/r_c and m_I Values.....	80
27	Flexiglas Model.....	39
28	End Detail of Aluminum Model with Gap.....	39
29	Aluminum Model with Vertical Load.....	40
30	Aluminum Model and Interchangeable Tie Girders.....	41

NOMENCLATURE

The letter symbols in this article are defined where they first appear. Those which appear frequently are listed below for reference.

A_a, A_c, A_g, A_r	cross-sectional areas
E, E_a, E_g, E_r	moduli of elasticity
F	horizontal force (external)
H, H_o	horizontal components of arch thrust
I, I_a, I_c, I_g	moments of inertia
K	a constant
L	span length between supports
M, M', M_a, M_g	bending moments
N, N'	axial forces
P, P_l	loads (external)
U	strain energy
X_l, X_i	unknown forces or moments (internal)
a_i, a_n	Fourier constants
h	rise at crown
h_i	height of arch at i^{th} suspension rod
k	$\frac{x}{L}$
m_g	$\frac{A_g E_g}{A_c E_a}$
m_I	$\frac{I_g E_g}{I_c E_a}$
m_r	$\frac{A_r E_r}{A_c E_a}$
q	membrane force along the span length
r_c, r_g	radii of gyration

NOMENCLATURE (CONT'D)

$\alpha_F, \alpha_G, \alpha_P$	constants
β_F	constant
δ_H, δ_{OH}	horizontal movements of arch at support
ϕ	slope along centerline of arch rib
Δ, Δ_G	initial horizontal gaps between arch and girder
Δ_q	vertical deflection of arch due to membrane force q
Δ_s	length along centerline of arch
Δx	length along girder or horizontal projection of
$\Delta X_1, \Delta X_1$	relative deflections or rotations at X_1, X_1

Subscripts

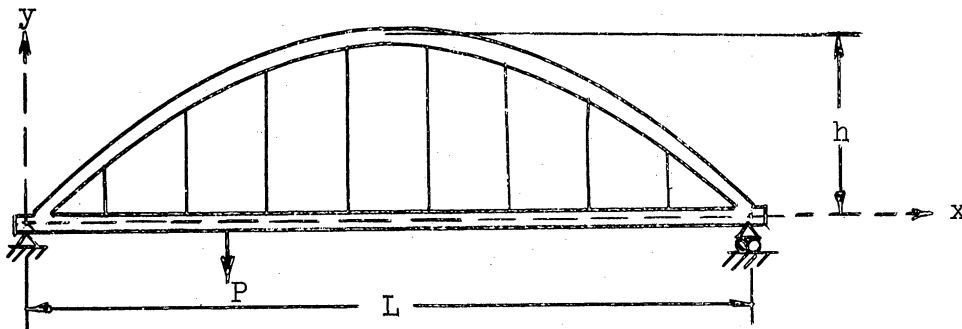
a	arch rib
c	crown
g	tie girder
r	suspension rod

I. INTRODUCTION

The purpose of this study is the analysis of the prestressed bowstring arch of which the structural system is highly indeterminate. With the ever-increasing use of prestressed concrete in construction, such an investigation is important to the structural designer.

Bowstring arches are often used when the abutments are not reliable for thrust, and when maximum clearance under the structure is desired.

As used in this study, the term "bowstring arch" denotes a combination of an arch rib with a tie girder. These elements are fastened to one another at the supports and connected to each other through equally spaced vertical suspension rods as shown in the diagram below.



Any load on the tie girder is resisted jointly both by the tie girder and the arch rib. In addition to its flexural action, the tie girder also resists the horizontal thrust of the arch.

This type of interaction which involves the flexural resistance of the girder makes the structure highly indeterminate. The exact redundancy will depend on the type of end connections and also on the number of suspension rods. Because of the extensibility of the suspension rods and the deflection of the arch rib, the tie girder resembles a continuous beam on elastic supports to a considerable degree.

The general practice is to simplify the above conditions by assuming that the suspension rods are inextensible, that the moment of inertia of the arch rib is small compared to that of the tie girder, i.e., the arch provides no bending resistance at all, and that the arch and the tie girder are pin-connected, although the latter may or may not be the case. Thus no matter how many suspension rods are used, the structure has only one redundant, that is, the horizontal reaction X_1 of the arch rib.

When the rigidity of the arch is considered, there is an additional degree of indeterminacy for every suspension rod. Hence, a bowstring arch with six suspension rods will have seven redundants for pin-connected ends and nine redundants when the ends are fixed.

The bowstring-arch structure differs from the usual tied arch in that the moment of inertia of the tie girder is many times greater than that of the arch rib. As a result, the total bending moment taken by the rib and girder together is divided between these two elements, the major part being resisted by the girder.

According to J. M. Garrelts⁽¹⁾ his design of St. Georges Tied Arch Span at St. Georges, Delaware, is the first to introduce

the bowstring-arch design to America. In his design, he assumes that the rib and the girder are hinged at the supports, and that the hangers are inextensible and resist axial forces only. For his first approximation he considers the arch rib to resist no bending moment, and subjected only to compression. Hence, the horizontal component H of the arch rib compression is the only redundant, and using the principle of virtual work, he determines its value. He then proceeds with his design and obtains preliminary sections to be used as a basis for his more accurate analysis.

Since the total bending moment (simple beam moment minus $H \cdot y$) at a section is actually taken by both the rib and the girder, Garrelts sets the second derivative of the vertical component of the arch-rib deflection equal to the second derivative of the girder deflection to find the right proportion for each. Thus he obtains the proper proportion of each and a more accurate formula for the value of H . A partial summary of his work is found in the Appendix.

Some seven years later, in 1948, in Budapest, Professor Viktor Haviar came out with his design.⁽²⁾ Were it not for the introduction of the extensibility of the suspension rods into his derivation, his work would be identical with Garrelt's. Unfortunately, however, his model analysis was not suitable for studying this point.

In 1954 Drs. S. Chandrangsou and S. R. Sparkes described a procedure called "The Method of Influence Coefficients"⁽³⁾ to design the bowstring arch. Here the relative displacement of the sides of every "cut" is expressed in terms of each force or moment applied, and as

many elastic equations are obtained as there are redundants in the system. To determine the coefficients in these equations, the principle of virtual work is used. A "null"-system bowstring arch is introduced to avoid seriously affecting the accuracy of the moment calculations. By transforming the elastic equations and calculating the differences, the bending moments are obtained directly.

Chandrangsu and Sparkes also describe the membrane-analogy method for a fixed-end bowstring arch by considering only the flexural strain energy in the system. However, a more complete and more accurate analysis must also consider the axial strain energy. This is especially important for low values of the slenderness ratio as well as prestressing forces. By slenderness ratio here is meant the span length of the bowstring arch divided by the radius of gyration of the arch rib at the crown around the horizontal axis.

The present study utilizes the strain-energy method to analyze the bowstring arch, and then applies this analysis to a bowstring arch which is pin-connected at each end and has six suspension rods equally spaced along its length. Five different tie-girder-to-arch-stiffness ratios have been used to each of ten different slenderness ratios of the arch. In addition, the effect of varying the cross-sectional area of the tie girder to the arch and the change in the suspension rod area were studied.

The results of the above calculations have been used to plot influence line diagrams and graphs with a view to using them in preliminary design work. Were it not for the electronic computing facilities of The University of Michigan, it would have been next to impossible to

obtain all these results; there were some 420 sets of seven equations with seven unknowns to be solved.

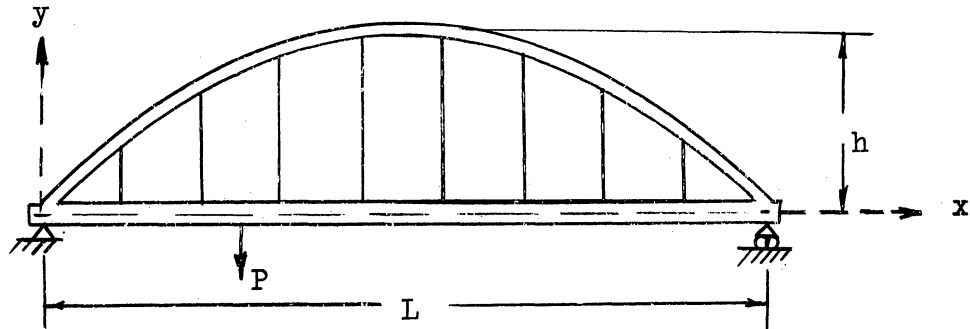
To make the analysis sufficiently general so that it may apply to any desired number of suspension rods and to all rise-to-span ratios, the membrane-analogy method has also been introduced here. (See Chapter III). This assumes that the arch and the tie girder are connected by an inextensible membrane, and the vertical force in the membrane is expressed as a single continuous function. To find the force in any suspension rod, one has only to integrate this force between the proper limits along the length. The accuracy of this method will depend on the number of suspension rods used. However, even with six suspension rods, the results are so accurate that its use for preliminary design work is recommended.

To verify the correctness of the various theories used in this study, an experiment was performed on an aluminum model of 49 in. length with two different tie girders. The model was properly instrumented with strain gauges, and gauges to measure the deflection. The experimental results thus obtained were in good harmony with those of the theories.

In case the reader has been wondering why the word prestressing has not occurred thus far, it should be emphasized that the analysis is one of determining redundant forces even when the forces applied are those of prestressing. This point will be clarified in the detailed study of the analytical and experimental results presented later. In this discussion, prestressing is regarded as a condition rather than the analysis itself.

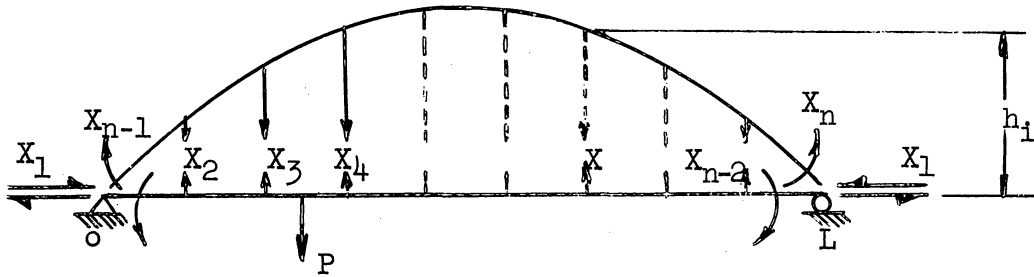
II. THE STRAIN-ENERGY METHOD

Derivation of the Equation for Bowstring Arch Having Any Number of Suspension Rods



The above diagram shows a fixed-end bowstring arch with equally spaced vertical suspension rods. To analyze this bowstring arch, "cuts" or "hinges", as the case may be, are imagined to be inserted at suitable places in the structure to make it statically determinate (see diagram below). Next, moments and forces are applied to both sides of these "cuts" or "hinges" to restore the structure to its initial condition. The total strain energy U , which is a function of all the forces and moments acting on the structure, can now be expressed in terms of all these forces and moments.

The derivative of this energy U with respect to any one force (or moment) will give the deflection (or the rotation) in the direction of that force (or moment). Hence one can get as many elastic continuity equations from U as there are unknowns in the structure. Since the relative deflection or rotation between the two faces of a "cut" is zero or a predetermined quantity, these equations can be solved simultaneously and the desired results are obtained.



The above is in accordance with Castigliano's theorem which states that, when a structure is acted upon by an equilibrated force system, the derivative of the total strain energy U in the structure with respect to any force gives the displacement in the direction of that force.

The unknown forces and the bending moments to restore the structure to its original condition are $X_1, X_2, X_3, \dots, X_n$ as seen in the above diagram. Let M and N denote, respectively, the bending moment and the axial force on the "cut" structure produced by the externally applied loads, say P ; and let M' and N' be the bending moment and the axial force caused by the unknown forces $X_1, X_2, X_3, \dots, X_n$. The total strain energy (neglecting shear and torsion) is

$$\begin{aligned}
 U = & \int_0^L \frac{(M_a + M'_a)^2}{2E_a I_a} ds + \int_0^L \frac{(N_a + N'_a)^2}{2E_a A_a} ds + \int_0^L \frac{(M_g + M'_g)^2}{2E_g I_g} dx \\
 & + \int_0^L \frac{(N_g + N'_g)^2}{2E_g A_g} dx + \sum_{i=2}^{(n-2)} \frac{(X_i)^2 h_i}{2E_r A_r} \quad (2.1)
 \end{aligned}$$

where subscripts "a", "g" and "r" stand, respectively, for the arch rib, tie girder, and suspension rod. The relative deflection or rotation at the i-th "cut" is

$$\frac{\partial U}{\partial X_i} = \Delta X_i$$

which, by means of Equation (2.1), can be expressed in the form

$$\begin{aligned} \Delta X_i = & \int_0^L \frac{(M_a + M'_a) \frac{\partial M'_a}{\partial X_i}}{E_a I_a} ds + \int_0^L \frac{(N_a + N'_a) \frac{\partial N'_a}{\partial X_i}}{E_a A_a} ds \\ & + \int \frac{(M_g + M'_g) \frac{\partial M'_g}{\partial X_i}}{E_g I_g} dx + \int \frac{(N_g + N'_g) \frac{\partial N'_g}{\partial X_i}}{E_g A_g} dx + \sum_{i=2}^{(n-2)} \frac{X_i h_i}{E_r A_r} \quad (2.2) \end{aligned}$$

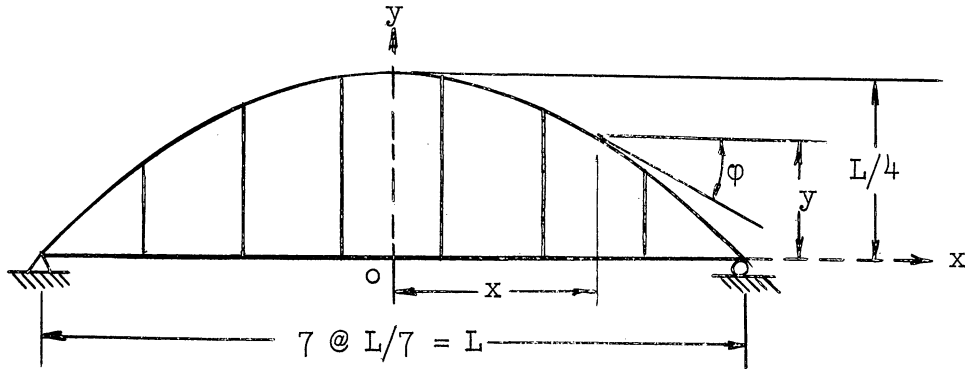
If, now the summation is used for the integration, the expression for ΔX_i becomes:

$$\begin{aligned} \Delta X_i = & \sum_0^L \frac{(M_a + M'_a) \frac{\partial M'_a}{\partial X_i}}{E_a I_a} \Delta s + \sum_0^L \frac{(N_a + N'_a) \frac{\partial N'_a}{\partial X_i}}{E_a A_a} \Delta s + \sum_0^L \frac{(M_g + M'_g) \frac{\partial M'_g}{\partial X_i}}{E_g I_g} \Delta x \\ & + \sum_0^L \frac{(N_g + N'_g) \frac{\partial N'_g}{\partial X_i}}{E_g A_g} \Delta x + \sum_{i=2}^{(n-2)} \frac{X_i h_i}{E_r A_r} \quad (2.3) \end{aligned}$$

Equation (2.3) gives "n" independent equations as "i" assumes values of 1, 2, 3, ..., n, respectively, i.e., one equation per "cut". Thus one gets as many equations as there are unknowns in the system. If there is no initial lack of fit of members, (ΔX_i) s are equal to zero. These "n" equations now can be solved simultaneously and the values of (X_i) s are obtained. Once the unknown forces are determined, finding the actual bending moment, the axial forces, and the shear at any section in the structure is a simple matter.

Solution of Hinged-End Bowstring Arch Having Six Suspension Rods

The arch being studied is parabolic in form and has the dimensions shown in the diagram below. For a 1 to 4 rise-to-span ratio,



the equation of the center line of the arch with its origin at mid point of the tie-girder is

$$y = -\frac{x^2}{L} + \frac{L}{4} \tag{2.4}$$

Further, the cross-sectional area of the arch A_a and the length along the center line of arch Δs_a are assumed, respectively, to vary according to equations

and

$$\left. \begin{aligned} A_a &= A_c \sec \phi \\ \Delta s_a &= \Delta s_c \sec \phi = \Delta x \sec \phi \end{aligned} \right\} \tag{2.5}$$

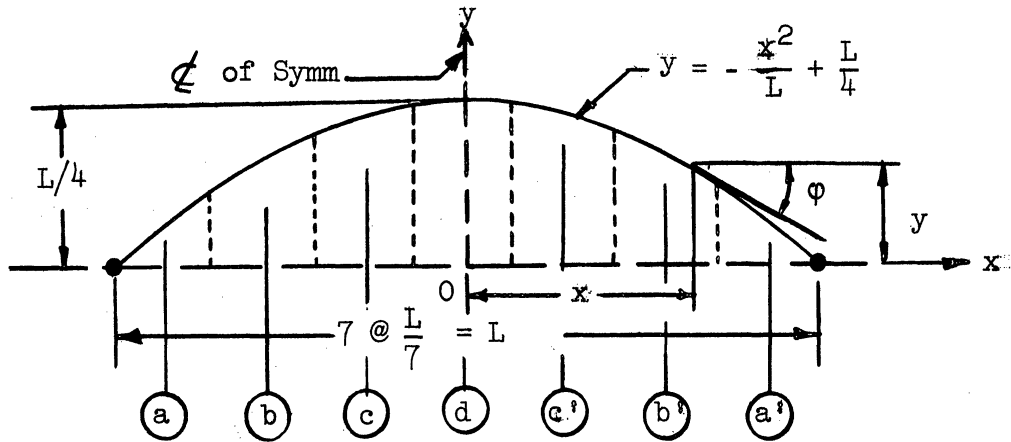
where the subscript c denotes crown; and taking the width of the arch to be constant throughout, the moment of inertia of the arch is given by

$$I_a = I_c \sec^3 \phi \tag{2.6}$$

To evaluate Equation (2.3), four tables have been prepared. Table I is the tabulated result of Equation (2.4) and its derivative. Tables II, III, and IV show all the forces, acting on the structure,

TABLE I

VALUES OF EQUATION (2.4), (ARCH RIB CENTERLINE) AND ITS DERIVATIVE



Point	x	y	$\frac{dy}{dx} = \tan \phi$	ϕ	$\cos \phi$
d	0	0.25000 · L	0	0	1
	1 · L/14	0.24490 · L	0.14286	8° 08'	.98994
c'	2 · L/14	0.22959 · L	0.28571	15° 57'	.96150
	3 · L/14	0.20408 · L	0.42857	23° 12'	.91914
b'	4 · L/14	0.16837 · L	0.57143	29° 45'	.86820
	5 · L/14	0.12245 · L	0.71429	35° 32'	.81378
a'	6 · L/14	0.06633 · L	0.85714	40° 36'	.75927
	7 · L/14	0	1	45° 00'	.70711

TABLE II

BENDING MOMENTS AND AXIAL FORCES
WITH PARTIAL DERIVATIVES IN ARCH


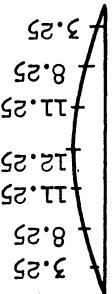

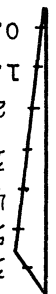

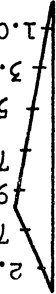
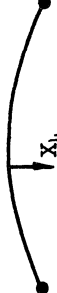


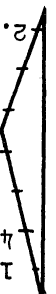

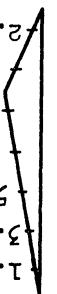

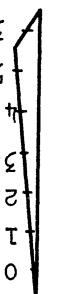
Load	Mult. Factor for $(M_B + M_A)$ & $\frac{\partial M_B}{\partial X_1}$ & $\frac{\partial M_A}{\partial X_1}$		Mult. Factor for $\frac{I_X}{EAC}$ & $\frac{I_X}{EAC}$		Mult. Factor for N_B & N_A & $\frac{\partial N_B}{\partial X_1}$ & $\frac{\partial N_A}{\partial X_1}$						
	$(M_B + M_A)$	$\frac{\partial M_B}{\partial X_1}$ & $\frac{\partial M_A}{\partial X_1}$	$(M_B + M_A)$	$\frac{I_X}{EAC}$ & $\frac{I_X}{EAC}$		N_B & N_A	$\frac{\partial N_B}{\partial X_1}$ & $\frac{\partial N_A}{\partial X_1}$				
		X_1	X_1	$\frac{64}{\pi}$	$\frac{64}{\pi}$	X_1	$\frac{64}{\pi}$	$\frac{64}{\pi}$	$\frac{I_X}{EAC}$ & $\frac{I_X}{EAC}$	X_1	1
		X_2	X_2	$\frac{64}{\pi}$	$\frac{64}{\pi}$	X_2	$\frac{64}{\pi}$	$\frac{64}{\pi}$	$\frac{I_X}{EAC}$ & $\frac{I_X}{EAC}$	X_2	1
		X_3	X_3	$\frac{64}{\pi}$	$\frac{64}{\pi}$	X_3	$\frac{64}{\pi}$	$\frac{64}{\pi}$	$\frac{I_X}{EAC}$ & $\frac{I_X}{EAC}$	X_3	1
		X_4	X_4	$\frac{64}{\pi}$	$\frac{64}{\pi}$	X_4	$\frac{64}{\pi}$	$\frac{64}{\pi}$	$\frac{I_X}{EAC}$ & $\frac{I_X}{EAC}$	X_4	1
		X_5	X_5	$\frac{64}{\pi}$	$\frac{64}{\pi}$	X_5	$\frac{64}{\pi}$	$\frac{64}{\pi}$	$\frac{I_X}{EAC}$ & $\frac{I_X}{EAC}$	X_5	1
		X_6	X_6	$\frac{64}{\pi}$	$\frac{64}{\pi}$	X_6	$\frac{64}{\pi}$	$\frac{64}{\pi}$	$\frac{I_X}{EAC}$ & $\frac{I_X}{EAC}$	X_6	1
		X_7	X_7	$\frac{64}{\pi}$	$\frac{64}{\pi}$	X_7	$\frac{64}{\pi}$	$\frac{64}{\pi}$	$\frac{I_X}{EAC}$ & $\frac{I_X}{EAC}$	X_7	1

TABLE IV
 AXIAL FORCES WITH PARTIAL
 DERIVATIVES IN SUSPENSION-RODS

Load	x_i & $\frac{\partial x_i}{\partial x_i}$	Mult. Factor for x_i	$\frac{\partial x_i}{\partial x_i}$
	(1) 0 0 0 0 0	- x2	-1
	0 (1) 0 0 0 0	- x3	-1
	0 0 (1) 0 0 0	- x4	-1
	0 0 0 (1) 0 0	- x5	-1
	0 0 0 0 (1) 0	- x6	-1
	0 0 0 0 0 (1)	- x7	-1
	7 @ L/7 = L		

and the bending moments successively produced in the arch and in the tie girder by all the redundants X_1, X_2, \dots, X_7 and the external forces $P_1, P_2, P_3,$ and P_4 .

With the help of these tables, and making the following substitutions, i.e., letting

$$m_g = \frac{A_g E_g}{A_c E_a}$$

$$m_r = \frac{A_r E_r}{A_c E_a}$$

$$m_I = \frac{I_g E_g}{I_c E_a}$$

and by recognizing that $(L/r_c)^{-2}$ is identical to $I_c/L^2 A_c$, and that

$\Delta X_1, \Delta X_2, \dots, \Delta X_7$ are all equal to zero, a set of seven equations

[Equation (2.7)]* is obtained for solving the values of X_1, X_2, \dots, X_7 .

The numerical values of X_1, X_2, \dots, X_7 of Equation (2.7) depend no doubt on the external load, $L/r_c, m_g, m_r$ and m_I . Once these parameters are known, X_1, X_2, \dots, X_7 can be determined, and one can now proceed to find the bending moments as well as the shearing and the axial forces along the entire structure, and thus design the bowstring arch.

For additional prestressing of the tie girder, whenever desirable, a specified initial (vertically restrained) horizontal gap Δ is provided between the ends of the arch and the tie girder. A horizontal force X_1 , just large enough to close this gap completely, is applied next. Since there is a relative motion now between the ends of the arch and the tie girder, a different set of equations must be obtained. This is done by satisfying the new geometric boundary conditions and by setting all the

* The detailed calculation of ΔX_1 as a sample may be found in Appendix B.

$$\Delta X_1 = 0$$

$$(i) \quad [498.8567 + 13228.3095 \left(\frac{L}{r_c}\right)^{-2} + 16807 \times \frac{1}{m_g} \times \left(\frac{L}{r_c}\right)^{-2}]X_1 + [165.7657 - 1186.3341 \left(\frac{L}{r_c}\right)^{-2}]X_2 + [303.2085 - 2220.6849 \left(\frac{L}{r_c}\right)^{-2}]X_3 \\ + [382.4850 - 2855.2692 \left(\frac{L}{r_c}\right)^{-2}]X_4 + [382.4850 - 2855.2692 \left(\frac{L}{r_c}\right)^{-2}]X_5 + [303.2085 - 2220.6849 \left(\frac{L}{r_c}\right)^{-2}]X_6 + [165.7657 - 1186.3341 \left(\frac{L}{r_c}\right)^{-2}]X_7 \\ + 16807 \frac{P_1}{m_g} \left(\frac{L}{r_c}\right)^{-2} = 0$$

$$\Delta X_2 = 0$$

$$(ii) \quad [165.7656 - 1186.3341 \left(\frac{L}{r_c}\right)^{-2}]X_1 + [66.5788 + 799.2929 \left(\frac{L}{r_c}\right)^{-2} + 80.50 \frac{1}{m_I} + 2058.8575 \frac{1}{m_r} \left(\frac{L}{r_c}\right)^{-2}]X_2 + [112.5944 + 642.7477 \left(\frac{L}{r_c}\right)^{-2} + 131.25 \frac{1}{m_I}]X_3 \\ + [129.5393 - 544.5468 \left(\frac{L}{r_c}\right)^{-2} + 147.00 \frac{1}{m_I}]X_4 + [119.6737 + 472.2767 \left(\frac{L}{r_c}\right)^{-2} + 134.75 \frac{1}{m_I}]X_5 + [89.4689 + 374.0758 \left(\frac{L}{r_c}\right)^{-2} + 101.50 \frac{1}{m_I}]X_6 \\ + [47.2175 + 217.5306 \left(\frac{L}{r_c}\right)^{-2} + 54.25 \frac{1}{m_I}]X_7 - [80.50 \frac{P_2}{m_I} + 131.25 \frac{P_3}{m_I} + 147.00 \frac{P_4}{m_I}] = 0$$

$$\Delta X_3 = 0$$

$$(iii) \quad [303.2085 - 2220.6849 \left(\frac{L}{r_c}\right)^{-2}]X_1 + [112.5944 + 642.7477 \left(\frac{L}{r_c}\right)^{-2} + 131.25 \frac{1}{m_I}]X_2 + [200.3580 + 981.2887 \left(\frac{L}{r_c}\right)^{-2} + 227.50 \frac{1}{m_I} + 3430.3087 \frac{1}{m_r} \left(\frac{L}{r_c}\right)^{-2}]X_3 \\ + [239.2140 + 845.8723 \left(\frac{L}{r_c}\right)^{-2} + 266.00 \frac{1}{m_I}]X_4 + [224.4488 + 762.3175 \left(\frac{L}{r_c}\right)^{-2} + 248.50 \frac{1}{m_I}]X_5 + [169.0053 + 626.6610 \left(\frac{L}{r_c}\right)^{-2} + 189.00 \frac{1}{m_I}]X_6 \\ + [89.4689 + 374.0758 \left(\frac{L}{r_c}\right)^{-2} + 101.50 \frac{1}{m_I}]X_7 - [131.25 \frac{P_2}{m_I} + 227.50 \frac{P_3}{m_I} + 266.00 \frac{P_4}{m_I}] = 0$$

$$\Delta X_4 = 0$$

$$(iv) \quad [382.2850 - 2855.2692 \left(\frac{L}{r_c}\right)^{-2}]X_1 + [129.5393 + 544.5468 \left(\frac{L}{r_c}\right)^{-2} + 147.00 \frac{1}{m_I}]X_2 + [239.2140 + 845.8723 \left(\frac{L}{r_c}\right)^{-2} + 266.00 \frac{1}{m_I}]X_3 \\ + [300.7027 + 912.8602 \left(\frac{L}{r_c}\right)^{-2} + 329.00 \frac{1}{m_I} + 4116.0343 \frac{1}{m_r} \left(\frac{L}{r_c}\right)^{-2}]X_4 + [293.0846 + 876.3650 \left(\frac{L}{r_c}\right)^{-2} + 320.25 \frac{1}{m_I}]X_5 \\ + [224.4488 + 762.3175 \left(\frac{L}{r_c}\right)^{-2} + 248.50 \frac{1}{m_I}]X_6 + [119.2637 + 472.2767 \left(\frac{L}{r_c}\right)^{-2} + 134.75 \frac{1}{m_I}]X_7 - [147.00 \frac{P_2}{m_I} + 266.00 \frac{P_3}{m_I} + 329.00 \frac{P_4}{m_I}] = 0$$

$$\Delta X_5 = 0$$

$$(v) \quad [382.4850 - 2855.2692 \left(\frac{L}{r_c}\right)^{-2}]X_1 + [119.6737 + 472.2767 \left(\frac{L}{r_c}\right)^{-2} + 134.75 \frac{1}{m_I}]X_2 + [224.4488 + 762.3175 \left(\frac{L}{r_c}\right)^{-2} + 248.50 \frac{1}{m_I}]X_3 \\ + [293.0846 + 876.3650 \left(\frac{L}{r_c}\right)^{-2} + 320.25 \frac{1}{m_I}]X_4 + [300.7027 + 912.8602 \left(\frac{L}{r_c}\right)^{-2} + 329.00 \frac{1}{m_I} + 4116.0343 \frac{1}{m_r} \left(\frac{L}{r_c}\right)^{-2}]X_5 \\ + [239.2140 + 845.8723 \left(\frac{L}{r_c}\right)^{-2} + 266.00 \frac{1}{m_I}]X_6 + [129.5393 + 544.5468 \left(\frac{L}{r_c}\right)^{-2} + 147.00 \frac{1}{m_I}]X_7 - [134.75 \frac{P_2}{m_I} + 248.50 \frac{P_3}{m_I} + 320.25 \frac{P_4}{m_I}] = 0$$

$$\Delta X_6 = 0$$

$$(vi) \quad [303.2085 - 2220.6849 \left(\frac{L}{r_c}\right)^{-2}]X_1 + [89.4689 + 374.0758 \left(\frac{L}{r_c}\right)^{-2} + 101.50 \frac{1}{m_I}]X_2 + [169.0053 + 626.6610 \left(\frac{L}{r_c}\right)^{-2} + 189.00 \frac{1}{m_I}]X_3 \\ + [224.4488 + 762.3175 \left(\frac{L}{r_c}\right)^{-2} + 248.50 \frac{1}{m_I}]X_4 + [239.2140 + 845.8723 \left(\frac{L}{r_c}\right)^{-2} + 266.00 \frac{1}{m_I}]X_5 + [200.3580 + 981.2887 \left(\frac{L}{r_c}\right)^{-2} + 227.50 \frac{1}{m_I} + 3430.3087 \frac{1}{m_r} \left(\frac{L}{r_c}\right)^{-2}]X_6 \\ + [112.5944 + 642.7477 \left(\frac{L}{r_c}\right)^{-2} + 131.25 \frac{1}{m_I}]X_7 - [101.50 \frac{P_2}{m_I} + 189.00 \frac{P_3}{m_I} + 248.50 \frac{P_4}{m_I}] = 0$$

$$\Delta X_7 = 0$$

$$(vii) \quad [165.7656 - 1186.3341 \left(\frac{L}{r_c}\right)^{-2}]X_1 + [47.2175 + 217.5306 \left(\frac{L}{r_c}\right)^{-2} + 54.25 \frac{1}{m_I}]X_2 + [89.4689 + 374.0758 \left(\frac{L}{r_c}\right)^{-2} + 101.50 \frac{1}{m_I}]X_3 \\ + [119.6737 + 472.2767 \left(\frac{L}{r_c}\right)^{-2} + 134.75 \frac{1}{m_I}]X_4 + [129.5393 + 544.5468 \left(\frac{L}{r_c}\right)^{-2} + 147.00 \frac{1}{m_I}]X_5 + [112.5944 + 642.7477 \left(\frac{L}{r_c}\right)^{-2} + 131.25 \frac{1}{m_I}]X_6 \\ + [66.5788 + 799.2929 \left(\frac{L}{r_c}\right)^{-2} + 80.50 \frac{1}{m_I} + 2058.8575 \frac{1}{m_r} \left(\frac{L}{r_c}\right)^{-2}]X_7 - [54.25 \frac{P_2}{m_I} + 101.50 \frac{P_3}{m_I} + 134.75 \frac{P_4}{m_I}] = 0$$

(2.7)

external forces P_1 , P_2 , P_3 , and P_4 equal to zero.

Thus for the case with a gap, Equation (2.7) becomes Equation (2.8).

Influence Line Diagrams and Graphs

Bending-moment and axial-force diagrams have been prepared from Equations (2.7) and (2.8) for various parameters and are shown in Appendix C. (See Figure 3 through 26). These will facilitate the preliminary design because the graphs can be read directly and bending moments and axial forces can be obtained at a glance. In all these diagrams the parameters m_g and m_r were held constant at 2.0 and 0.1, respectively, while L/r_c varied from 25 to 300 and m_I from 2.5 to 20. Thus they cover a wide range of values.

The bending moments and the axial forces, for the vertical loads, are drawn as influence lines. For the horizontal loads the bending moments and the axial forces are drawn as a function of m_I for different values of L/r_c or vice versa.

To use Figures 21 through 26, one must first find the particular value of Δ for which the graphs are prepared and then by direct proportion obtain the values wanted. To find the particular gap Δ , set

$$\Delta = KL$$

where $K = 5000/E_a A_c$. Thus, once $E_a A_c$ is known, Δ can easily be determined.

The effects of varying the parameters m_g and m_r on the bending moments are shown in Figures 3 and 4.

$$\Delta X_1 = \Delta$$

$$(i) \quad [498.8567 + 13228.3095 \left(\frac{L}{r_c}\right)^{-2}]X_1 + [165.7657 - 1186.3341 \left(\frac{L}{r_c}\right)^{-2}]X_2 + [303.2085 - 2220.6849 \left(\frac{L}{r_c}\right)^{-2}]X_3 + [382.4850 - 2855.2692 \left(\frac{L}{r_c}\right)^{-2}]X_4 + [382.4850 - 2855.2692 \left(\frac{L}{r_c}\right)^{-2}]X_5 + [303.2085 - 2220.6849 \left(\frac{L}{r_c}\right)^{-2}]X_6 + [165.7657 - 1186.3341 \left(\frac{L}{r_c}\right)^{-2}]X_7 = \Delta \frac{7}{1^3} \frac{E_0 I_c}{L^3}$$

$$\Delta X_2 = 0$$

$$(ii) \quad [165.7656 - 1186.3341 \left(\frac{L}{r_c}\right)^{-2}]X_1 + [66.5788 + 799.2929 \left(\frac{L}{r_c}\right)^{-2} + 80.50 \frac{1}{m_1} + 2058.8575 \frac{1}{m_1} \left(\frac{L}{r_c}\right)^{-2}]X_2 + [112.5944 + 642.7477 \left(\frac{L}{r_c}\right)^{-2} + 131.25 \frac{1}{m_1}]X_3 + [129.5393 + 544.5468 \left(\frac{L}{r_c}\right)^{-2} + 147.00 \frac{1}{m_1}]X_4 + [119.6737 + 472.2767 \left(\frac{L}{r_c}\right)^{-2} + 134.75 \frac{1}{m_1}]X_5 + [89.4689 + 374.0758 \left(\frac{L}{r_c}\right)^{-2} + 101.50 \frac{1}{m_1}]X_6 + [47.2175 + 217.5306 \left(\frac{L}{r_c}\right)^{-2} + 54.25 \frac{1}{m_1}]X_7 = 0$$

$$\Delta X_3 = 0$$

$$(iii) \quad [303.2085 - 2220.6849 \left(\frac{L}{r_c}\right)^{-2}]X_1 + [112.5944 + 642.7477 \left(\frac{L}{r_c}\right)^{-2} + 131.25 \frac{1}{m_1}]X_2 + [200.3580 + 981.2887 \left(\frac{L}{r_c}\right)^{-2} + 227.50 \frac{1}{m_1} + 3430.3087 \frac{1}{m_1} \left(\frac{L}{r_c}\right)^{-2}]X_3 + [239.2140 + 845.8723 \left(\frac{L}{r_c}\right)^{-2} + 266.00 \frac{1}{m_1}]X_4 + [224.4488 + 762.3175 \left(\frac{L}{r_c}\right)^{-2} + 248.50 \frac{1}{m_1}]X_5 + [169.0053 + 626.6610 \left(\frac{L}{r_c}\right)^{-2} + 189.00 \frac{1}{m_1}]X_6 + [89.4689 + 374.0758 \left(\frac{L}{r_c}\right)^{-2} + 101.50 \frac{1}{m_1}]X_7 = 0$$

$$\Delta X_4 = 0$$

$$(iv) \quad [382.4850 - 2855.2692 \left(\frac{L}{r_c}\right)^{-2}]X_1 + [129.5393 + 544.5468 \left(\frac{L}{r_c}\right)^{-2} + 147.00 \frac{1}{m_1}]X_2 + [239.2140 + 845.8723 \left(\frac{L}{r_c}\right)^{-2} + 266.00 \frac{1}{m_1}]X_3 + [300.7027 + 912.8602 \left(\frac{L}{r_c}\right)^{-2} + 329.00 \frac{1}{m_1} + 4116.0343 \frac{1}{m_1} \left(\frac{L}{r_c}\right)^{-2}]X_4 + [293.0846 + 876.3650 \left(\frac{L}{r_c}\right)^{-2} + 320.25 \frac{1}{m_1}]X_5 + [224.4488 + 762.3175 \left(\frac{L}{r_c}\right)^{-2} + 248.50 \frac{1}{m_1}]X_6 + [119.6737 + 472.2767 \left(\frac{L}{r_c}\right)^{-2} + 134.75 \frac{1}{m_1}]X_7 = 0$$

(2.8)

$$\Delta X_5 = 0$$

$$(v) \quad [382.4850 - 2855.2692 \left(\frac{L}{r_c}\right)^{-2}]X_1 + [119.6737 + 472.2767 \left(\frac{L}{r_c}\right)^{-2} + 134.75 \frac{1}{m_1}]X_2 + [224.4488 + 762.3175 \left(\frac{L}{r_c}\right)^{-2} + 248.50 \frac{1}{m_1}]X_3 + [293.0846 + 876.3650 \left(\frac{L}{r_c}\right)^{-2} + 320.25 \frac{1}{m_1} + 4116.0343 \frac{1}{m_1} \left(\frac{L}{r_c}\right)^{-2}]X_4 + [239.2140 + 845.8723 \left(\frac{L}{r_c}\right)^{-2} + 266.00 \frac{1}{m_1}]X_5 + [129.5393 + 544.5468 \left(\frac{L}{r_c}\right)^{-2} + 147.00 \frac{1}{m_1}]X_7 = 0$$

$$\Delta X_6 = 0$$

$$(vi) \quad [303.2085 - 2220.6849 \left(\frac{L}{r_c}\right)^{-2}]X_1 + [89.4689 + 374.0758 \left(\frac{L}{r_c}\right)^{-2} + 101.50 \frac{1}{m_1}]X_2 + [169.0053 + 626.6610 \left(\frac{L}{r_c}\right)^{-2} + 189.00 \frac{1}{m_1}]X_3 + [224.4488 + 762.3175 \left(\frac{L}{r_c}\right)^{-2} + 248.50 \frac{1}{m_1}]X_4 + [239.2140 + 845.8723 \left(\frac{L}{r_c}\right)^{-2} + 266.00 \frac{1}{m_1}]X_5 + [200.3580 + 981.2887 \left(\frac{L}{r_c}\right)^{-2} + 227.50 \frac{1}{m_1} + 3430.3087 \frac{1}{m_1} \left(\frac{L}{r_c}\right)^{-2}]X_6 + [112.5944 + 642.7477 \left(\frac{L}{r_c}\right)^{-2} + 131.25 \frac{1}{m_1}]X_7 = 0$$

$$\Delta X_7 = 0$$

$$(vii) \quad [165.7656 - 1186.3341 \left(\frac{L}{r_c}\right)^{-2}]X_1 + [47.2175 + 217.5306 \left(\frac{L}{r_c}\right)^{-2} + 54.25 \frac{1}{m_1}]X_2 + [89.4689 + 374.0758 \left(\frac{L}{r_c}\right)^{-2} + 101.50 \frac{1}{m_1}]X_3 + [119.6737 + 472.2767 \left(\frac{L}{r_c}\right)^{-2} + 134.75 \frac{1}{m_1}]X_4 + [129.5393 + 544.5468 \left(\frac{L}{r_c}\right)^{-2} + 147.00 \frac{1}{m_1}]X_5 + [112.5944 + 642.7477 \left(\frac{L}{r_c}\right)^{-2} + 131.25 \frac{1}{m_1}]X_6 + [66.5788 + 799.2929 \left(\frac{L}{r_c}\right)^{-2} + 80.50 \frac{1}{m_1} + 2058.8575 \frac{1}{m_1} \left(\frac{L}{r_c}\right)^{-2}]X_7 = 0$$

Sign Convention

Bending-moments producing compression on the upper fibers of the arch rib and the tie girder are considered positive throughout the text.

III. THE MEMBRANE-ANALOGY METHOD

For a Concentrated Vertical Force on the Girder

To simplify the analysis of the hinged-end bowstring arch by the membrane theory, the membrane has been assumed to be inextensible so that the deflections of the arch rib and the tie girder are the same.

The arch is assumed to be of parabolic form

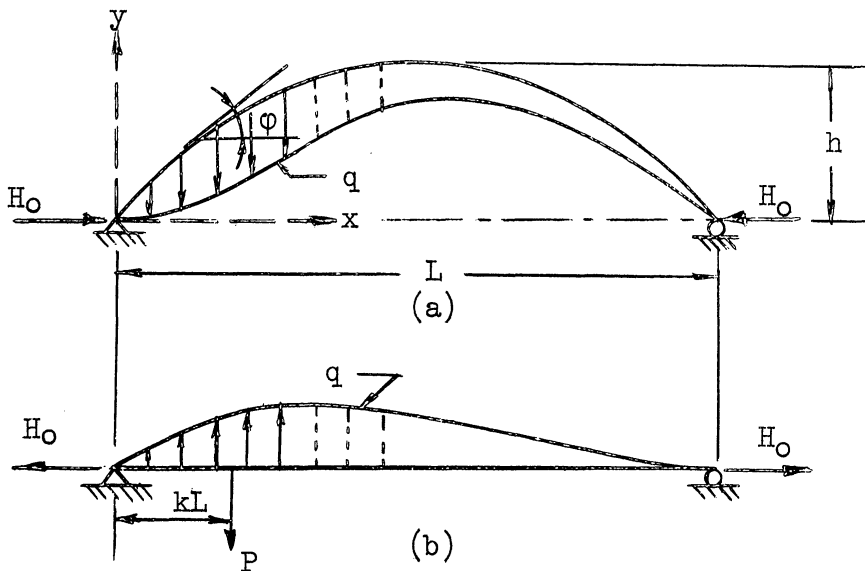
$$y = 4h \left[\left(\frac{x}{L} \right) - \left(\frac{x}{L} \right)^2 \right] \quad (3.1)$$

Moments of inertia and the cross-sectional area of the arch vary, respectively, as

$$I_a = I_c \sec \phi \quad (3.2)$$

$$A_a = A_c \sec \phi$$

Now separate the arch from the girder as shown below.



\$P\$ above is any vertical load applied on the girder. The membrane connecting the arch and the girder is assumed to function in the same

way as an infinite number of suspension rods, and carries a vertical force q of varying intensity along the span length.

The vertical deflection of the arch due to membrane force q , in the preceding diagram may be obtained from the equation:

$$q = EI_a \cos \varphi \frac{d^4 \Delta_q}{dx^4} \quad (3.3)$$

$$M_a^q = EI_a \cos \varphi \frac{d^2 \Delta_q}{dx^2} \quad (3.4)$$

where Δ_q denotes the vertical deflection and M_a^q the bending moment due to the membrane force only.

This deflection can be represented by the Fourier series:

$$\Delta_q = \frac{a_0}{EI_c} + \sum_{n=1}^{\infty} \frac{a_n}{EI_c} \sin \frac{n\pi x}{L} + \sum_{n=1}^{\infty} \frac{b_n}{EI_c} \cos \frac{n\pi x}{L} \quad (3.5)$$

where a_0 , a_n , and b_n denote constants to be determined.

Considering the end conditions of the arch, $\Delta_q = 0$ at $x = 0$ and $x = L$; also $d^2 \Delta_q / dx^2 = 0$ at $x = 0$ and $x = L$; it is convenient to use the simplified form:

$$\Delta_q = \sum_{n=1}^{\infty} \frac{a_n}{EI_c} \sin \frac{n\pi x}{L} \quad (3.6)$$

By successive differentiation of Δ_q and replacing I_a by $I_c \sec \varphi$, the membrane force q and the bending moment M^q are found:

$$M^q = - \sum_{n=1}^{\infty} a_n \left(\frac{n\pi}{L} \right)^2 \sin \frac{n\pi x}{L} \quad (3.7)$$

and

$$q = \sum_{n=1}^{\infty} a_n \left(\frac{n\pi}{L} \right)^4 \sin \frac{n\pi x}{L} \quad (3.8)$$

Equation (3.8) indicates that the membrane force can be regarded as being composed of an infinite number of distributed vertical loads whose magnitudes vary sinusoidally along the span length. It can be expressed to any desired degree of accuracy depending upon the number of terms considered.

The vertical deflection of any point on the arch is equal to that of the point on the girder immediately below it, and in the arch it is the sum of the deflections produced by the horizontal force H_0 , and the membrane force q , that is:

$$\Delta = \Delta_H + \Delta_q \quad (3.9)$$

The deflection due to H_0 is given by:

$$\frac{d^2\Delta_H}{dx^2} = \frac{H_0 y}{EI_c} = \frac{4H_0 h}{EI_c} \left[\frac{x}{L} - \left(\frac{x}{L}\right)^2 \right]$$

integrating and satisfying the end conditions that $\Delta_H = 0$ at $x = 0$ and $x = L$:

$$\Delta_H = -\frac{H_0 h L^2}{3EI_c} \left[\left(\frac{x}{L}\right)^4 - 2\left(\frac{x}{L}\right)^3 + \left(\frac{x}{L}\right) \right] \quad (3.10)$$

Hence from Equations (3.6) and (3.10)

$$\Delta = -\frac{H_0 h L^2}{3EI_c} \left[\left(\frac{x}{L}\right)^4 - 2\left(\frac{x}{L}\right)^3 + \left(\frac{x}{L}\right) \right] + \sum_{n=1}^{\infty} \frac{a_n}{EI_c} \sin \frac{n\pi x}{L} \quad (3.11)$$

and when $x = kL$, the deflection Δ_p under the load P is:

$$\Delta_p = -\frac{H_0 h L^2}{3EI_c} (k^4 - 2k^3 + k) + \sum_{n=1}^{\infty} \frac{a_n}{EI_c} \sin n\pi k \quad (3.12)$$

H_0 and the constants $a_1 \dots a_n$ remain to be determined.

Since the relative horizontal movement on each side of the cut section at H_0 is zero,

$$\delta_H = \delta_{OH} + H_0 \delta_{HH} = 0 \quad (3.13)$$

from which

$$H_0 = - \frac{\delta_{OH}}{\delta_{HH}} \quad (3.14)$$

δ_{OH} and δ_{HH} denote, respectively, the horizontal movement of the arch at H_0 due to the membrane load force q and to the load H_0 taken as unity.

$$\begin{aligned} \bar{\delta}_{OH} &= EI_c \delta_{OH} = -16 \frac{h}{L} \sum_{1 \cdot 3 \cdot 5}^{\infty} a_n \left(\frac{1}{n\pi} \right) \\ \bar{\delta}_{HH} &= EI_c \delta_{HH} = \frac{8}{15} h^2 L \end{aligned}$$

Substituting the above in Equation (3.14) and reducing, we obtain:

$$H_0 = 30 \frac{L}{h} \sum_{1 \cdot 3 \cdot 5}^{\infty} \frac{a_n}{L^3} \frac{1}{n\pi} \quad (3.15)$$

Thus, H_0 can be determined when the Fourier constants are known, and these in turn can be calculated by consideration of the energy in the system. If a small increment da_1 is given to a Fourier coefficient a_1 , there will be a small change in the internal stresses and also a small consequent deformation of the whole system including the load point. To satisfy equilibrium, the change in potential energy in the system must equal the change in work done by the external load.

$$\text{Thus} \quad \frac{\partial U}{\partial a_1} da_1 = P \left(\frac{\partial}{\partial a_1} \Delta P \right) da_1 \quad (3.16)$$

The total potential energy in the system is:

$$U = \int_0^L \frac{M_a^2}{2EI_c} dx + \int_0^L \frac{M_g^2}{2E_g I_g} dx + \int_0^L \frac{(H_o \cos \phi)^2}{2EA_c} dx + \int_0^L \frac{(-H_o)^2}{2E_g A_g} dx \quad (3.17)$$

$$M_a = H_o y - \sum_{n=1}^{\infty} a_n \left(\frac{n\pi}{L}\right)^2 \sin \frac{n\pi x}{L} \quad (3.18)$$

$$\begin{aligned} M_g &= P(1-k)x - \sum_{n=1}^{\infty} a_n \left(\frac{n\pi}{L}\right)^2 \sin \frac{n\pi x}{L} \quad \text{for } 0 \leq x \leq kL \\ &= Pk(L-x) - \sum_{n=1}^{\infty} a_n \left(\frac{n\pi}{L}\right)^2 \sin \frac{n\pi x}{L} \quad \text{for } kL \leq x \leq L \end{aligned} \quad (3.19)$$

From Equation (1)

$$\cos^2 \phi = \left[1 + \frac{16h^2}{L^2} - \frac{64h^2}{L^2} \left(\frac{x}{L}\right) + \frac{64h^2}{L^2} \left(\frac{x}{L}\right)^2 \right]^{-1}$$

and for $L/h = 4$

$$\int_0^L \cos^2 \phi dx = \frac{\pi}{4} L \quad (3.20)$$

Substituting these values in Equation (3.17), and integrating it and

reducing gives

$$\begin{aligned} U &= \frac{1}{2EI_c} \left[\frac{8}{15} H_o^2 h^2 L - \frac{32H_o h}{L} \sum_{n=1}^{\infty} \frac{a_n}{1 \cdot 3 \cdot 5} \frac{1}{n\pi} + \frac{1}{2L^3} \sum_{n=1}^{\infty} a_n^2 (n\pi)^4 + \frac{\pi}{4} H_o^2 r_c^2 L \right] \\ &+ \frac{1}{2m_I EI_c} \left[\frac{P^2 k^2 L^3}{3} (1-k)^2 - 2P \sum_{n=1}^{\infty} a_n \sin (n\pi k) \right. \\ &\left. + \frac{1}{2} \sum_{n=1}^{\infty} \frac{a_n^2}{L^3} (n\pi)^4 + H_o r_g^2 L \right] \quad (3.21) \end{aligned}$$

Substituting for H_0 in the above equation and differentiating with respect to a_1 , we obtain:

$$\begin{aligned} \frac{\partial U}{\partial a_1} = & \frac{1}{2EI_c} \cdot \frac{a_1}{L^3} \left\{ (i\Pi)^4 - \frac{1}{(i\Pi)^2} \left[960 - 1800 \frac{\Pi}{4} \left(\frac{r_c}{h} \right)^2 \right] \right\} \\ & + \frac{1}{2m_I EI_c} \left\{ -2P \sin(i\Pi k) + \frac{a_1}{L^3} \left[(i\Pi)^4 + \frac{1800}{(i\Pi)^2} \left(\frac{r_g}{h} \right)^2 \right] \right\} \end{aligned} \quad (3.22)$$

The change in potential energy in the bowstring arch due to the increment da_1 is:

$$\begin{aligned} \frac{\partial U}{\partial a_1} da_1 = & \frac{1}{2EI_c} \left\langle \frac{a_1}{L^3} \left\{ (i\Pi)^4 - \frac{1}{(i\Pi)^2} \left[960 - 1800 \frac{\Pi}{4} \left(\frac{r_c}{h} \right)^2 \right] \right\} \right. \\ & \left. + \frac{1}{m_I} \left\{ -2P \sin(i\Pi k) + \frac{a_1}{L^3} \left[(i\Pi)^4 + \frac{1800}{(i\Pi)^2} \left(\frac{r_g}{h} \right)^2 \right] \right\} \right\rangle da_1 \end{aligned} \quad (3.23)$$

Substituting for H_0 in Equation (3.12) and differentiating, we obtain:

$$\frac{\partial}{\partial a_1} \Delta_P = \frac{P}{EI_c} \left[-\frac{10}{i\Pi} (k^4 - 2k^3 + k) + \sin(i\Pi k) \right] \quad (3.24)$$

and the work done by P is:

$$P \left(\frac{\partial}{\partial a_1} \Delta_P \right) da_1 = \frac{P}{EI_c} \left[-\frac{10}{i\Pi} (k^4 - 2k^3 + k) + \sin(i\Pi k) \right] da_1 \quad (3.25)$$

The change in work done by P is equal to the change in the potential energy of the system, so equating Equations (3.23) and (3.25) and simplifying gives:

$$a_1 = 2PL^3 \frac{\frac{m_I + 1}{m_I} \sin(i\Pi k) - \frac{10}{i\Pi} (k^4 - 2k^3 + k)}{\frac{m_I + 1}{m_I} (i\Pi)^4 - \frac{120}{(i\Pi)^2} \alpha_P} \quad (3.26)$$

where

$$\alpha_P = 8 - 15 \left[\frac{\Pi}{4} \left(\frac{r_c}{h} \right)^2 + \frac{1}{m_I} \left(\frac{r_g}{h} \right)^2 \right] \quad (3.27)$$

Note that even values of "i" have no effect on H_0 .

The Fourier constants from Equation (3.26) can now be substituted in Equation (3.15) to give H_0 ; Equations (3.7) and (3.8) can be used to give M^q and q , and the bending moments in the arch and tie girder are then given by:

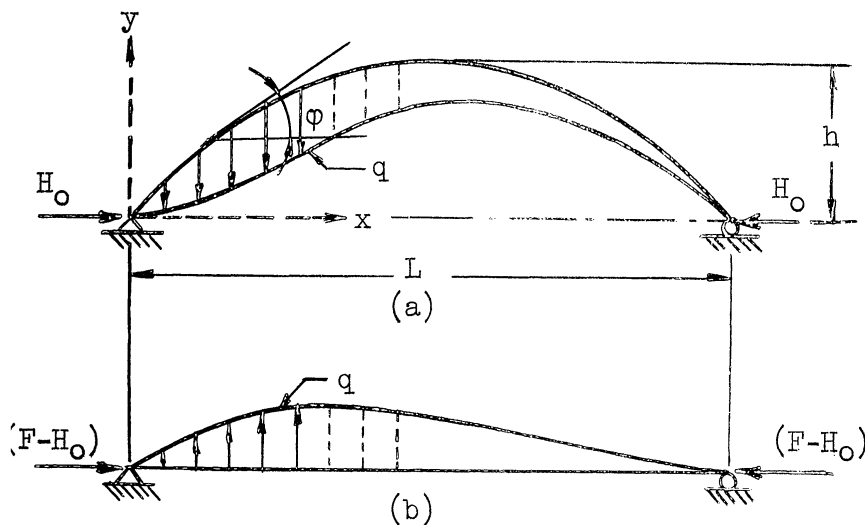
$$M_a = H_0 y - \sum_{n=1}^{\infty} a_n \left(\frac{n\pi}{L}\right)^2 \sin \frac{n\pi x}{L} \quad (3.28)$$

$$M_g = M_P - \sum_{n=1}^{\infty} a_n \left(\frac{n\pi}{L}\right)^2 \sin \frac{n\pi x}{L} \quad (3.29)$$

The suspension-rod forces are given by integrating Equation (3.8) between the proper limits.

For a Prestressing Force F as Shown in the Diagram Below

Since all assumptions for this case are the same as before, Equations (3.1) through (3.8) are valid here as well. The difference is in the application of the external load.



Likewise, the relative horizontal movement on each side of the cut section at H_0 is zero:

$$\delta_H = \delta_{OH} + H_0 \delta_{HH} + (F - H_0) \delta_{GH} = 0 \quad (3.30)$$

from which

$$H_0 = \frac{\delta_{OH} + F\delta_{GH}}{\delta_{GH} - \delta_{HH}} \quad (3.31)$$

denotes the horizontal movement of the arch at H_0 due to a unit load on the tie girder. δ_{OH} and δ_{HH} denote the same as before and

$$\delta_{GH} = -\frac{L}{EA_g}$$

Substituting the values of δ_{OH} , δ_{HH} and δ_{GH} into Equation (3.31) and reducing, we obtain:

$$H_0 = \frac{F \frac{1}{m_g} \left(\frac{r_g}{L}\right)^2 + 16 \frac{h}{L} \sum_{n=1}^{\infty} \frac{a_n}{L^3} \cdot \frac{1}{n\pi}}{\alpha_F} \quad (3.32)$$

where

$$\alpha_F = \frac{8}{15} \left(\frac{h}{L}\right)^2 + \frac{1}{m_g} \left(\frac{r_g}{L}\right)^2$$

Thus H_0 can be determined when the Fourier constants are known; and with the same reasoning as before:

$$\frac{\partial U}{\partial a_i} da_i = F \left(\frac{\partial}{\partial a_i} \Delta_F \right) da_i \quad (3.33)$$

where Δ_F is the horizontal movement of force F . The total potential energy in the system is:

$$U = \int_0^L \frac{M_a^2}{2EI_c} dx + \int_0^L \frac{M_g^2}{2E_g I_g} dx + \int_0^L \frac{(H_0 \cos \varphi)^2}{2E A_c} dx + \int_0^L \frac{(F - H_0)^2}{2E_g A_g} dx \quad (3.34)$$

where

$$M_a = H_o y - \sum_{n=1}^{\infty} a_n \left(\frac{n\pi}{L}\right)^2 \sin \frac{n\pi x}{L}, \quad \text{see Equation (3.18)}$$

$$M_g = - \sum_{n=1}^{\infty} a_n \left(\frac{n\pi}{L}\right)^2 \sin \frac{n\pi x}{L}, \quad \text{see Equation (3.7)} \quad (3.35)$$

and

$$\int_0^L \cos^2 \varphi dx = \frac{\pi}{4} L, \quad \text{see Equation (3.20)}$$

Substituting these in Equation (3.34), and integrating and reducing gives:

$$U = \frac{1}{2EI_c} \left\{ \left[\frac{8}{15} H_o^2 h^2 L - \frac{32H_o h}{L} \sum_{n=1}^{\infty} a_n \frac{1}{n\pi} + \frac{1}{2L^3} \sum_{n=1}^{\infty} a_n^2 (n\pi)^4 \right] \right.$$

$$\left. + \frac{1}{m_I} \cdot \frac{1}{2L^3} \sum_{n=1}^{\infty} a_n^2 (n\pi)^4 + \frac{\pi}{4} H_o^2 r_c^2 L + \frac{(F - H_o)^2}{m_I} r_g^2 L \right\} \quad (3.36)$$

Replacing the value of H_o from Equation (3.32) in (3.36) and differentiating with respect to a_i , we obtain:

$$\frac{\partial U}{\partial a_i} = \frac{1}{2EI_c} \left\langle \frac{a_i}{L^3} \left\{ \frac{h^2}{L^2} \cdot \frac{1}{(i\pi)^2 \alpha_F} \left[\frac{1}{\alpha_F} \left(\frac{4096}{15} \cdot \frac{h^2}{L^2} + \frac{512}{m_I} \frac{r_g^2}{L^2} + 512 \frac{\pi}{4} \cdot \frac{r_c^2}{L^2} \right) \right. \right. \right.$$

$$\left. \left. - 1024 \right] + \frac{m_I + 1}{m_I} (i\pi)^4 \right\} + \frac{8}{m_I} \cdot \frac{r_g^2}{L^2} \cdot \frac{h}{L} \cdot \frac{1}{(i\pi)} \cdot \frac{F}{\alpha_F} \left[\frac{1}{\alpha_F} \left(\frac{32}{15} \cdot \frac{h^2}{L^2} \right. \right.$$

$$\left. \left. + \frac{4}{m_I} \cdot \frac{r_g^2}{L^2} + 4 \frac{\pi}{4} \cdot \frac{r_c^2}{L^2} \right) - 8 \right] \right\rangle \quad (3.37)$$

The change in potential energy in the bowstring arch due to the increment da_i is:

$$\begin{aligned} \frac{\partial U}{\partial a_1} da_1 = \frac{1}{2EI_c} \left\langle \frac{a_1}{L^3} \left\{ \frac{h^2}{L^2} \frac{1}{(i\Pi)^2 \alpha_F} \left[\frac{1}{\alpha_F} \left(\frac{4096}{15} \cdot \frac{h^2}{L^2} + \frac{512}{m_I} \cdot \frac{r_g^2}{L^2} + 512 \frac{\Pi}{4} \cdot \frac{r_c^2}{L^2} \right) \right. \right. \right. \\ \left. \left. \left. - 1024 \right] + \frac{m_I + 1}{m_I} (i\Pi)^4 \right\} + \frac{8}{m_I} \cdot \frac{r_g^2}{L^2} \cdot \frac{h}{L} \cdot \frac{1}{(i\Pi)} \cdot \frac{F}{\alpha_F} \left[\frac{1}{\alpha_F} \left(\frac{32}{15} \cdot \frac{h^2}{L^2} \right. \right. \right. \\ \left. \left. \left. + \frac{4}{m_I} \cdot \frac{r_g^2}{L^2} + 4 \frac{\Pi}{4} \cdot \frac{r_c^2}{L^2} \right) - 8 \right] \right\rangle da_1 \end{aligned} \quad (3.38)$$

The horizontal movement of force F is

$$\Delta_F = C \frac{FL}{EI_c} \quad (3.39)$$

where C is a constant. Differentiating Equation (3.39) with respect to a_1 gives

$$\frac{\partial}{\partial a_1} \Delta_F = 0 \quad (3.40)$$

and the work done by F is:

$$F \left(\frac{\partial}{\partial a_1} \Delta_F \right) da_1 = 0 \quad (3.41)$$

The change in work done by F is equal to the change in the potential energy of the system. Thus, equating Equations (3.38) and (3.41) and reducing gives:

$$a_1 = FL^3 \frac{\frac{8}{(i\Pi)m_I} \left(\frac{r_g}{L} \right)^2 \frac{h}{L} \beta_F}{\frac{m_I+1}{m_I} (i\Pi)^4 \alpha_F - \frac{128}{(i\Pi)^2} \left(\frac{h}{L} \right)^2 \beta_F} \quad (3.42)$$

where

$$\alpha_F = \frac{8}{15} \cdot \left(\frac{h}{L} \right)^2 + \frac{1}{m_I} \left(\frac{r_g}{L} \right)^2 \quad (3.43)$$

and

$$\beta_F = 4 - \frac{4}{\alpha_F} \left(\frac{\Pi}{4} \right) \cdot \left(\frac{r_c}{L} \right)^2$$

As before, even values of "i" do not effect H_0 .

From Equation (3.42) Fourier constants can now be substituted in Equation (3.32) to give H_0 ; Equations (3.7) and (3.8) can be used to give M^q and q , and the bending moments in the arch and tie girder are then given by:

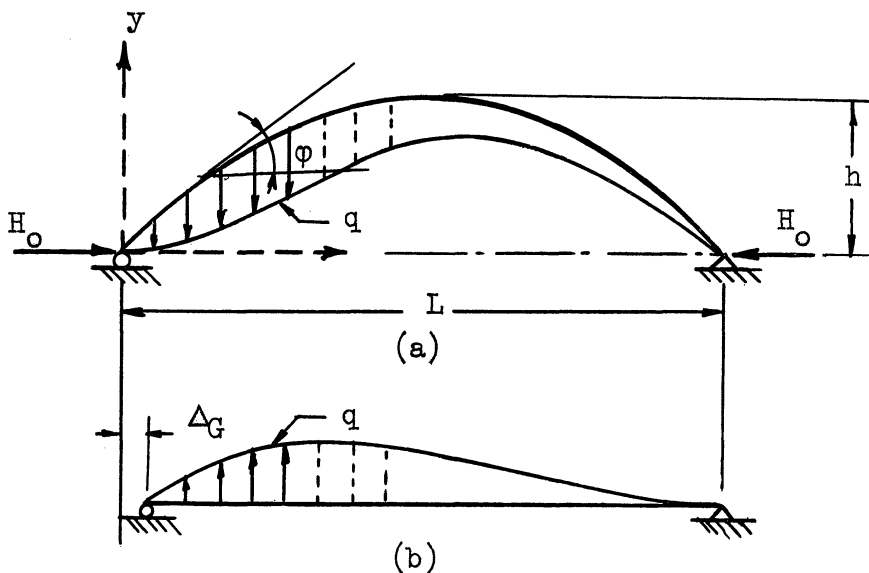
$$M_a = H_0 y - \sum_{n=1}^{\infty} a_n \left(\frac{n\pi}{L}\right)^2 \sin \frac{n\pi x}{L} \quad (3.44)$$

$$M_g = - \sum_{n=1}^{\infty} a_n \left(\frac{n\pi}{L}\right)^2 \sin \frac{n\pi x}{L} \quad (3.45)$$

The suspension-rod forces are given by integrating Equation (3.8) between the proper limits as before.

For an Initial Predetermined Gap Δ_G , as Shown in the Diagram Below

All assumptions and Equations (3.1) through (3.8) apply for this condition also.



The relative horizontal movement on each side of the cut section at the origin "0" is Δ_G :

$$\Delta_G = \delta_{OH} + H_0 \delta_{HH} \quad (3.46)$$

from which

$$H_0 = \frac{\Delta_G - \delta_{OH}}{\delta_{HH}} \quad (3.47)$$

Substituting the values of δ_{OH} and δ_{HH} in Equation (3.47) and reducing we obtain

$$H_0 = \frac{15}{8} \frac{EI_c}{h^2 L} \Delta_G + 30 \frac{L}{h} \sum_{n=1,3,5}^{\infty} \frac{a_n}{L^3} \frac{1}{n\pi} \quad (3.48)$$

As before, H_0 can be determined once the Fourier constants are known. With the same reasoning as in previous cases,

$$\frac{\partial U}{\partial a_1} da_1 = \Delta_G \left(\frac{\partial H_0}{\partial a_1} \right) da_1 \quad (3.49)$$

The total potential energy in the system is:

$$U = \int_0^L \frac{M_a^2}{2EI_c} dx + \int_0^L \frac{M_g^2}{2E_g I_g} dx + \int_0^L \frac{(H_0 \cos \varphi)^2}{2EA_c} dx \quad (3.50)$$

where

$$M_a = H_0 y - \sum_{n=1}^{\infty} a_n \left(\frac{n\pi}{L} \right)^2 \sin \frac{n\pi x}{L}, \quad [\text{see Equation (3.18)}]$$

$$M_g = - \sum_{n=1}^{\infty} a_n \left(\frac{n\pi}{L} \right)^2 \sin \frac{n\pi x}{L} \quad . \quad [\text{see Equation (3.7)}]$$

and

$$\int_0^L \cos^2 \varphi dx = \frac{\pi}{4} L \quad . \quad [\text{see Equation (3.20)}]$$

Substituting these in Equation (3.50), and integrating and reducing gives:

$$U = \frac{1}{2EI_c} \left\{ \left[\frac{8}{15} H_o^2 h^2 L - \frac{32H_o h}{L} \sum_{1 \cdot 3 \cdot 5}^{\infty} a_n \frac{1}{n\pi} + \frac{1}{2L^3} \sum_{n=1}^{\infty} a_n^2 (n\pi)^4 \right] \right. \\ \left. + \frac{1}{m_I} \cdot \frac{1}{2L^3} \sum_{n=1}^{\infty} a_n^2 (n\pi)^4 + \frac{\pi}{4} H_o^2 r_c^2 L \right\} \quad (3.51)$$

Substituting H_o from Equation (3.48) in Equation (3.51) and differentiating with respect to a_1 gives:

$$\frac{\partial U}{\partial a_1} = \frac{1}{2EI_c} \cdot \frac{a_1}{L^3} \left[\frac{m_I + 1}{m_I} (i\pi)^4 - \frac{30}{(i\pi)^2} \left(32 - 60 \frac{\pi}{4} \frac{r_c^2}{h^2} \right) \right] \\ + \frac{225}{4(i\pi)} \cdot \frac{\pi}{4} \cdot \frac{r_c^2}{h^2 L^2} \Delta_G \quad (3.52)$$

The change in potential energy in the bowstring arch due to the increment da_1 is:

$$\frac{\partial U}{\partial a_1} da_1 = \left\{ \frac{1}{2EI_c} \cdot \frac{a_1}{L^3} \left[\frac{m_I + 1}{m_I} (i\pi)^4 - \frac{30}{(i\pi)^2} \left(32 - 60 \frac{\pi}{4} \frac{r_c^2}{h^2} \right) \right] \right. \\ \left. + \frac{225}{4(i\pi)} \cdot \frac{\pi}{4} \cdot \frac{r_c^2}{h^2 L^2} \Delta_G \right\} da_1 \quad (3.53)$$

From Equation (3.48) the horizontal force is:

$$H_o = \frac{15}{8} \cdot \frac{EI_c}{h^2 L} \Delta_G + 30 \frac{L}{h} \sum_{1 \cdot 3 \cdot 5}^{\infty} \frac{a_n}{L^3} \cdot \frac{1}{n\pi}$$

Differentiating H_o with respect to a_1 gives:

$$\frac{\partial H_o}{\partial a_1} = \frac{30}{(i\pi)} \cdot \frac{1}{hL^2} \quad (3.54)$$

and the work done due this change in H_o is:

$$\Delta_G \left(\frac{\partial H_o}{\partial a_1} \right) da_1 = \Delta_G \frac{30}{(i\pi)} \cdot \frac{1}{hL^2} da_1 \quad (3.55)$$

The work done by the change in H_o is equal to the change in the potential energy of the system; thus equating Equations (3.53) and (3.55) and reducing gives:

$$a_i = L^3 \frac{\frac{30}{(i\pi)} \alpha_G \cdot \frac{\Delta_G EI_G}{h L^2}}{\frac{m_I + 1}{m_I} (i\pi)^4 - \frac{480}{(i\pi)^2} \alpha_G} \quad (3.56)$$

where "i" is odd for H_0

$$\text{and} \quad \alpha_G = 2 - \frac{15}{4} \cdot \left(\frac{\pi}{4}\right) \cdot \left(\frac{r_c}{h}\right)^2 \quad (3.57)$$

From Equation (3.56) the Fourier constants can now be substituted in Equation (3.48) to give H_0 ; Equations (3.7), (3.8), (3.44), and (3.45) can be used to give, respectively, M^q , q , the bending moments M_a in the arch, and M_g in the tie girder. The suspension rod forces, as before, are given by integrating Equation (3.8) between the proper limits.

IV. EXPERIMENTAL STUDY

Preliminary Work

To determine the load-deflection relationship in the bowstring arch, prior to any analytical work, a preliminary experiment was carried out on a 21-inch-length double-plane Plexiglas model, shown in Figure 27. The model was loaded in several increments either by a vertical load at a panel point or by a horizontal force at the ends (produced by tightening the bolts on the prestressing rod) and the corresponding deflections on the tie girder were measured at all the panel points. The results of the tests, when plotted load vs. deflection, indicated the existence of a linear behavior between the applied load and the deflection produced by it.

Main Experiment

The main experimental work was carried out on an aluminum model of 49 in. c. to c. span, and the results were compared with exact and approximate theoretical study.

Dimensions

The arch rib, cut from 1-inch-thick aluminum (6061-T6) plate, was 1 in. wide at the crown, making $L/r_c = 169.74$, and varied according to $A_a = A_c \sec \phi$ and $I_a = I_c \sec^3 \phi$ toward the abutments. The interchangeable tie girders were made of extruded aluminum (6063-T5) rectangular tubing. There were two different sizes, 1 1/2 x 1 1/2 x 1/8 inches for two, and 1 1/2 x 2 x 1/8 inches for one tie girder. One of the former was for the case with an initial gap. This had horizontally slotted holes at each end

to permit relative horizontal motion between the ends of the arch and the tie girder. The suspension-rods were made of 7/32-inch-diameter brass rods.

To find the moduli of elasticity for aluminum and brass, samples prepared from the same stock as the model were tested from which the following ratios were obtained:

$$m_I = 2.6208 \text{ for } 1 \frac{1}{2} \times 1 \frac{1}{2} \times \frac{1}{8} \text{ inch,}$$

$$m_I = 5.3004 \text{ for } 1 \frac{1}{2} \times 2 \times \frac{1}{8} \text{ inch,}$$

and $m_r = 0.0637$ throughout.

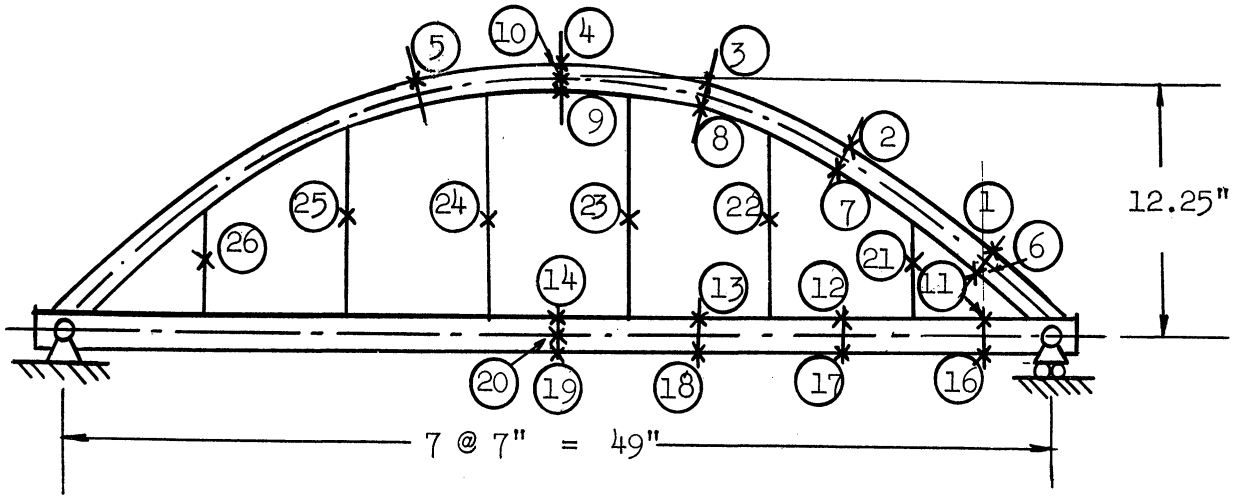
Loading and Measurements

The model, in vertical position, was loaded in two increments of 100 lb at each panel point, and strains of a total of 25 points (the distribution and location of which are shown in the diagram below) were measured by SR-4 electric strain gages after the application of each increment of load. To minimize the errors in strain measurements, two gages in series were used per point. These were glued one on each side of the point in question.

The horizontal prestressing load was applied in increments of 1000 lb to a maximum of 4000 lb. This was done with the help of a hydraulic jack, a calibrated 3/4-inch-diameter load rod, prestressing wire that ran concentrically inside the tie girder and anchor plates. See Figures 28 through 30. As with the panel point loading, strain measurements were taken after every increment of load.

For the case with the initial gap, the relative horizontal deflection were varied in different decrements to a maximum of 181.7×10^{-3} in. and the corresponding horizontal force and strain measurements were

taken for every decrement of the relative deflection.

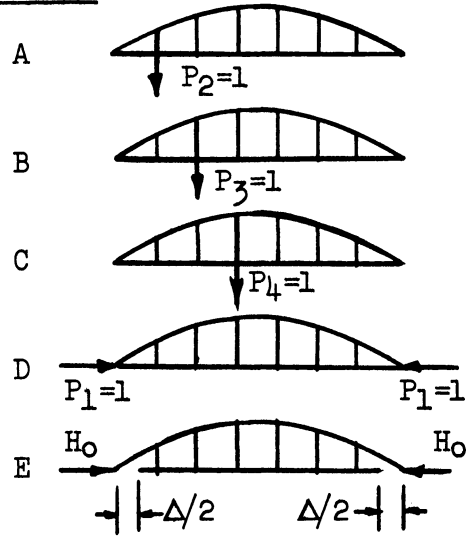


The theoretical and experimental values of the axial force and the bending moments in the arch and the tie girder are shown compared in Table V and Figures 1 and 2.

TABLE V

ANALYTICAL AND EXPERIMENTAL VALUES
OF HORIZONTAL FORCE X_1 COMPARED

LOAD CASES



$$\Delta = KL \text{ \& } K = \frac{5000}{E_a A_c}$$

Load Case	m_I	Horizontal Force		
		By Energy Method	By Membrane Analogy	By Experiment
A	2.62	0.3329	0.3296	0.3300
B		0.5999	0.6064	0.5892
C		0.7482	0.7662	0.7161
D		0.005615	0.005422	
E		19.41	18.74	20.14
A	5.30	0.3304	0.3190	0.3304
B		0.5938	0.6000	0.5648
C		0.7390	0.7682	0.7114
D		0.008061	.007915	
E		33.01	32.41	

Full Lines show bending moments calculated by the energy method with extensible suspension rods.

⊙ — Indicates Experimental Values

△ — Indicates Membrane Analogy Values

Bending Moments are in units of in-lb x 49

$$m_I = 2.62$$

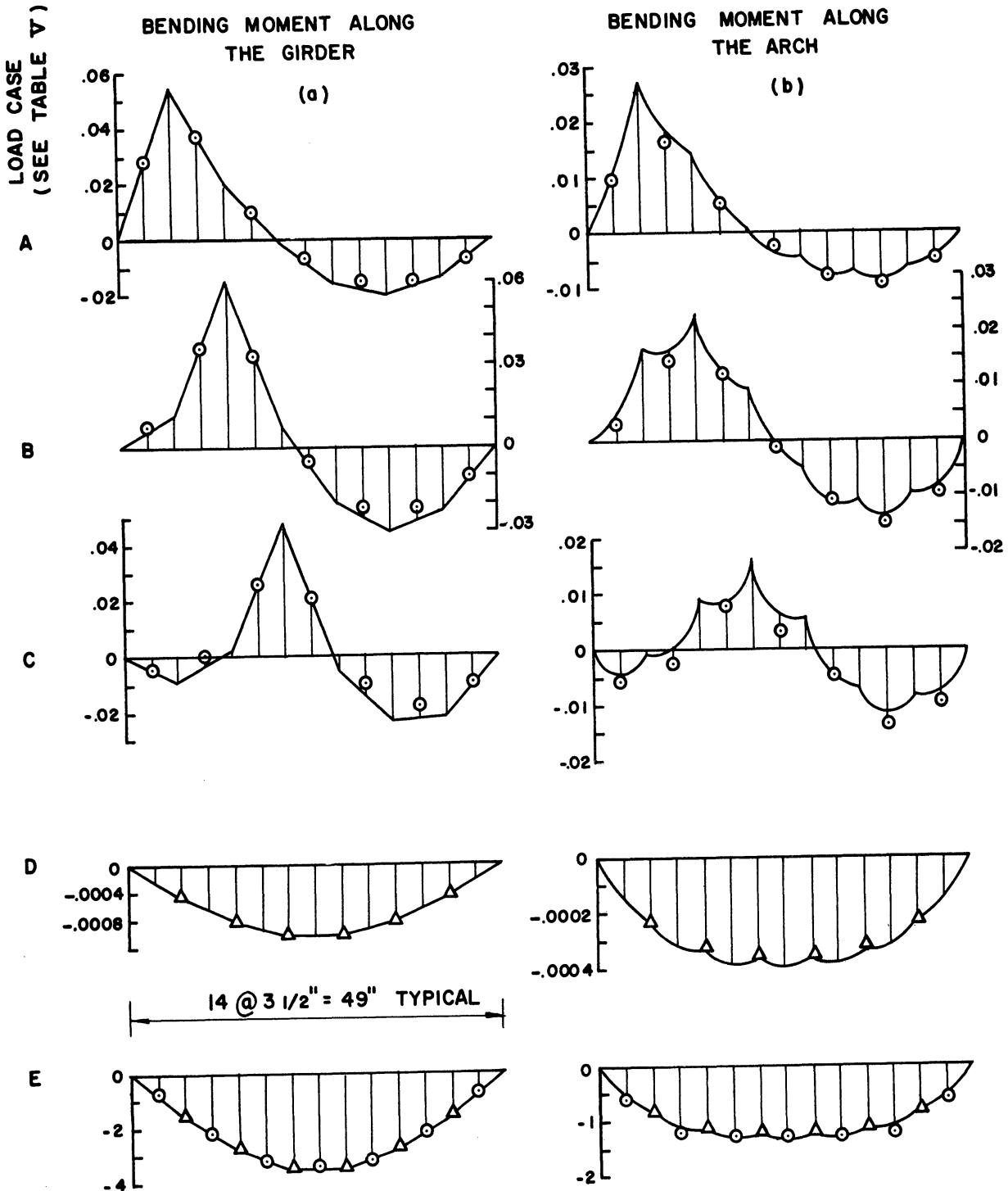


Figure 1. Analytical and Experimental Values of Bending Moments Compared for $m_I = 2.62$

Full lines show bending moments calculated by the energy method with extensible suspension rods.

⊙—Indicates Experimental Values

△—Indicates Membrane Analogy Values

Bending Moments are in Units of in-lb = 49

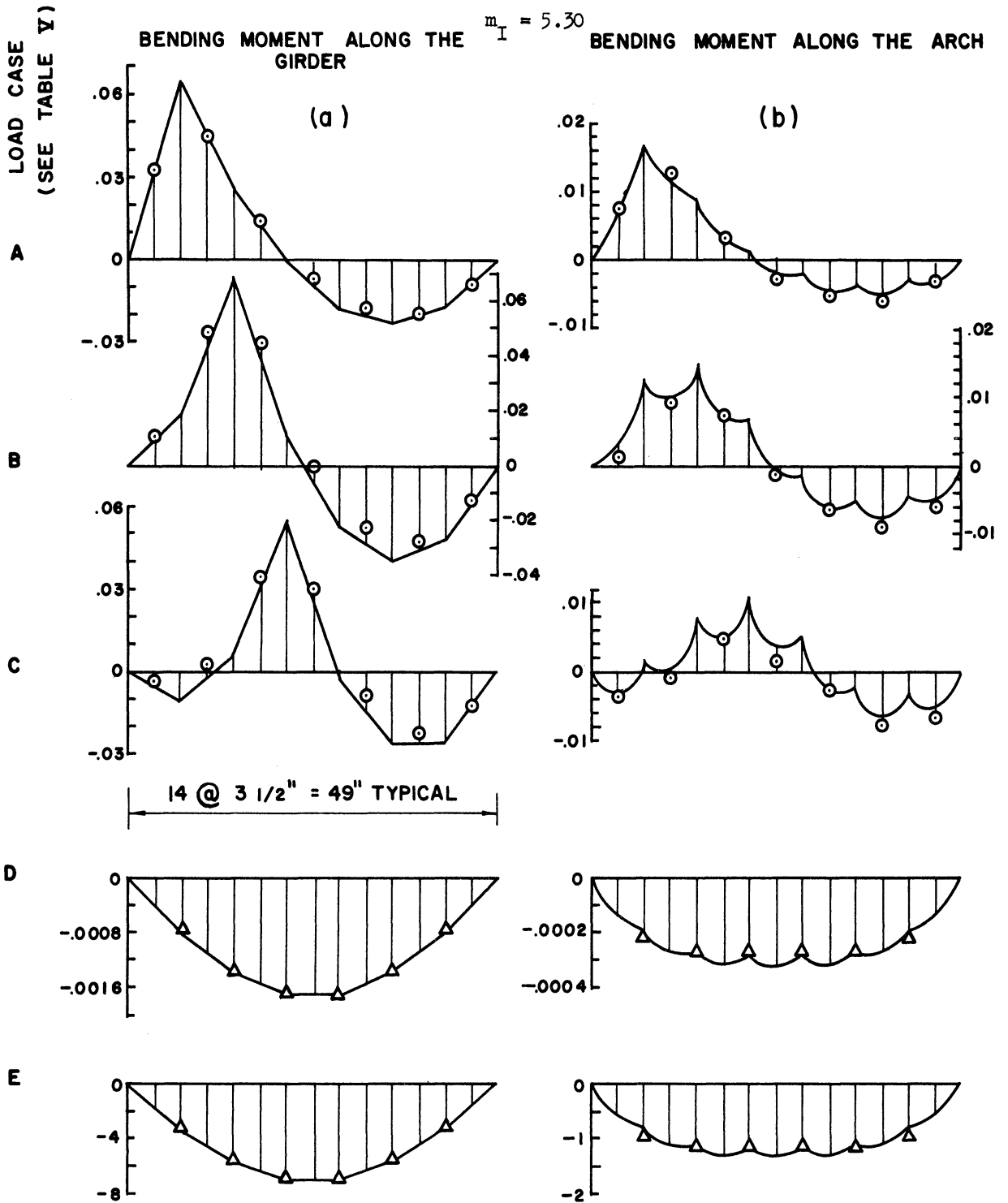


Figure 2. Analytical and Experimental Values of Bending Moments Compared for $m_I = 5.30$.

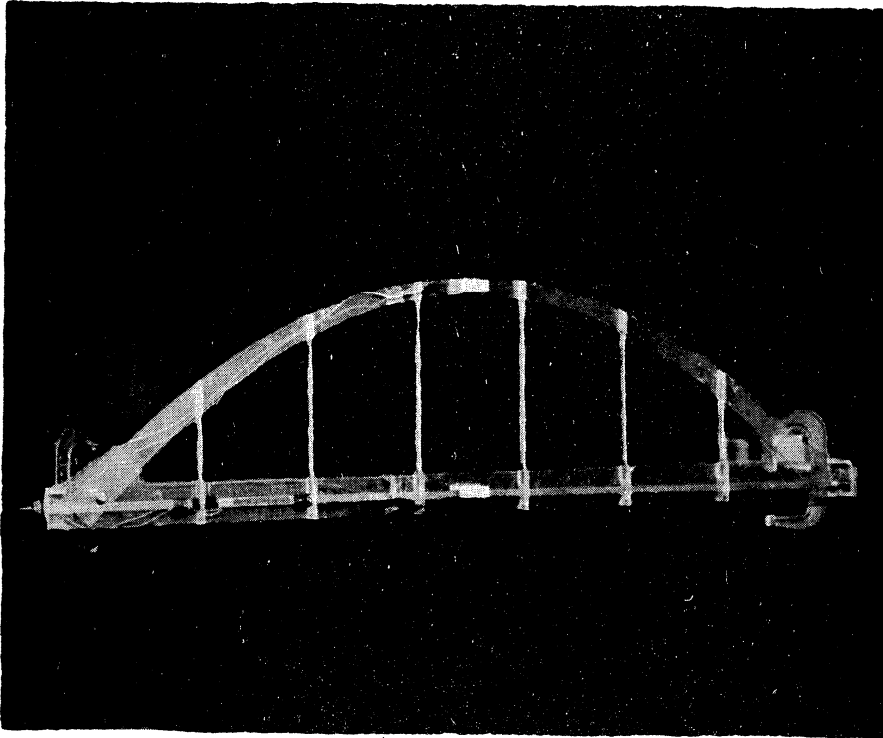


Figure 27. Plexiglas Model.

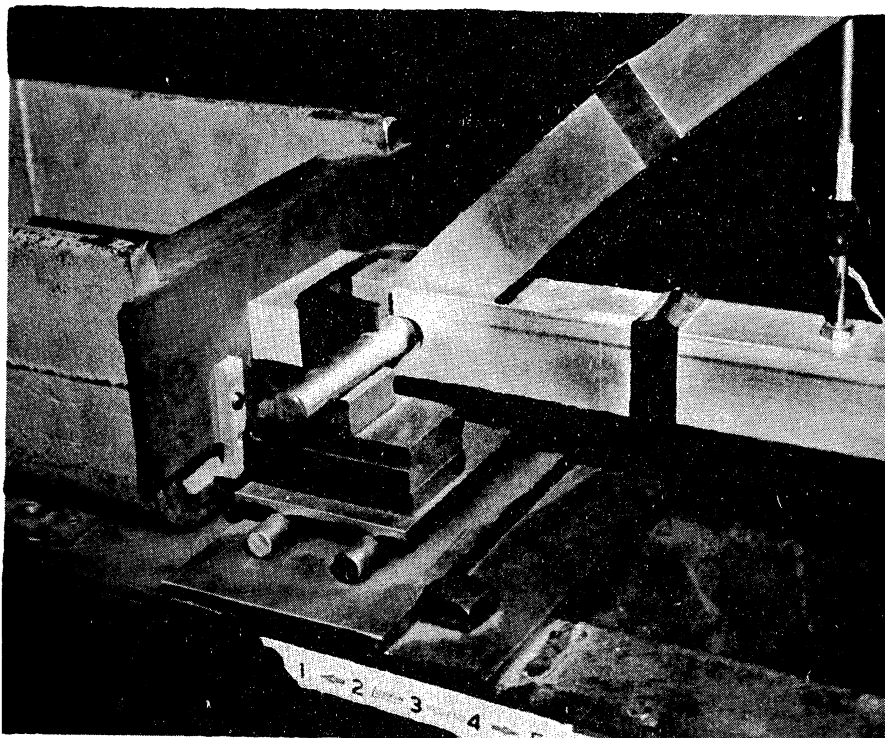


Figure 28. End Detail for Aluminum Model with Gap.

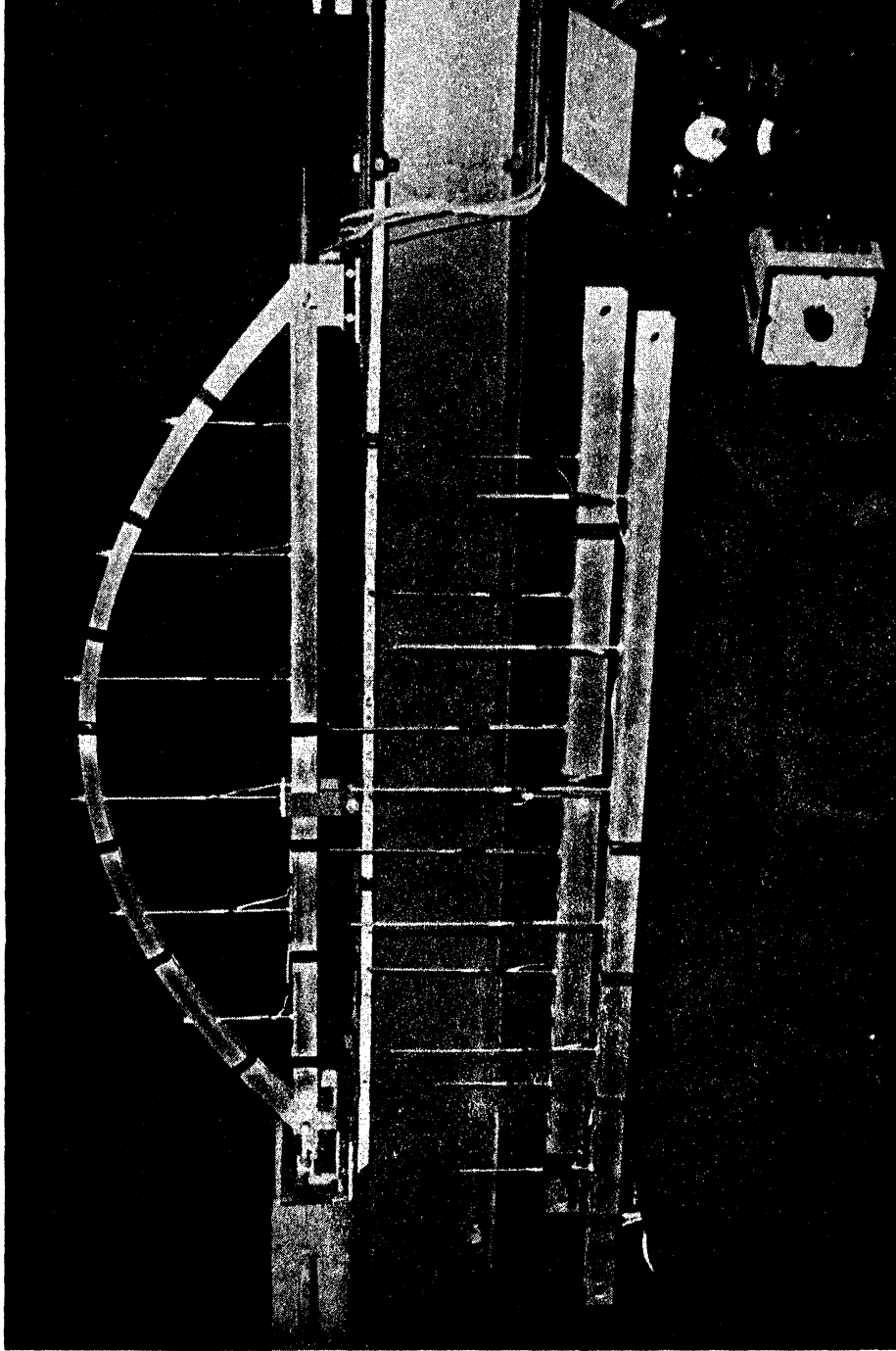


Figure 29. Aluminum Model and Interchangeable Tie-Girders.

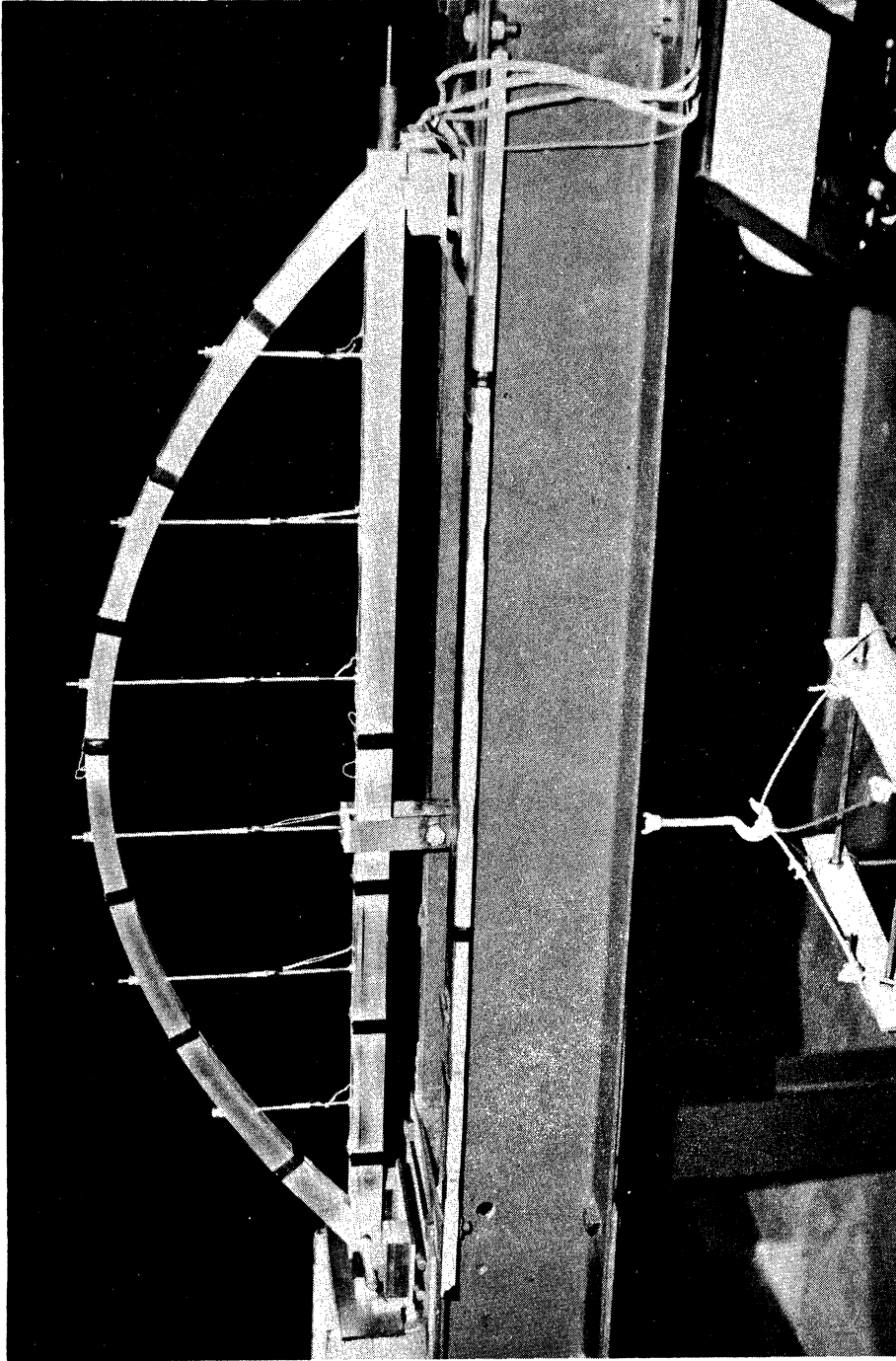


Figure 30. Aluminum Model with Vertical Load.

V. SUMMARY AND CONCLUSIONS

In the foregoing chapters, different methods of solving the prestressed bowstring arch for various types of loadings and their experimental verification have been described.

In Chapter I, the problem was described and a brief history of previous work on bowstring-arch design was given.

In Chapter II, a general expression for solving bowstring arches with extensible suspension rods was obtained from the strain energy of the structure. Then specific equations were derived for a hinged-end bowstring arch with six suspension rods. Lastly, from these equations (with the help of a high-speed digital computer), influence line and other diagrams were prepared for the bending moments and the axial forces to be used in design.

In Chapter III, the membrane-analogy method of solving the bowstring arch was introduced. This method is of special value since it covers a wider range of parameters (i.e., all rise-to-span ratios, as many suspension rods as desired, and even different curves for the arch rib) with almost no additional work.

In Chapter IV, the experimental work carried on 49-inch-span aluminum models was described briefly and the results obtained were compared with those given in Chapters II and III.

From the results of the work discussed in this study, the following conclusions can be drawn.

(1) The assumption that the total moment at a section (simple bending moment minus $H \cdot y$) is distributed between the rib and the girder according to their respective moment of inertia is quite justified. For horizontal loading the error in the maximum moment is within 2% (Figures 1 and 2) and for vertical loading the error is around 10% at the load point at best, but away from the load there is a much larger error (Figures 1 and 2.)

(2) A good correspondence between the results of strain-energy and membrane-analogy methods (Table V and Figures 1 and 2) seems to suggest that the assumption of inextensible suspension rods in simplified design is not unreasonable. ^{*} Suspension rods were assumed to be extensible in the former and inextensible in the latter.

(3) The manner in which I_a varied along the arch rib did not affect the results appreciably. (I_a was assumed to be $I_c \sec^3 \phi$ in the strain-energy method and $I_c \sec \phi$ in the membrane-analogy method.)

(4) Omitting the axial energy in the arch rib caused by the suspension-rod force components produced only a maximum error of 0.3% anywhere in the bowstring arch. This item can safely be left out from the design.

(5) For horizontal loading an inverselinear variation was noticed to exist between m_g and the bending moment in both the girder and the arch (Figure 3). The maximum error in this assumption, as m_g varied from 0.5 to 10, was 1.0%. For vertical loads the same variation in m_g changes the bending moment by only -3.3% in the arch and by -5.6% in the girder (Figure 4) (i.e., the effect of varying m_g on vertical loads can be totally neglected).

* This can also be due in part to (3)

(6) Varying m_r from 0.05 to ∞ produced a maximum bending moment change of -2.4% in the arch and 2.7% in the girder for the horizontal loads, and 26.7% in the arch and -9.8% in the girder for the vertical loads (Figures 3 and 4). This same variation in m_r caused in the largest of the suspension rod forces an increase of about 21%. In practice the percentages mentioned above can be considerably less, for m_r may take values a few times larger than 0.05.

(7) For vertical loads: The horizontal force in the arch and the bending moment along the girder were found to be very sensitive to variations in m_I when L/r_c was small (Figures 5, 12-14), but for large values of L/r_c , changing m_I had very little affect on the bending moment and practically none on the horizontal force.

Suspension-rod and horizontal forces were directly proportional to L/r_c and inversely to m_I . They never changed sign (Figures 5-8).

The bending moment varied with m_I , directly in the girder and inversely in the arch (Figures 9-14). As L/r_c increased, along the girder, the (-) bending moment increased and the (+) moment decreased.

For horizontal loads: Suspension-rod and horizontal forces as well as the bending moments both in the arch and in the girder were all found to vary inversely with L/r_c and except for the bending moment in the arch, directly with m_I . They were very sensitive to changes in L/r_c when the latter had low values and became insensitive as L/r_c took on large values (Figures 15-26).

(8) As a whole the results of the experimental work showed very good agreement with those of the analytical methods. The maximum error in the horizontal force, using the strain-energy method as the standard for comparison, was 3.4% for the membrane-analogy method and 4.9% for the experimental work. (See Table V.) For the vertical loading the bending-moment curve of the experimental work showed a small shift upwards along the girder, and downwards along the arch (Figures 1 and 2).

The bending moment along the arch (Figures 1b and 2b) was not a smooth curve, while upper and lower-envelope curves, if drawn, tend to be smooth. Figure 3 shows upper-envelope curves only.

(9) The membrane-analogy method yielded very satisfactory results. The maximum error in the bending moments for horizontal loading did not exceed 2.6% along the girder and 6.6% along the arch (Figures 1 and 2) compared with the results of the strain-energy method. It was further observed that, as m_I increased, the error in the bending moment increased in the arch and decreased in the girder in a linear fashion. This can be attributed to the assumption that the suspension rods were inextensible.

In some cases the results from the membrane-analogy method can be obtained by using only the first term of the series. This is especially true for finding the horizontal force for all types of loading and the bending moment along the girder and the arch for horizontal loads. In other cases, say to find the bending moment for a vertical load, since here the series does not converge so rapidly, one must use a few more terms of the series. The latter will no doubt depend on the accuracy

desired. One can assume ($I_a = I_c \sec \phi$) variation without introducing any error which is significant for preliminary design. In conclusion, the use of the Membrane Analogy method for design is highly recommended.

(10) When a uniform load is applied over the entire length of the bowstring arch, the bending moment along the arch is found to be positive (Figures 9-11). On the other hand, prestressing the bowstring arch, with or without gap, by a horizontal force always produces a negative bending moment in the arch rib (Figures 3, 16, and 22). Thus prestressing the bowstring arch to counteract the dead-load bending moment is very advantageous for the arch rib.

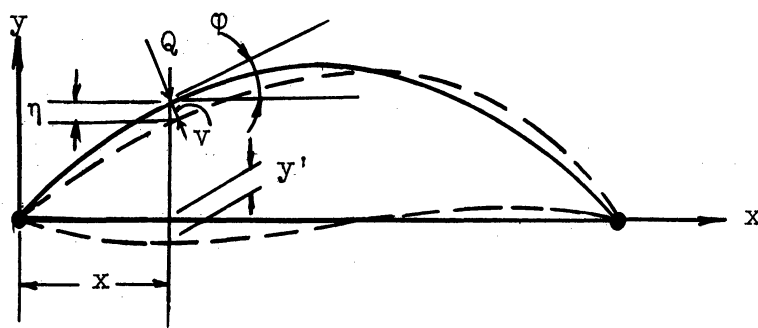
In the tie girder for low L/r_c values the bending moment is also positive when m_I is around 10 or larger (Figures 12-14). Here again there is an advantage to prestressing for the dead-load bending moment. When L/r_c has large values (Figures 12-14), the girder part of the structure does not profit from this combined prestressing; it may even suffer. In this case, the gap prestressing system may be followed and the suspension rods released when the gap is being closed. After prestressing, the suspension rods are fastened back. This will allow one to get the benefit of prestressing without its harmful effect. If the tie girder is to be made of prestressed concrete, the two prestressing operations can be performed in one. Thus, within the limits described above, there are definite advantages to prestressing the bowstring arch.

NOTE: It may be of interest also to mention here that for short spans, the roadway floor may be designed as part of the tie girder itself.

APPENDIX A

RELATION BETWEEN THE VERTICAL COMPONENTS OF THE DEFLECTION OF THE ARCH RIB AND THE TIE GIRDER⁽¹⁾

Let v represent the component of deflection along a normal to the arch-rib curve at point Q in the diagram below.



From the differential equation for the deflection of a curved beam:

$$\frac{d^2v}{ds^2} + \frac{v}{\rho^2} = \pm \frac{M_a}{EI_a} \quad (\text{A.1a})$$

in which ds is an element of length of the arch rib and ρ is the radius of curvature of the rib at point Q .

The second term of Equation (A.1a) can be neglected without appreciable error, and the equation reduces to

$$\frac{d^2v}{ds^2} = \pm \frac{M_a}{EI_a} \quad (\text{A.1b})$$

Neglecting the tangential component of deflection at Q , the vertical component η of v is:

$$\eta = v \cos \phi \quad (\text{A.2})$$

The first term of Equation (A.1b) can be replaced by an expression involving η , x , and ϕ as follows: from Equation (A.2)

$$\frac{d\eta}{ds} = \frac{dv}{ds} \cos \phi - v \frac{d\phi}{ds} \sin \phi$$

and

$$\begin{aligned} \frac{d^2\eta}{ds^2} &= \cos \phi \frac{d^2v}{ds^2} - 2 \frac{dv}{ds} \frac{d\phi}{ds} \sin \phi - v \frac{d^2\phi}{ds^2} \sin \phi - v \left(\frac{d\phi}{ds} \right)^2 \cos \phi \\ &= \cos \phi \frac{d^2v}{ds^2} - 2 \frac{dv}{ds} \frac{1}{\rho} \sin \phi + \frac{v}{\rho^2} \frac{d\rho}{ds} \sin \phi - \frac{v}{\rho^2} \cos \phi \end{aligned} \quad (A.3)$$

Neglecting the last three terms of Equation (A.3), we obtain:

$$\frac{d^2v}{ds^2} = \sec \phi \frac{d^2\eta}{ds^2} \quad (\text{approx.}) \quad (A.4)$$

Using $dx = ds \cos \phi$, Equation (A.4) reduces to

$$\frac{d^2v}{ds^2} = \cos \phi \frac{d^2\eta}{dx^2} \quad (A.5a)$$

or

$$\pm \frac{M_a}{EI_a} = \cos \phi \frac{d^2\eta}{dx^2} \quad (\text{approx.}) \quad (A.5b)$$

For the girder (see preceding diagram).

$$\pm \frac{M_g}{EI_g} = \frac{d^2y'}{dx^2} \quad (A.6)$$

The total moment M_T is equal to $M_a + M_g$; and neglecting the change in lengths of the hangers, we obtain:

$$\frac{d^2\eta}{dx^2} = \frac{d^2y'}{dx^2}$$

and from Equations (A.5b) and (A.6), letting $m = I_g/I_a$,

$$M_g = M_T \left(\frac{m}{m + \cos \varphi} \right) \quad (\text{A.7a})$$

and

$$M_a = M_T \left(\frac{\cos \varphi}{m + \cos \varphi} \right) \quad (\text{A.7b})$$

Professor Haviár and Drs. Chandrangsu and Sparkes in their respective designs replace $\cos \varphi$ of Equations (A.7a, b) by one.

APPENDIX B

SAMPLE CALCULATION

Calculation for ΔX_1 :

To find ΔX_1 , from Table II, III, and IV evaluate all five terms of Equation (3) and add them up together. Thus,

$$\sum_0^L \frac{(M_a + M_a^i) \frac{\partial M_a^i}{\partial X_1}}{E_a I_a} \Delta s = (498.8567X_1 + 165.7656X_2 + 303.2085X_3 + 382.4850X_4 + 382.4850X_5 + 303.2085X_6 + 165.7656X_7) \frac{L^3}{7^5 E_a I_c}$$

(See page 52 for detailed calculations of this first term).

$$\sum_0^L \frac{(N_a + N_a^i) \frac{\partial N_a^i}{\partial X_1}}{E_a A_a} \Delta s = (5.5095X_1 - .4941X_2 - .9249X_3 - 1.1892X_4 - 1.1892X_5 - .9249X_6 - .4941X_7) \frac{L}{7 E_a A_c}$$

(See page 53 for details of this second term).

$$\sum_0^L \frac{(M_g + M_g^i) \frac{\partial M_g^i}{\partial X_1}}{E_g I_g} \Delta x = 0, \text{ see Table III}$$

$$\sum_0^L \frac{(N_g + N_g^i) \frac{\partial N_g^i}{\partial X_1}}{E_g A_g} \Delta x = \frac{(P_1 + X_1) L}{E_g A_g}, \text{ see Table III}$$

$$\sum_{i=2}^{(n-2)} \frac{X_i h_i}{E_r A_r} = 0, \text{ see Table IV}$$

and after adding and simplifying,

$$\begin{aligned} \Delta X_1 = & \left\{ [498.8567 + 13228.3095 \left(\frac{L}{r_c}\right)^{-2} + 16807 - \frac{1}{m_g} \cdot \left(\frac{L}{r_c}\right)^{-2}] X_1 \right. \\ & + [165.7657 - 1186.3341 \left(\frac{L}{r_c}\right)^{-2}] X_2 \\ & + [303.2085 - 2220.6849 \left(\frac{L}{r_c}\right)^{-2}] X_3 \\ & + [382.4850 - 2855.2692 \left(\frac{L}{r_c}\right)^{-2}] X_4 \\ & + [382.4850 - 2855.2692 \left(\frac{L}{r_c}\right)^{-2}] X_5 \\ & + [303.2085 - 2220.6849 \left(\frac{L}{r_c}\right)^{-2}] X_6 \\ & + [165.7657 - 1186.3341 \left(\frac{L}{r_c}\right)^{-2}] X_7 \\ & \left. + 16807 \cdot \frac{P_1}{m_g} \cdot \left(\frac{L}{r_c}\right)^{-2} \right\} \cdot \frac{L^3}{75 E_a I_c} \end{aligned}$$

Point	$(M_a + M_a^1) \cdot \frac{\Delta s}{E_a I_a}$	$\frac{\partial M_a^1}{\partial X_1}$
a	$(3.25 X_1 + 3.0 X_2 + 2.5 X_3 + 2.0 X_4 + 1.5 X_5 + 1.0 X_6 + 0.5 X_7) \cdot \frac{L^2 (.75927)^2}{7^3 E_a I_c} \cdot (3.25) \cdot \frac{L}{49}$	
b	$(8.25 X_1 + 5.5 X_2 + 7.5 X_3 + 6.0 X_4 + 4.5 X_5 + 3.0 X_6 + 1.5 X_7) \cdot \frac{L^2 (.86820)^2}{7^3 E_a I_c} \cdot (8.25) \cdot \frac{L}{49}$	
c	$(11.25 X_1 + 4.5 X_2 + 9.0 X_3 + 10.0 X_4 + 7.5 X_5 + 5.0 X_6 + 2.5 X_7) \cdot \frac{L^2 (.96150)^2}{7^3 E_a I_c} \cdot (11.25) \cdot \frac{L}{49}$	
d	$(12.25 X_1 + 3.5 X_2 + 7.0 X_3 + 10.5 X_4 + 10.5 X_5 + 7.0 X_6 + 3.5 X_7) \cdot \frac{L^2 (1)^2}{7^3 E_a I_c} \cdot (12.25) \cdot \frac{L}{49}$	
c'	$(11.25 X_1 + 2.5 X_2 + 5.0 X_3 + 7.5 X_4 + 10.0 X_5 + 9.0 X_6 + 4.5 X_7) \cdot \frac{L^2 (.96150)^2}{7^3 E_a I_c} \cdot (11.25) \cdot \frac{L}{49}$	
b'	$(8.25 X_1 + 1.5 X_2 + 3.0 X_3 + 4.5 X_4 + 6.0 X_5 + 7.5 X_6 + 5.5 X_7) \cdot \frac{L^2 (.86820)^2}{7^3 E_a I_c} \cdot (8.25) \cdot \frac{L}{49}$	
a'	$(3.25 X_1 + 0.5 X_2 + 1.0 X_3 + 1.5 X_4 + 2.0 X_5 + 2.5 X_6 + 3.0 X_7) \cdot \frac{L^2 (.75927)^2}{7^3 E_a I_c} \cdot (3.25) \cdot \frac{L}{49}$	
	$= (498.8567X_1 + 165.7656X_2 + 303.2085X_3 + 382.4850X_4 + 382.4850X_5 + 303.2085X_6 + 165.7656X_7) \cdot \frac{L^3}{7^5 E_a I_c}$	
	$= \sum_0^L \frac{(M_a + M_a^1) \frac{\partial M_a^1}{\partial X_1}}{E_a I_a} \Delta s$	

The first term of Equation (3) for ΔX_1 $\sum_0^L \frac{(M_a + M_a^1) \frac{\partial M_a^1}{\partial X_1}}{E_a I_a} \Delta s$, is evaluated, from Table II, as shown above.

Point *	$\frac{\partial N_i}{\partial X_1} \frac{\Delta s}{E_a A_a}$	$\frac{\partial N_i}{\partial X_1}$
a	$(-.75927X_1 + .55780X_2 + .46484X_3 + .37187X_4 + .27890X_5 + .18593X_6 + .09297X_7) \cdot \frac{L}{7 E_a A_c} \cdot (-.75927)$	$\frac{L}{7 E_a A_c} \cdot (-.75927)$
b	$+ (-.86820X_1 - .07089X_2 + .35445X_3 + .28356X_4 + .21267X_5 + .14178X_6 + .07089X_7) \cdot \frac{L}{7 E_a A_c} \cdot (-.86820)$	$\frac{L}{7 E_a A_c} \cdot (-.86820)$
c	$+ (-.96150X_1 - .03926X_2 - .07851X_3 + .15703X_4 + .11777X_5 + .07851X_6 + .03926X_7) \cdot \frac{L}{7 E_a A_c} \cdot (-.96150)$	$\frac{L}{7 E_a A_c} \cdot (-.96150)$
d	$+ (-1.0 X_1 + 0 + 0 + 0 + 0 + 0 + 0) \cdot \frac{L}{7 E_a A_c} \cdot (-1.0)$	$\frac{L}{7 E_a A_c} \cdot (-1.0)$
c'	$+ (-.96150X_1 + .03926X_2 + .07851X_3 + .11777X_4 + .15703X_5 - .07851X_6 - .03926X_7) \cdot \frac{L}{7 E_a A_c} \cdot (-.96150)$	$\frac{L}{7 E_a A_c} \cdot (-.96150)$
b'	$+ (-.86820X_1 + .07089X_2 + .14178X_3 + .21267X_4 + .28356X_5 + .35445X_6 - .07089X_7) \cdot \frac{L}{7 E_a A_c} \cdot (-.86820)$	$\frac{L}{7 E_a A_c} \cdot (-.86820)$
a'	$+ (-.75927X_1 + .09297X_2 + .18593X_3 + .27890X_4 + .37189X_5 + .46484X_6 + .55780X_7) \cdot \frac{L}{7 E_a A_c} \cdot (-.75927)$	$\frac{L}{7 E_a A_c} \cdot (-.75927)$
	$= (5.5095X_1 - .4941X_2 - .9249X_3 - 1.1892X_4 - 1.1892X_5 - .9249X_6 - .4941X_7) \cdot \frac{L}{7 E_a A_c}$	
	$= \sum_0^L \frac{(N_a + N_a') \frac{\partial N_a'}{\partial X_1}}{E_a A_a} \Delta s$	

The second term of Equation (3) for ΔX_1 is evaluated also from Table II as shown above.

* See Table I.

TABLE VI

VALUES OF $\sin(i\pi k)$ FOR DIFFERENT i AND k

k	i								
	1	2	3	4	5	6	7	8	9
1/7	.433879	.781836	.974928	.974928	.781836	.433879	0	-.433879	-.781836
2/7	.781836	.974928	.433879	-.433879	-.974928	-.781836	0	.781836	.974928
3/7	.974928	.433879	-.781836	-.781836	.433879	.974928	0	-.974928	-.433879
4/7	.974928	-.433879	-.781836	.781836	.433879	-.974928	0	.974928	-.433879
5/7	.781836	-.974928	.433879	.433879	-.974928	.781836	0	-.781836	.974928
6/7	.433879	-.781836	.974928	-.974928	.781836	-.433879	0	.433879	-.781836

TABLE VII

VALUES OF $\frac{10}{i\pi}(k^4 - 2k^2 + k)$ FOR DIFFERENT i AND k

k	i								
	1	2	3	4	5	6	7	8	9
1/7	.43749	.21875	.14583	.10937	.08750	.07292	.06250	.05469	.04861
2/7	.78218	.39109	.26073	.19555	.15644	.13036	.11174	.09777	.08691
3/7	.97044	.48522	.32348	.24261	.19409	.16174	.13863	.12130	.10783
4/7	.97044	.48522	.32348	.24261	.19409	.16174	.13873	.12130	.10783
5/7	.78218	.39109	.26073	.19555	.15644	.13036	.11174	.09777	.08691
6/7	.43749	.21875	.14583	.10937	.08750	.07292	.06250	.05469	.04861

APPENDIX C

Influence Line Diagrams and Graphs for
Preliminary Design Work
Figures 3 - 26

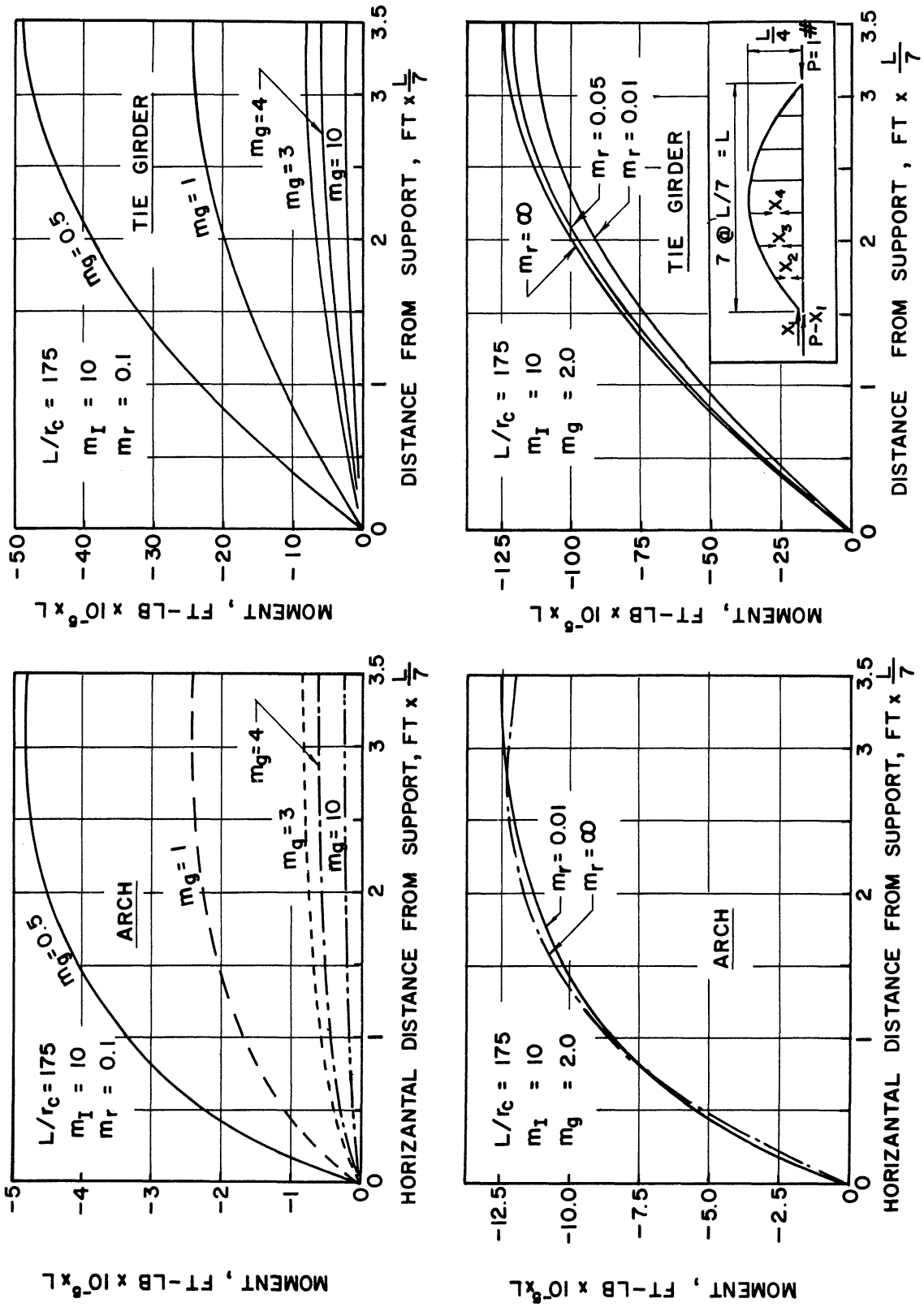


Figure 3. Bending Moment Along Arch and Girder For Different m_g and m_r Values.

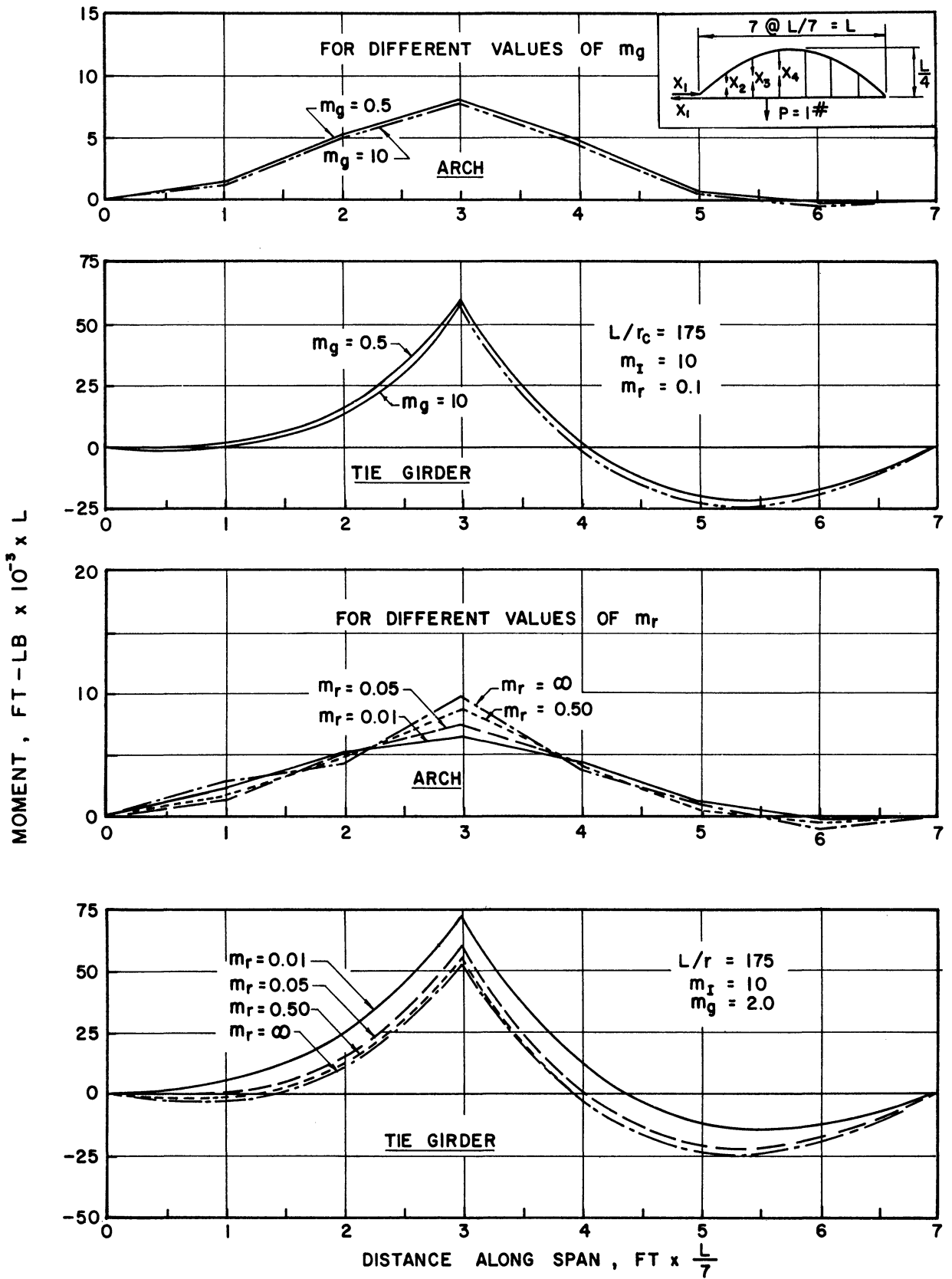


Figure 4. Influence Lines for Bending Moment at Panel Point X_4 For Different m_g and m_r Values.

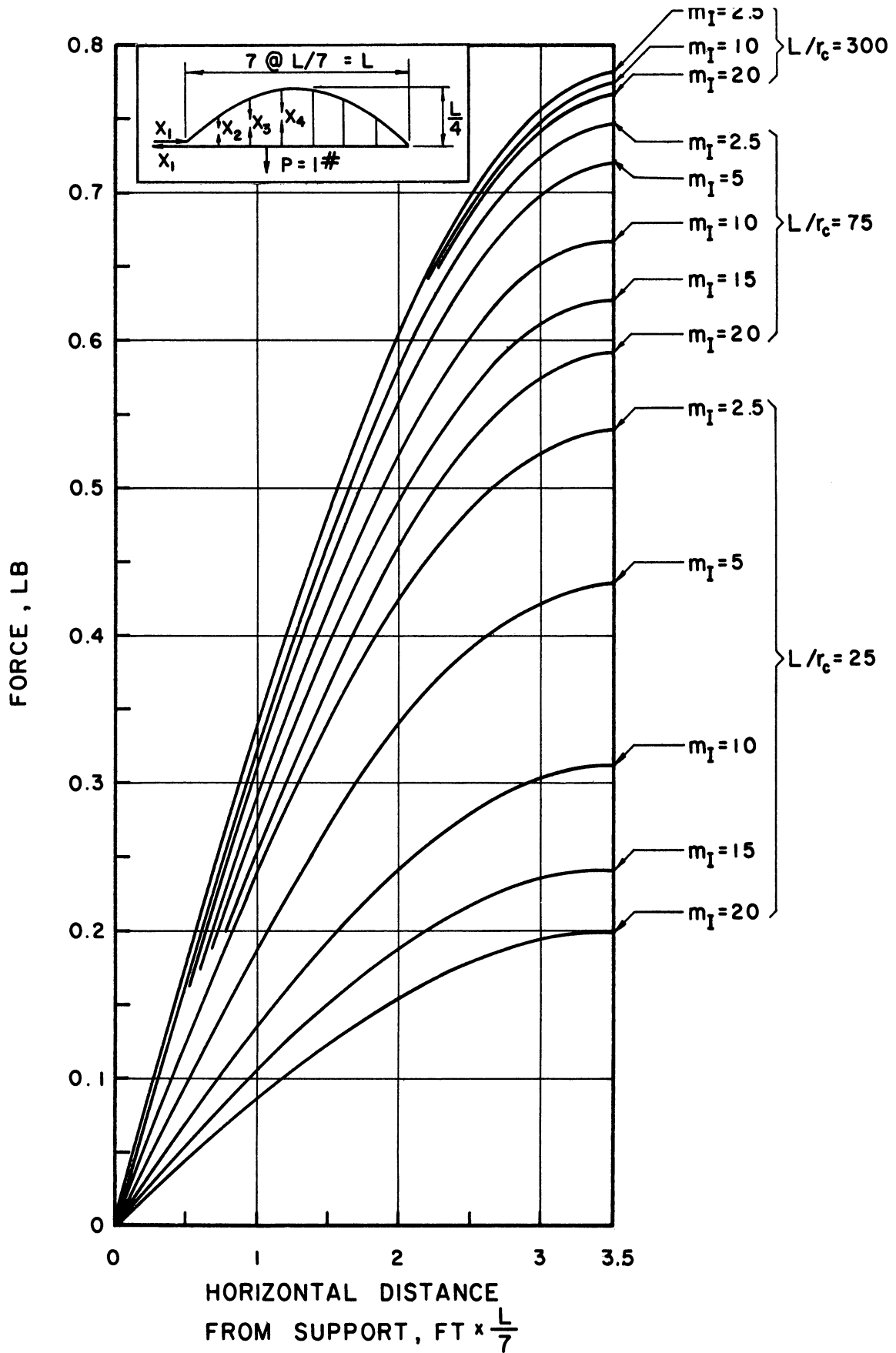


Figure 5. Influence Lines for Horizontal Force X_1 .

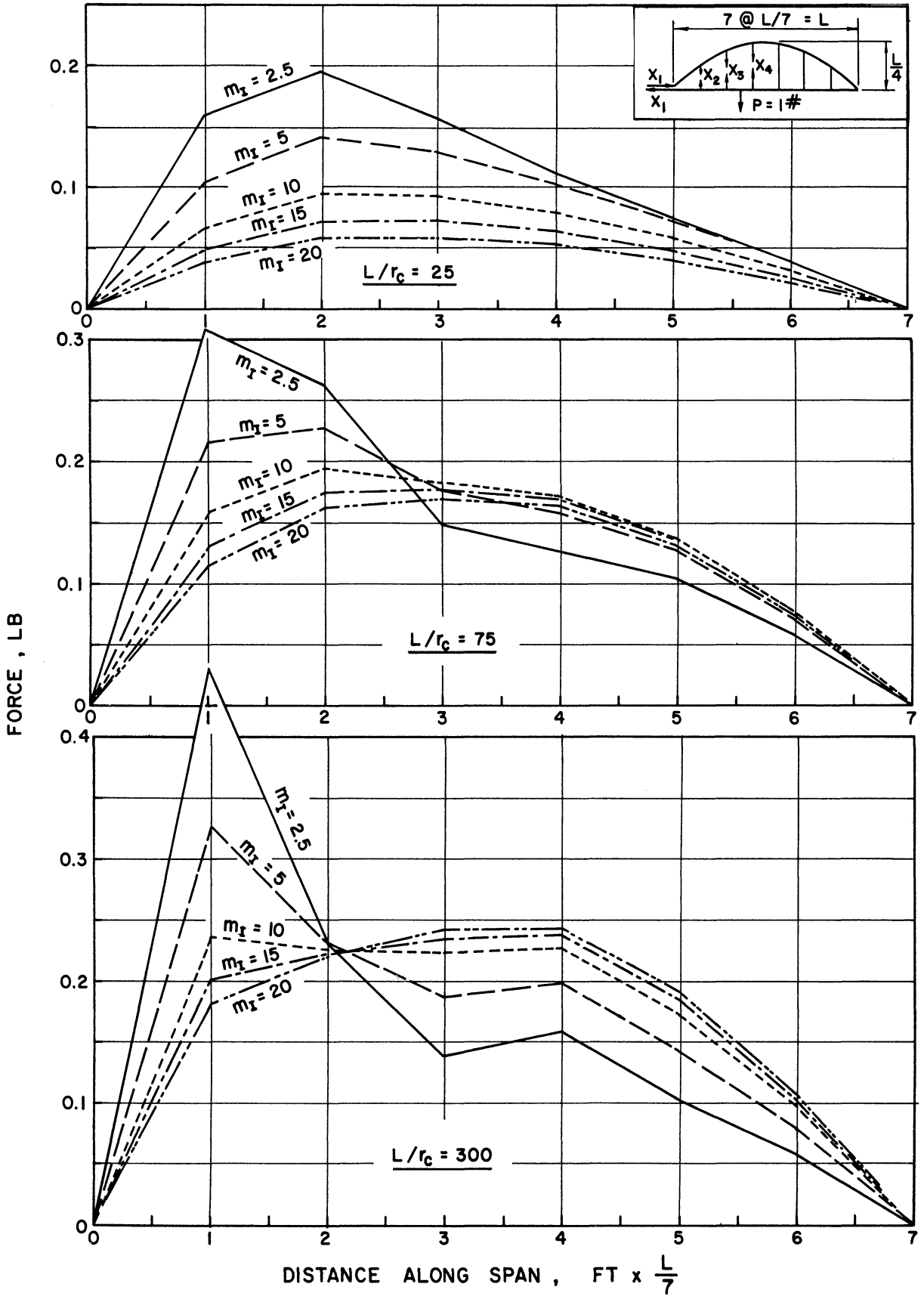


Figure 6. Influence Lines for Suspension-Rod Force X_2 .

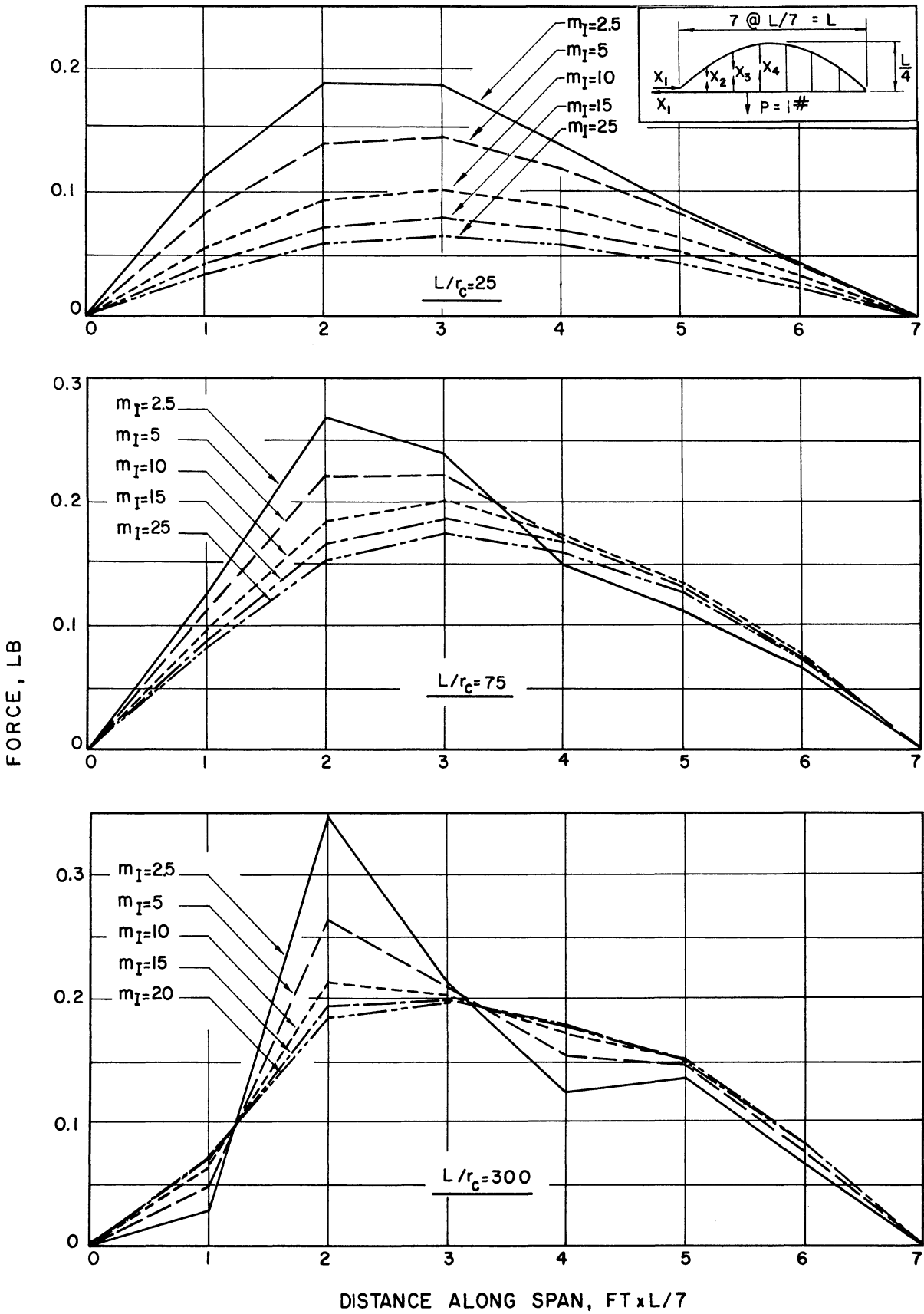


Figure 7. Influence Lines for Suspension-Rod Force X_3 .

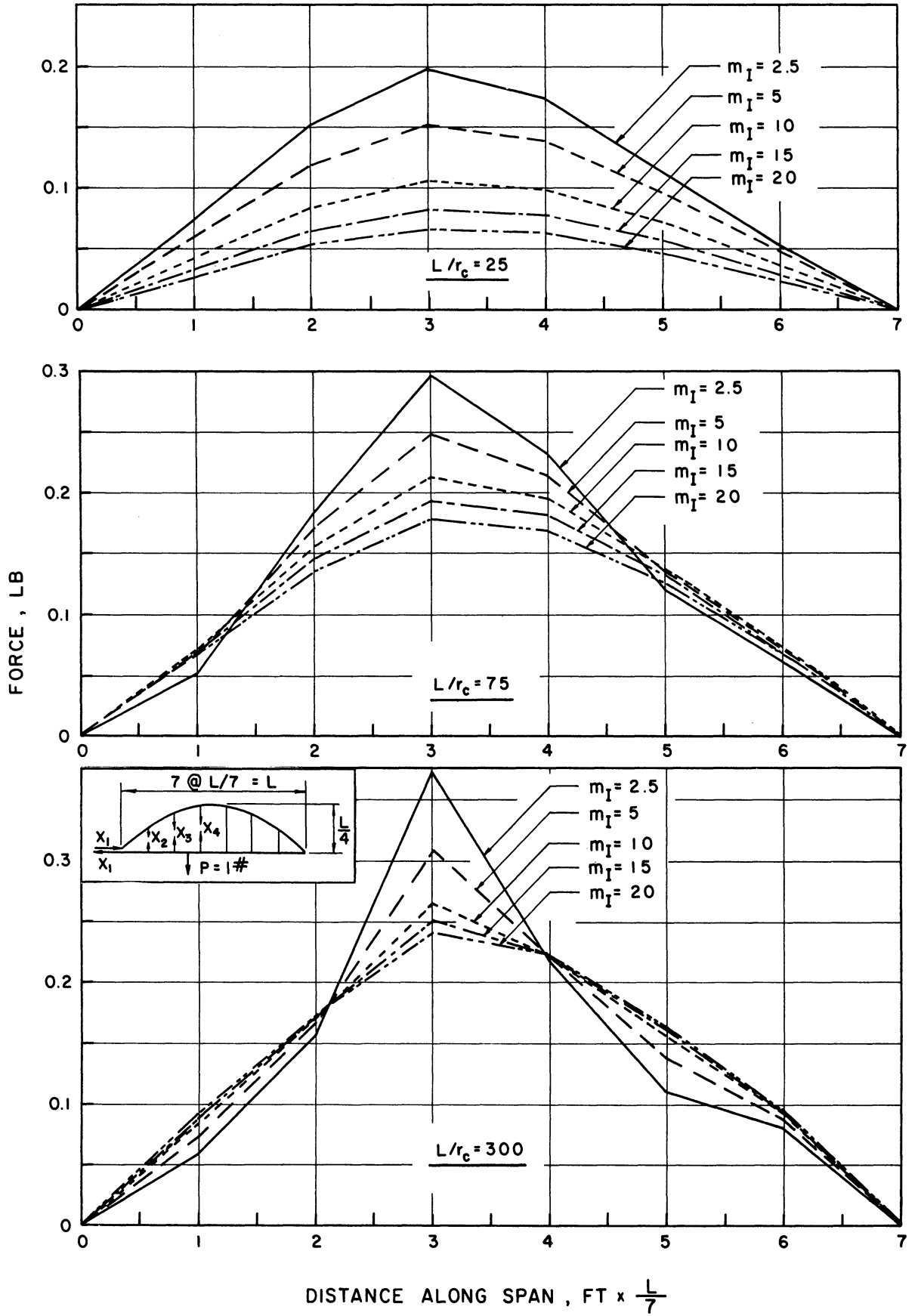


Figure 8. Influence Lines for Suspension-Rod Force X_4 .

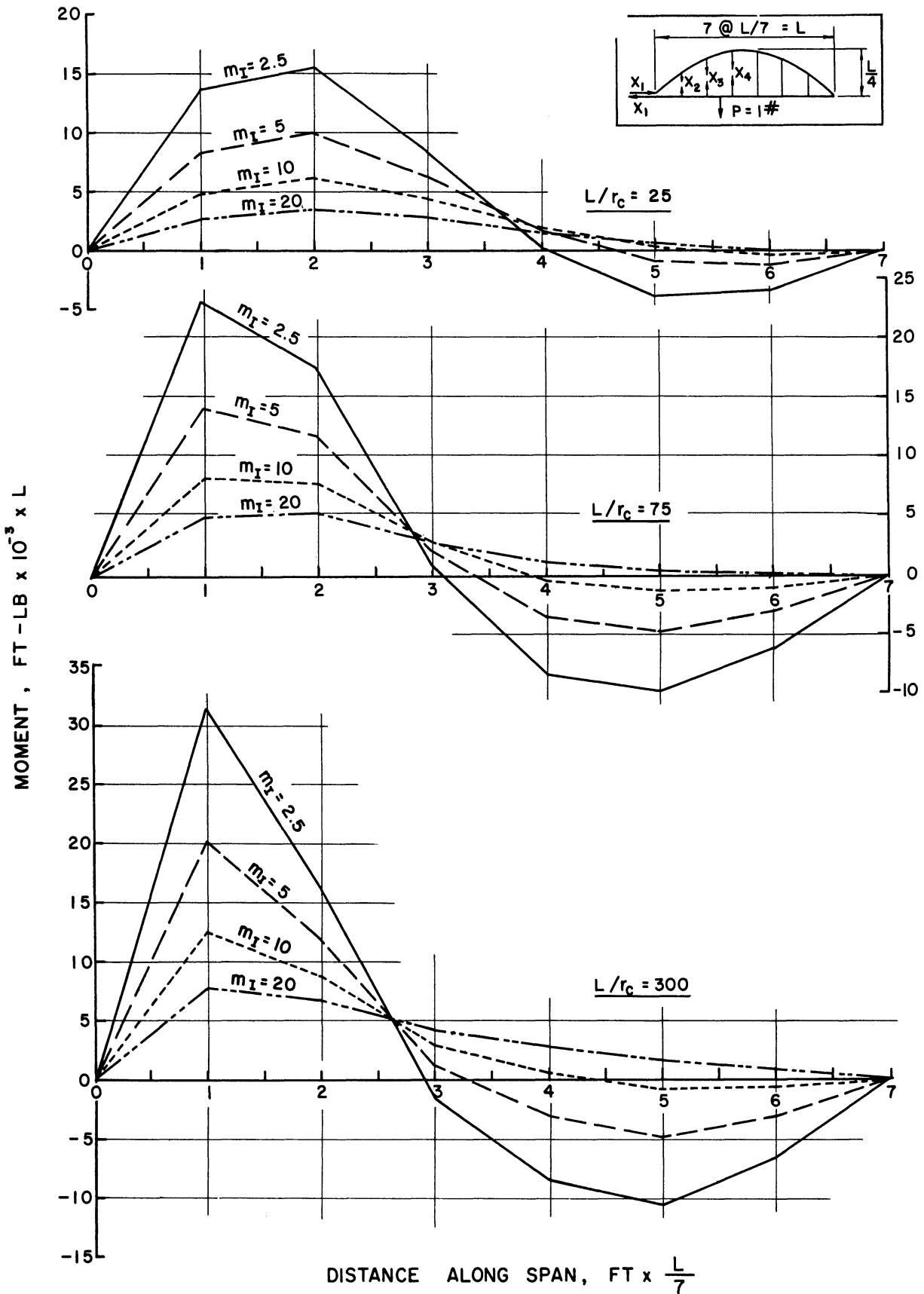


Figure 9. Influence Lines for Bending Moment at Panel Point X_2 for Arch.

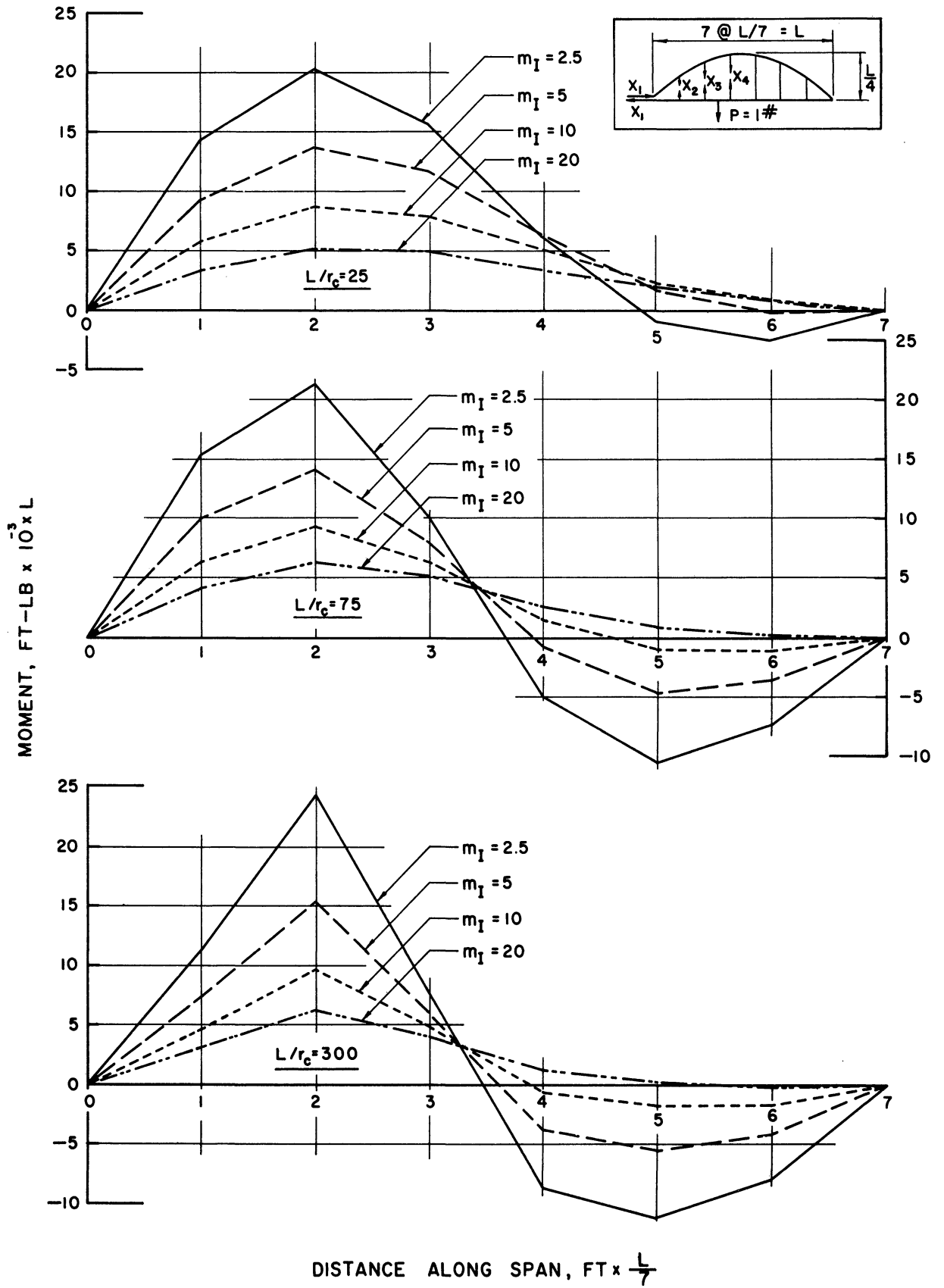


Figure 10. Influence Lines for Bending Moment at Panel Point X_3 for Arch.

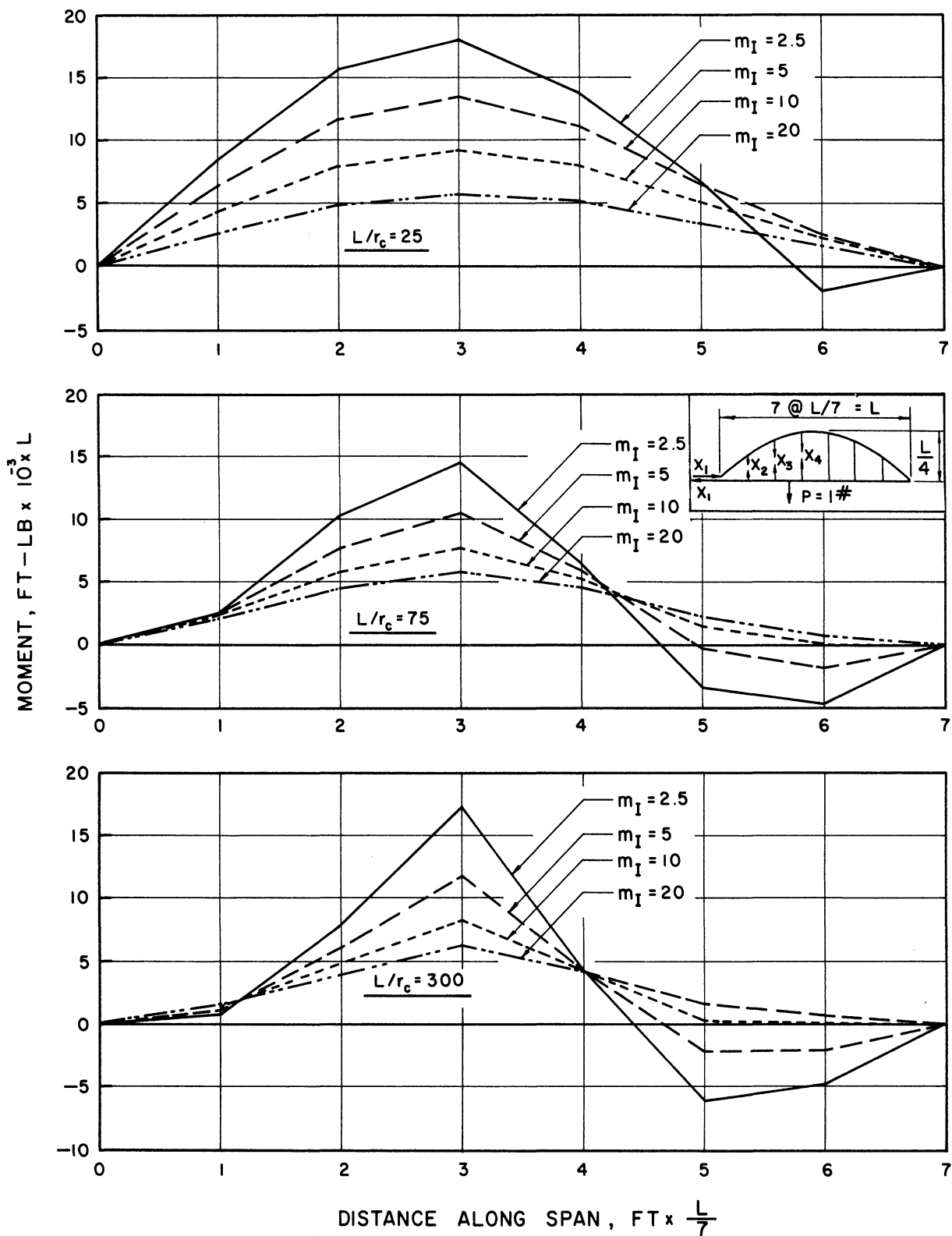


Figure 11. Influence Lines for Bending Moment at Panel Point X_4 for Arch.

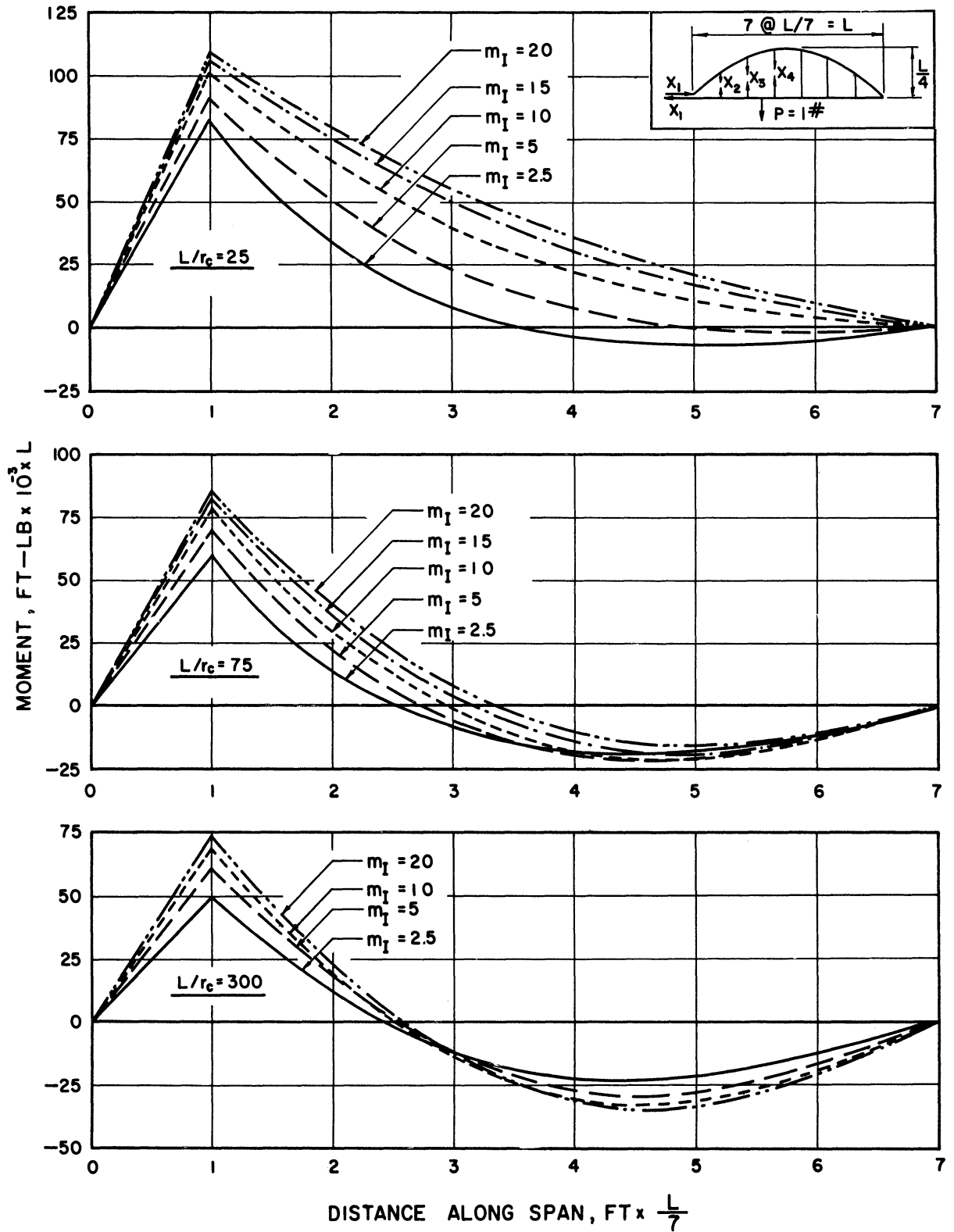


Figure 12. Influence Lines for Bending Moment at Panel Point X_2 for Tie Girder.

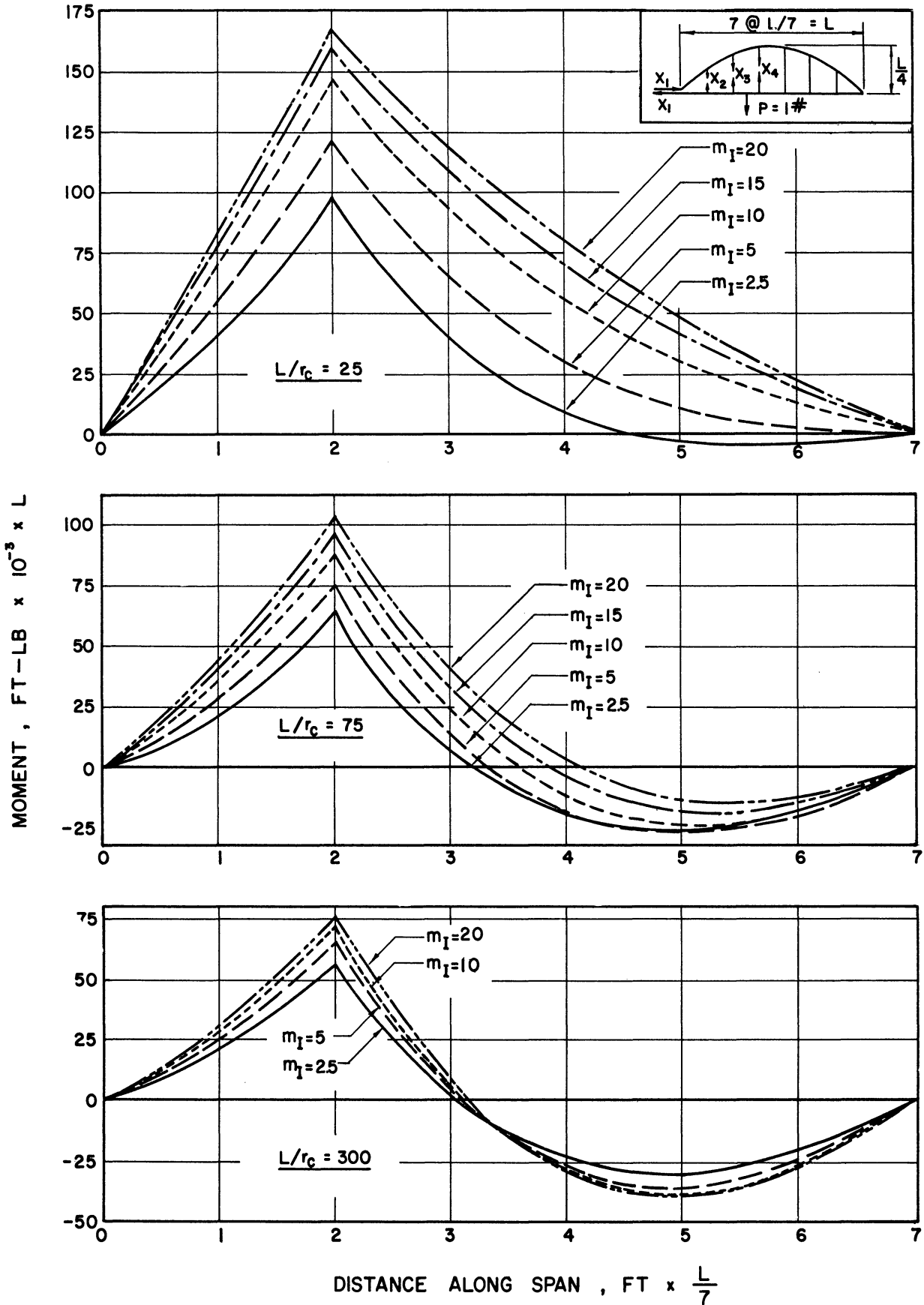


Figure 13. Influence Lines for Bending Moment at Panel Point X_3 for Tie Girder.

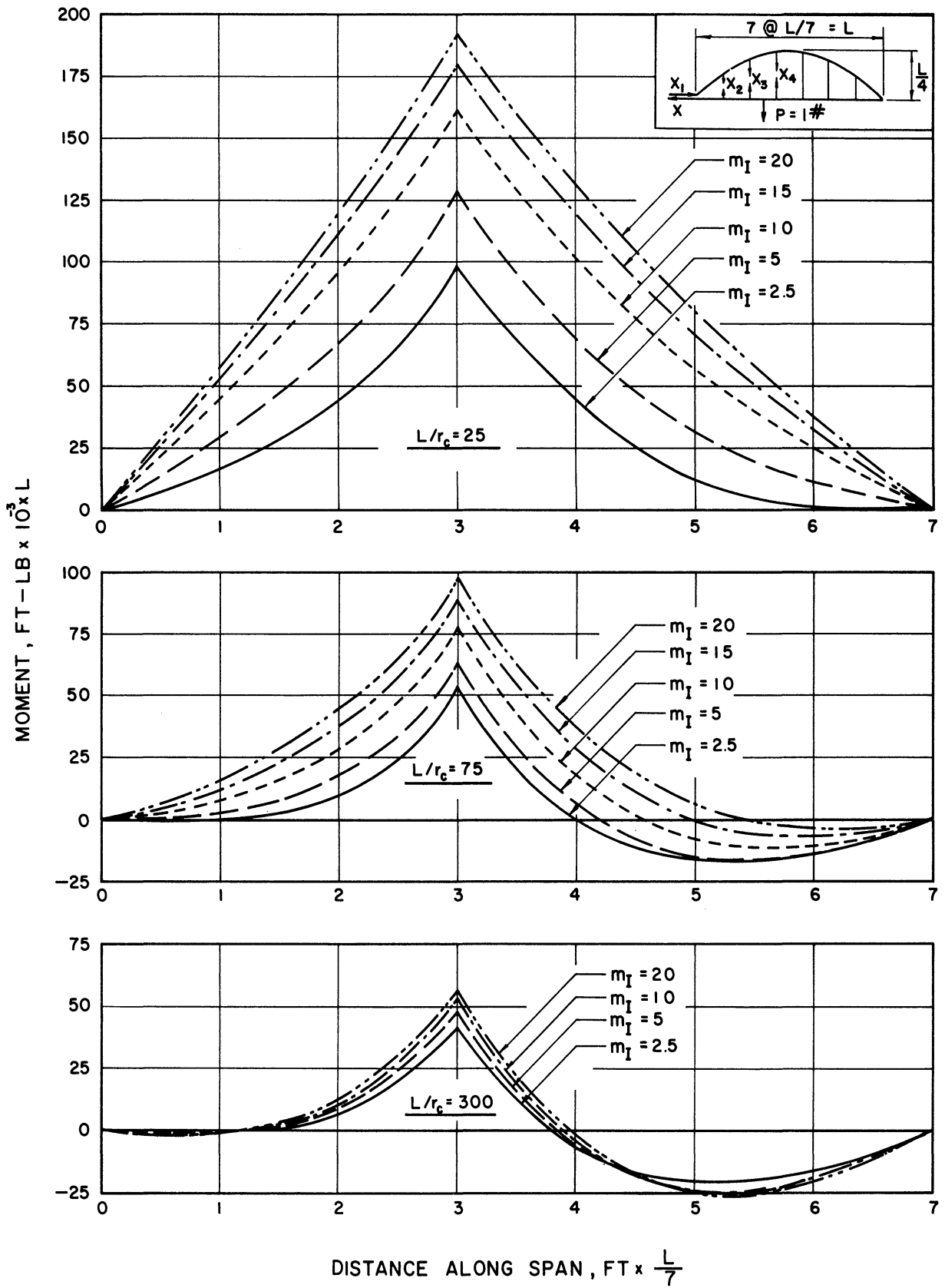


Figure 14. Influence Lines for Bending Moment at Panel Point X_4 for Tie Girder.

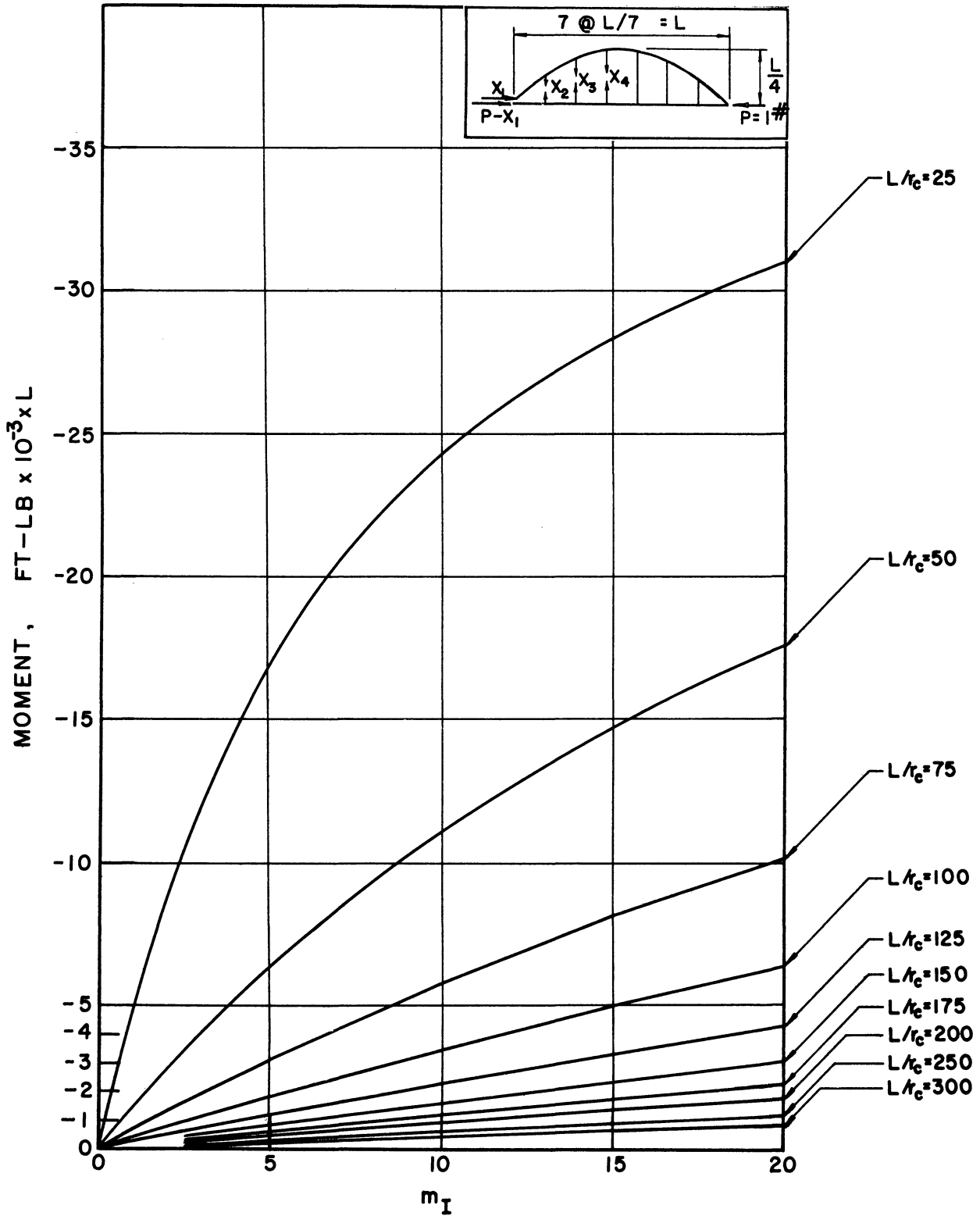


Figure 15. Bending Moment at Panel Point X₄ for Different Values of L/r_c and m_I for Tie Girder.

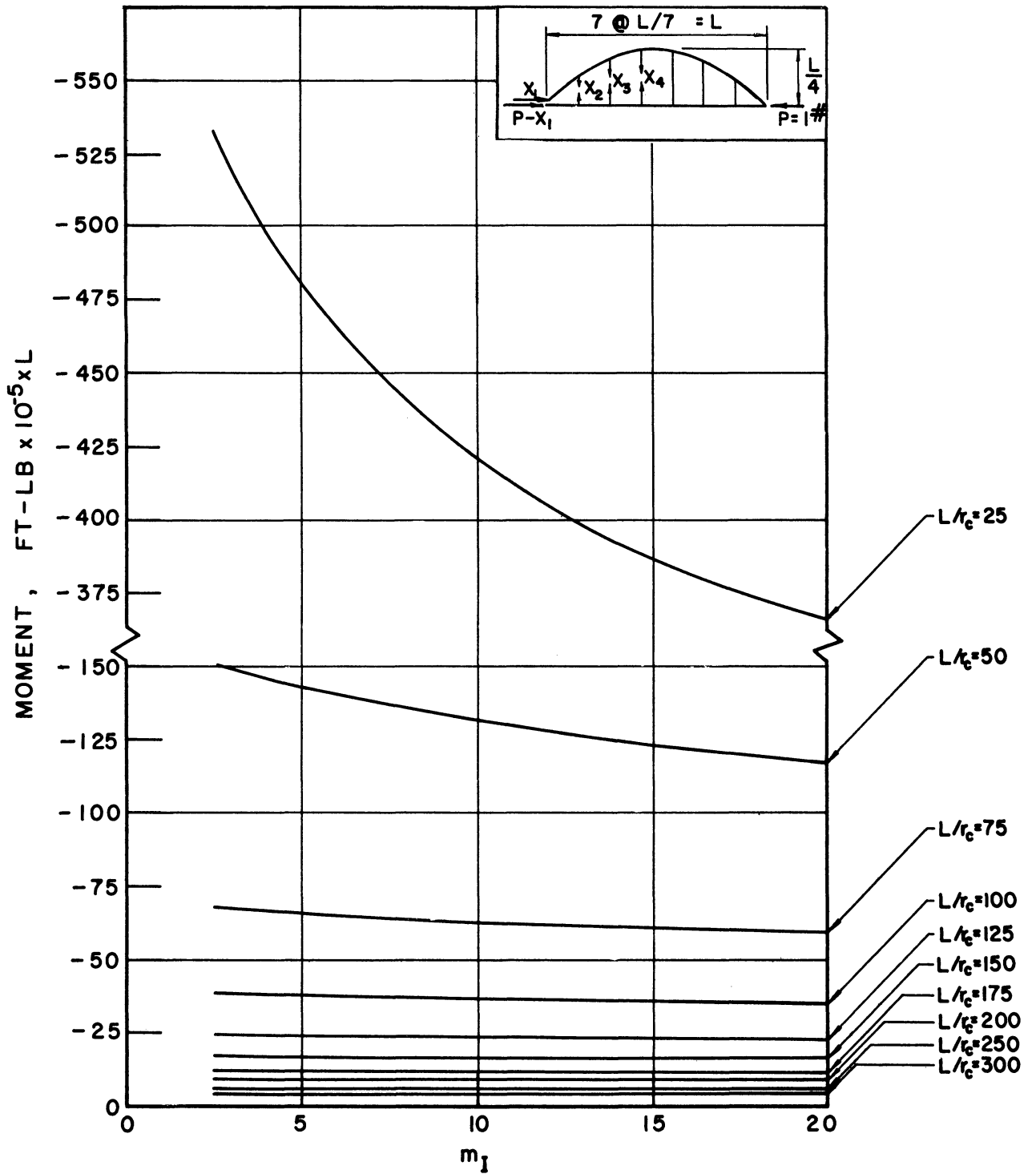


Figure 16. Bending Moment at Crown for Different Values of L/r_c and m_I for Arch.

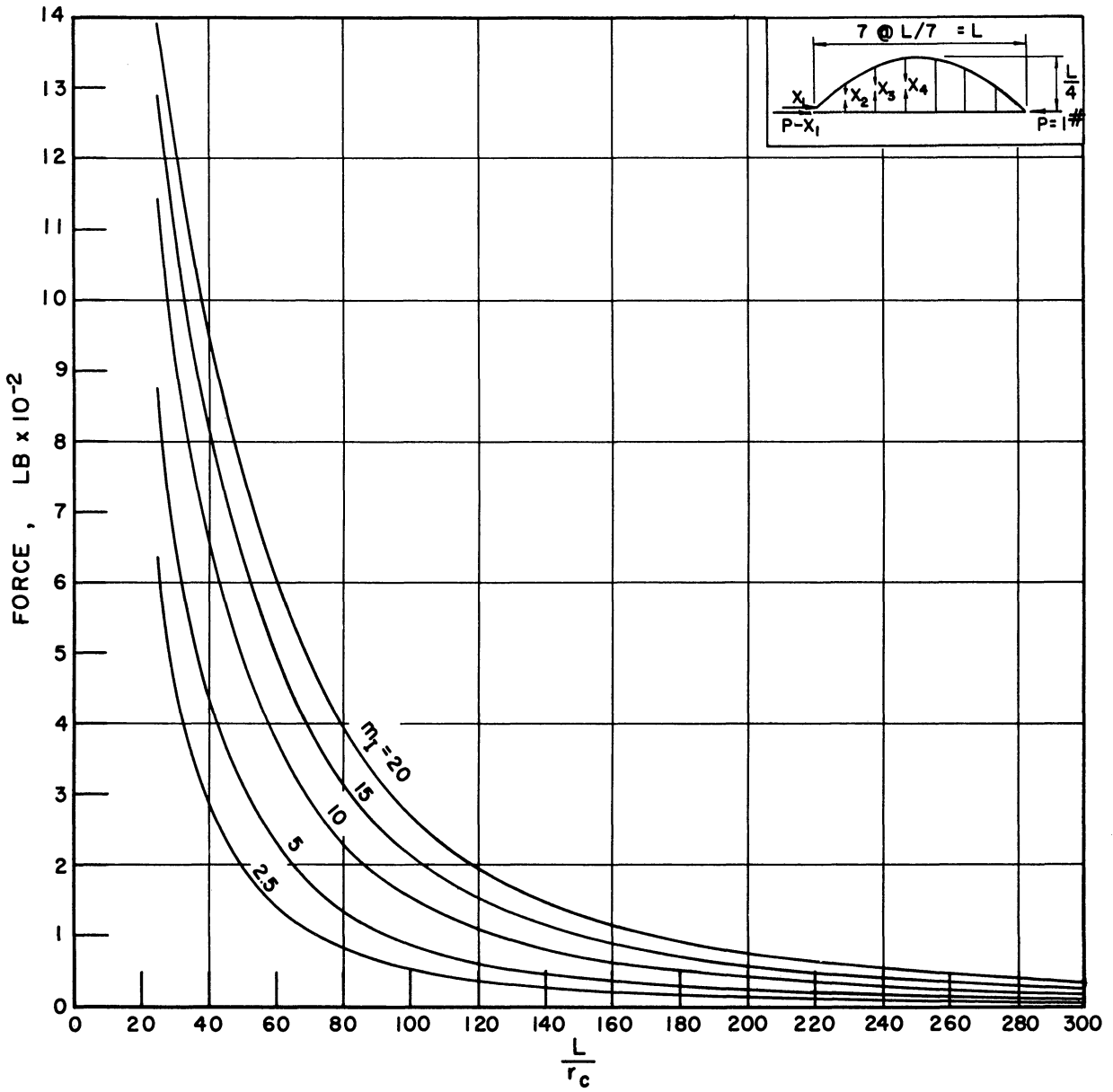


Figure 17. Horizontal Force X_1 for Different L/r_c and m_T Values.

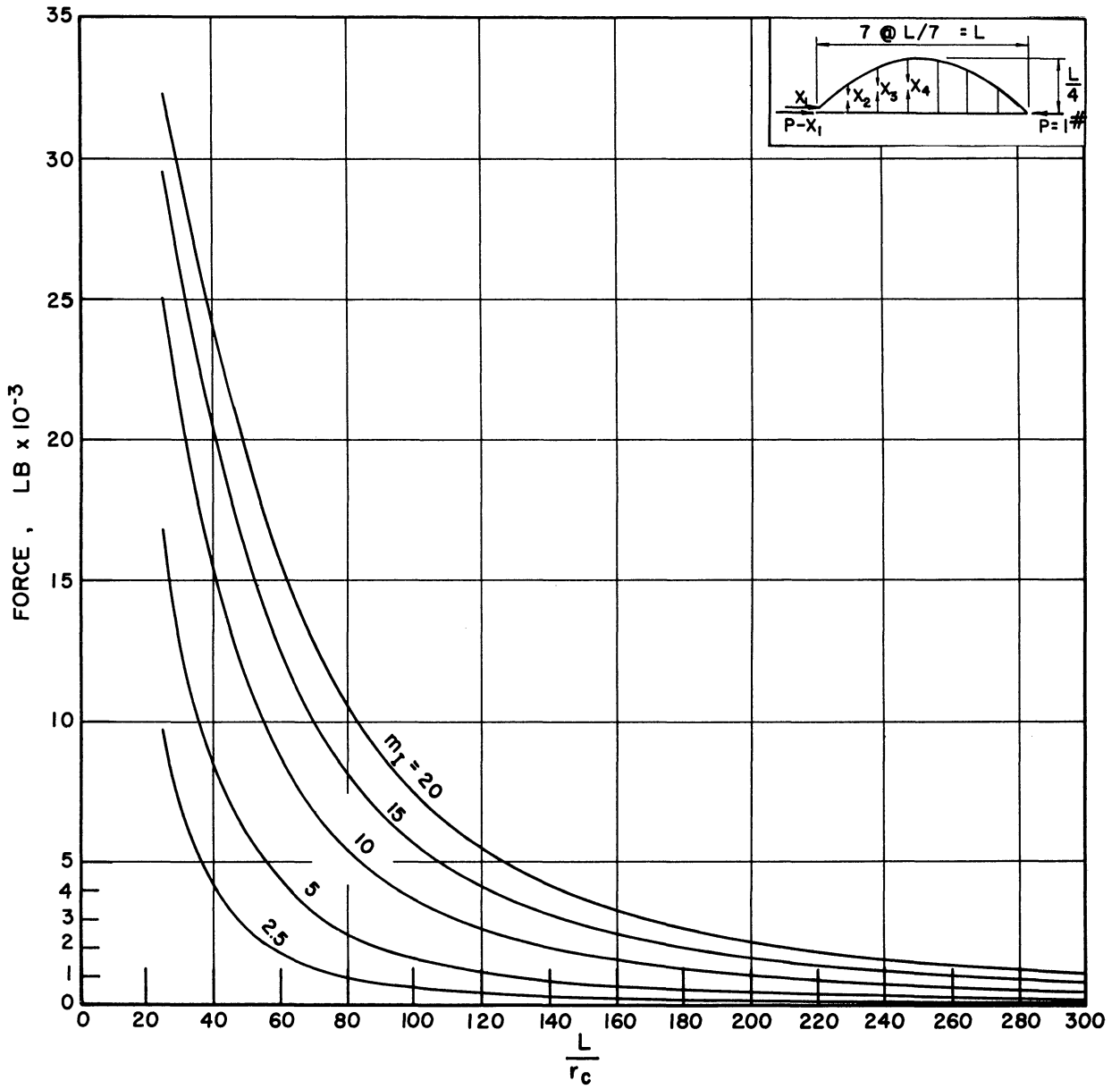


Figure 18. Suspension-Rod Force X_2 for Different L/r_c and m_I Values

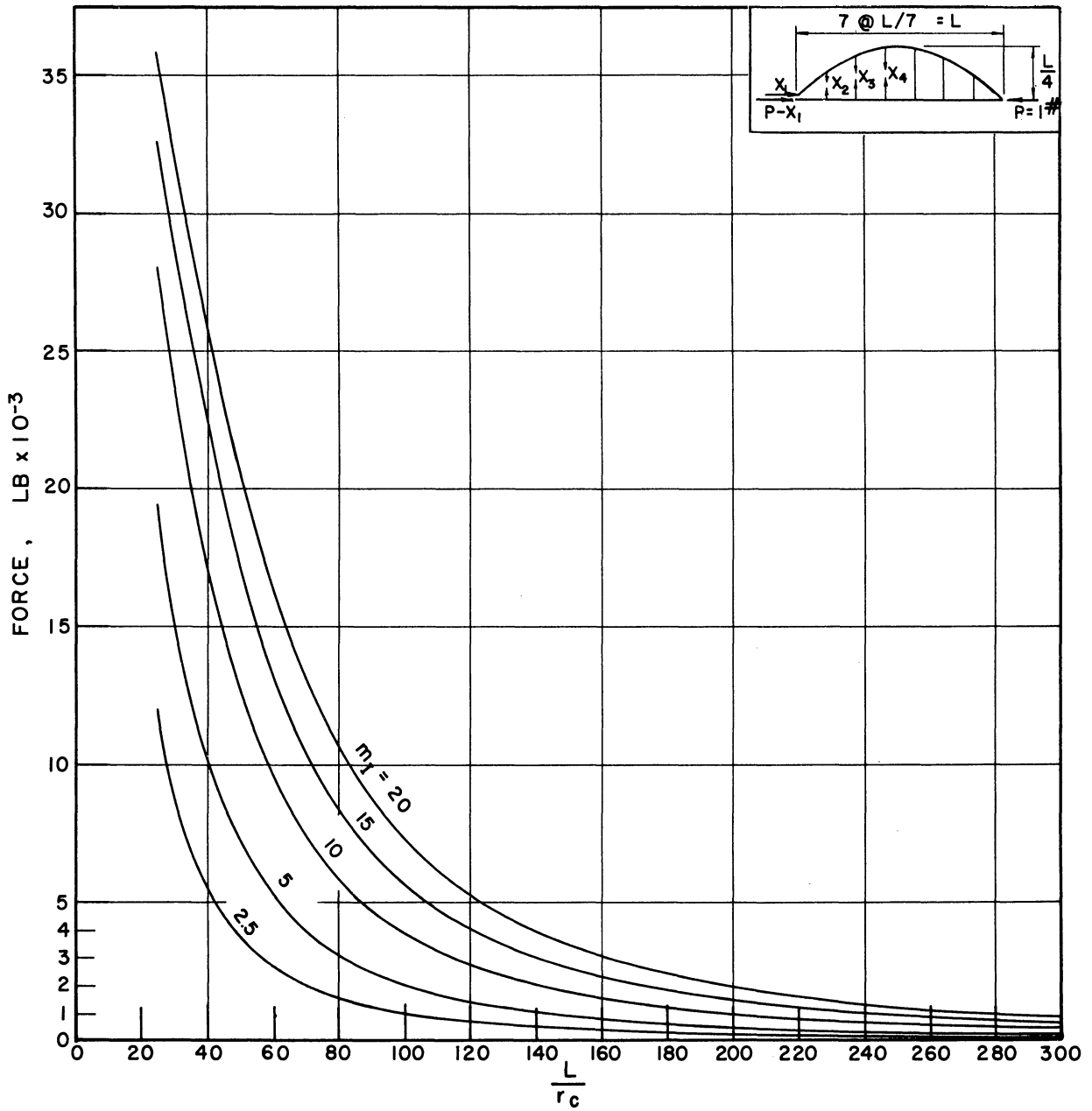


Figure 19. Suspension-Rod Force X_3 for Different L/r_c and m_I Values

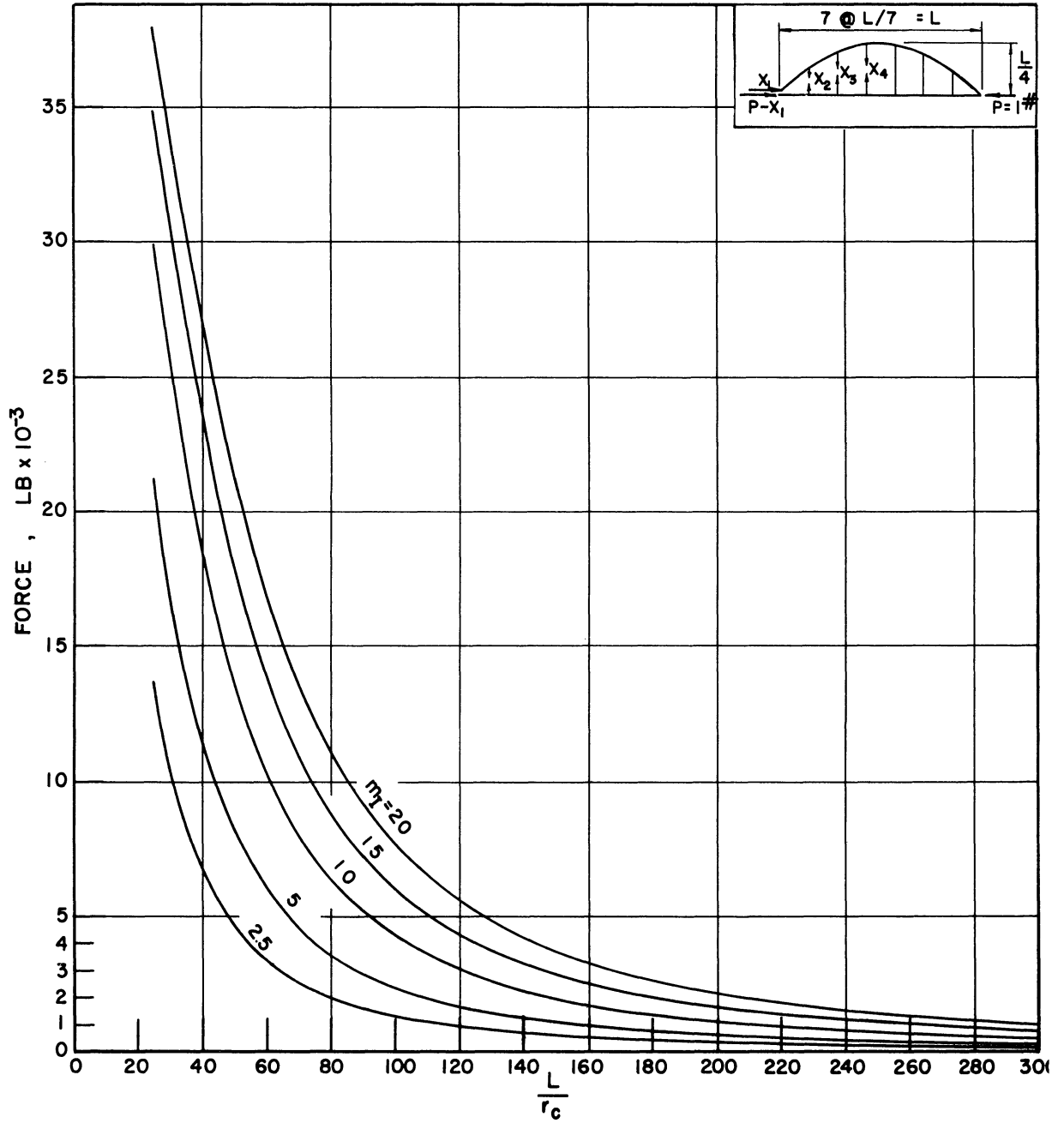


Figure 20. Suspension-Rod Force X_4 for Different L/r_c and m_I Values

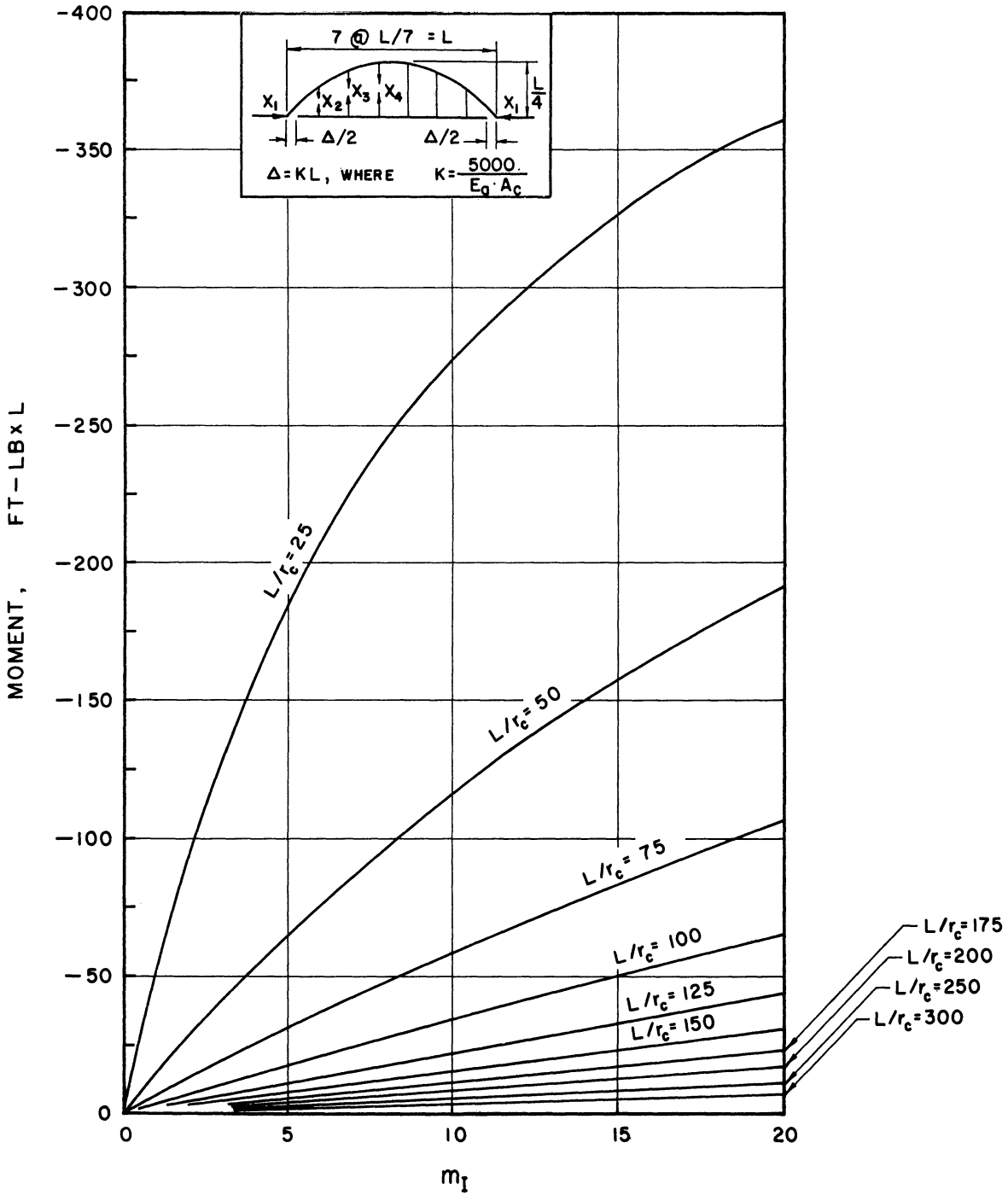


Figure 21. Bending Moment at Panel Point X_4 for Different Values of L/r_c and m_T for Tie Girder.

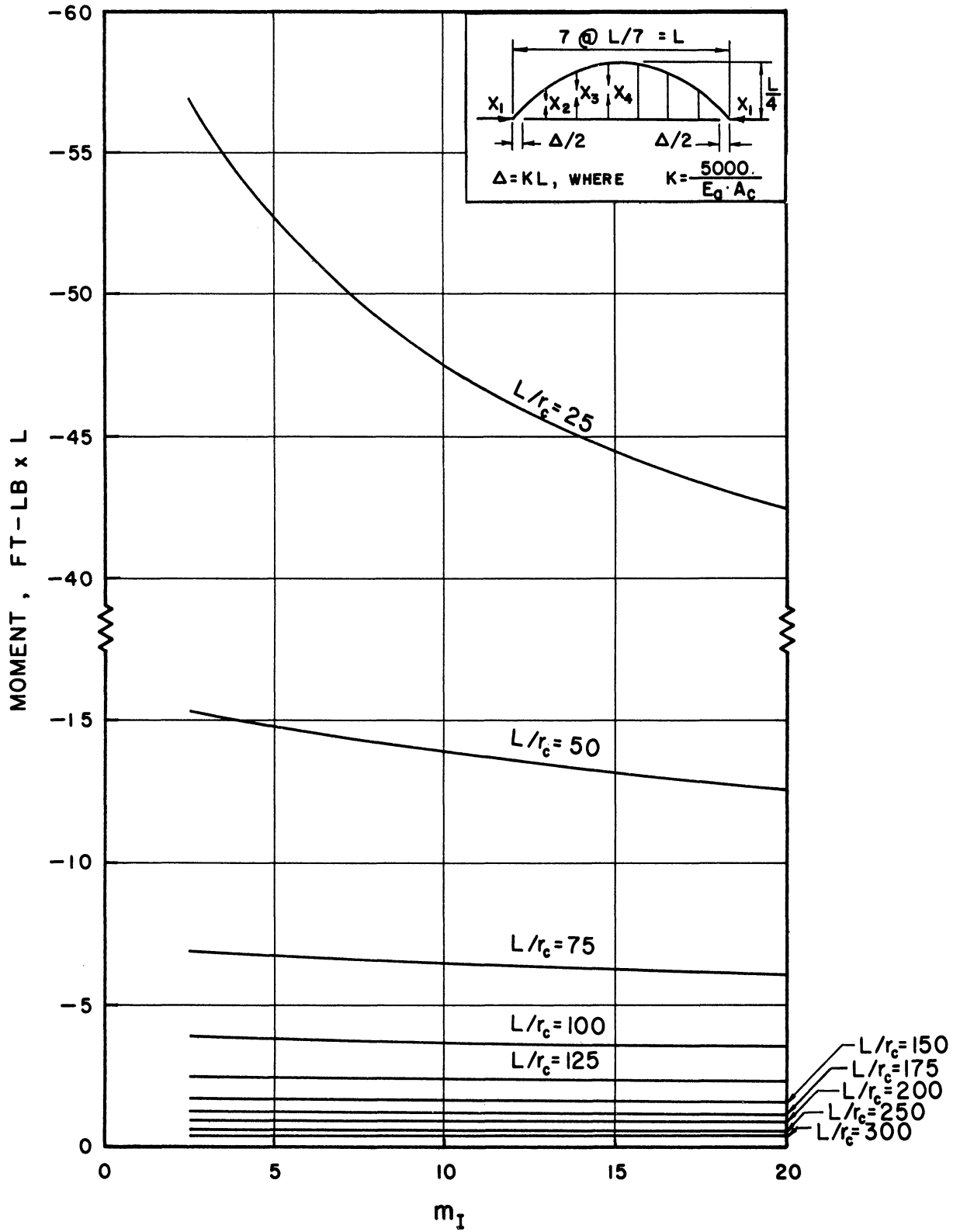


Figure 22. Bending Moment at Crown for Different Values of L/r_c and m_I for Arch.

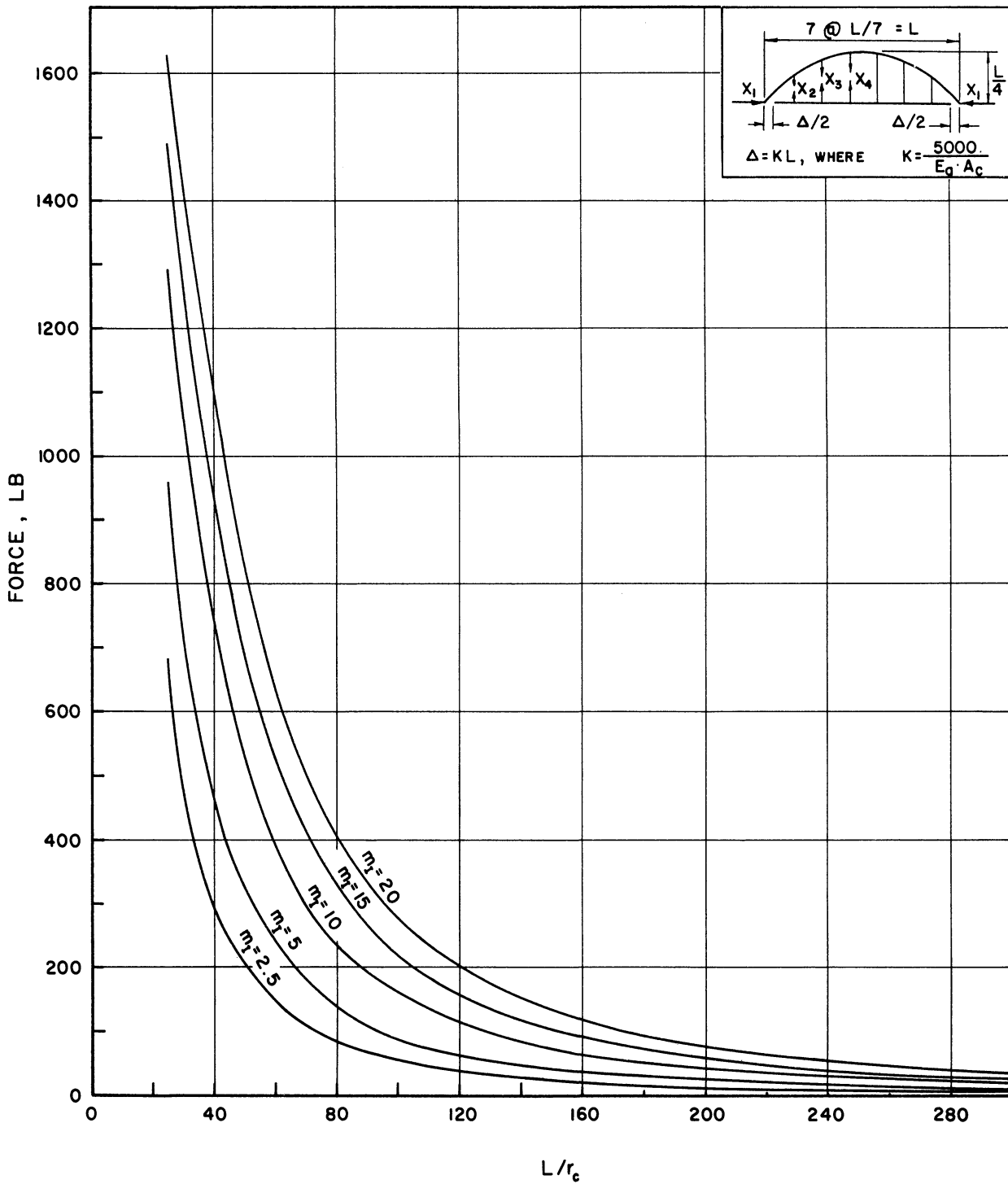


Figure 23. Horizontal Force X_1 for Different L/r_c and m_I Values

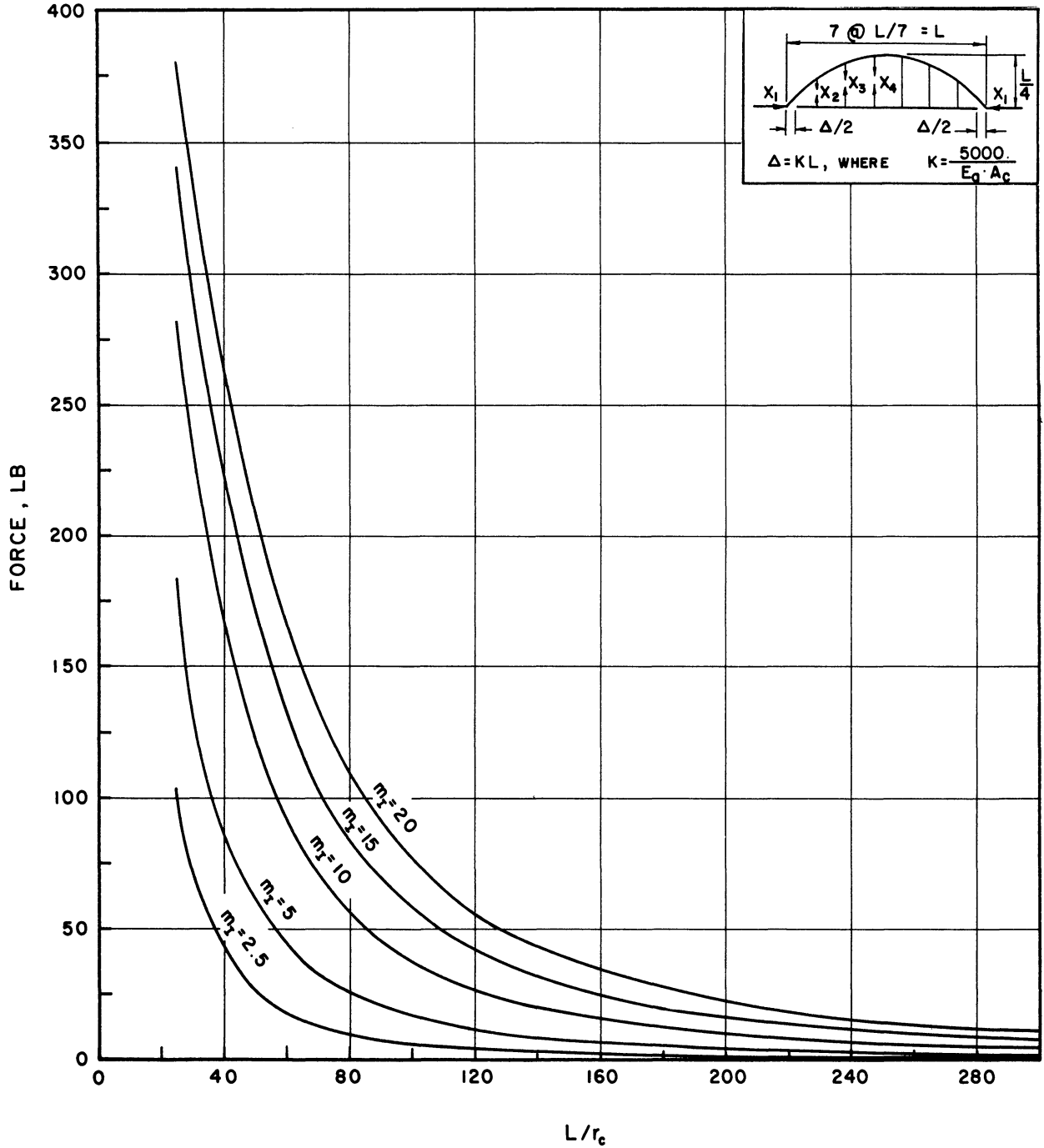


Figure 24. Suspension-Rod Force X_2 for Different L/r_c and m_I Values.

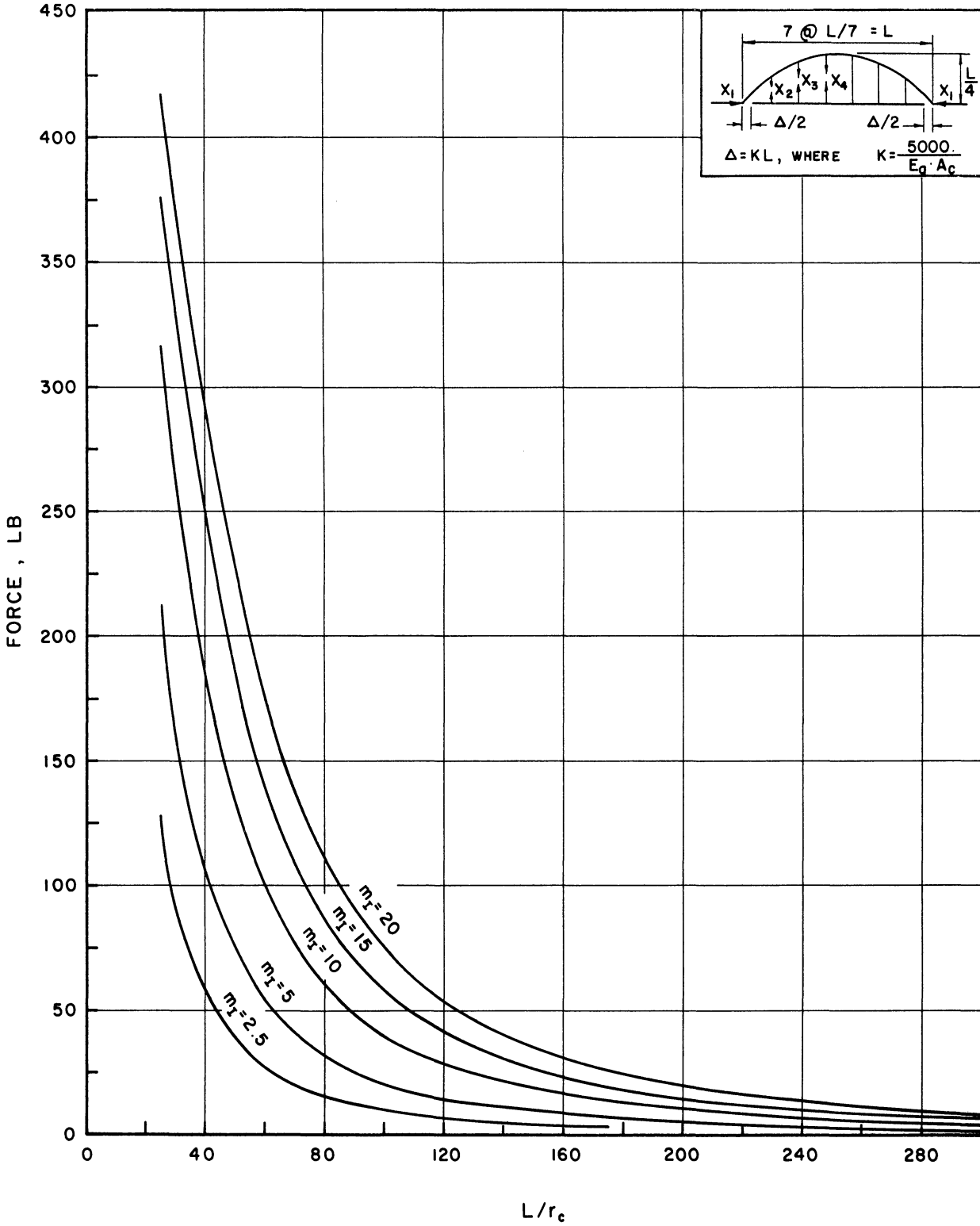


Figure 25. Suspension-Rod Force X_3 for Different L/r_c and m_I Values.

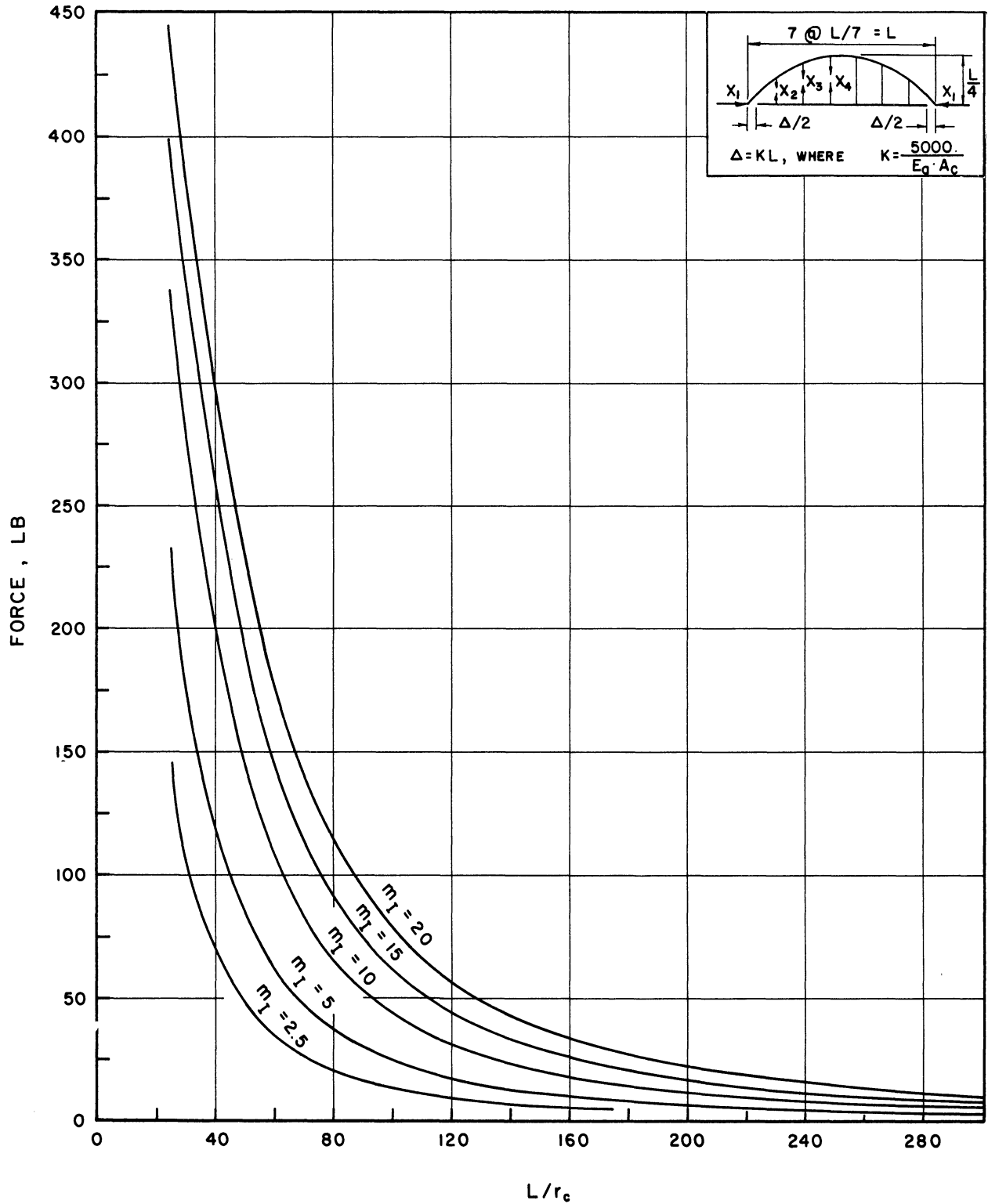


Figure 26. Suspension-Rod Force X_4 for Different L/r_c and m_I Values.

REFERENCES

1. Garrelts, J. M. "Design of St. Georges Tied Arch Span." Proceedings, ASCE, 67, (December, 1941) No. 10.
2. Haviar, V. "The Arch with Connected Stiffening Girder." Final Report of Third Congress, International Association for Bridge and Structural Engineering, Liege, Belgium, September, 1948.
3. Chandrangsou, S., and Sparkes, S. R., "A Study of the Bowstring Arch Having Extensible Suspension Rods and Different Ratios of Tie-Beam to Arch-Rib Stiffness." Proceedings of the Institution of Civil Engineers, 3, No. 2, (August, 1954) Paper No. 5966.
4. Maugh, L. C. Statically Indeterminate Structures New York: John Wiley and Sons, Inc., 1951.
5. Newmark, N. M. "The Distribution of Moment Between Rib and Girder." Transactions, ASCE, 103, (1938)
6. Melan, J., Theory of Arches and Suspension Bridges Chicago: The Myron C. Clark Publishing Co., 1913.
7. Courbon, J. "Bowstring Design." Les Annales des Ponts et Chaussees, (September-October, 1941)
8. Courbon, J. Pont de la Raterie sur la Sarthe Bulletin of the International Association for Bridge and Structural Engineering, August 15, 1958.
9. Chang, J. C. L., "Electronic Computers in Design of Tied-Arch Bridges." Civil Engineering, 28, No. 11 (November, 1958).
10. Anonymous, "A First in Bridge Construction." Engineering News-Record, 162, No. 22 (June, 1959).

UNIVERSITY OF MICHIGAN



3 9015 03024 4472